UNIVERSITY OF CALIFORNIA, SAN DIEGO

SpoIVFB regulation during *Bacillus subtilis* sporulation:

Evidence for a morphological checkpoint governing protease activity

A Thesis submitted in partial satisfaction of the requirement for the degree

Master of Science

in

Biology

by

Kristina Ann Coleman

Committee in Charge

Professor Kit Pogliano, Chair
Professor Joe Pogliano
Professor Milton Saier

2008

The Thesis of Kristina Ann Coleman is approved, and it is acceptable in quality and form for publication on microfilm:

Chair

University of California, San Diego

2008

TABLE OF CONTENTS

LIST OF ABBREVIATIONS

boe	bypass of engulfment
bof	bypass of forespore
bob	bypass of both
cat	chloramphenicol
kan	kanamycin
RIP	regulated intramembrane proteolysis
DNA	deoxyribonucleic acid
GTP	guanosine triphosphate
PCR	polymerase chain reaction
FB	SpoIVFB
FA	SpoIVFA
IVB	SpoIVB
IIQ	SpoIIQ
IID	SpoIID
FAB	SpoIVFAB
ECL	enhanced chemiluminescence
PBS	phosphate-buffered saline
FITC	Fluorescein-5-isothiocyanate
IPTG	isopropyl 1-thio-β-D-galactopyranoside
SDS	sodium dodecyl sulfate
DTT	dithiothreitol
PAGE	polyacrylamide gel electrophoresis

LIST OF FIGURES AND TABLES

Chapter I

Chapter III

ACKNOWLEDGEMENTS

Chapter 2 includes, in full, a reprint of material as it appears in The Journal of Biological Chemistry, Chiba, Shinobu; Coleman, Kristina; and Pogliano, Kit, JBC Papers in Press, 2007. The thesis author was a secondary author and investigator of this paper. Contributions made are mentioned in detail in Chapter 2, part A.

VITA

2005 Bachelor of Science, University of California, San Diego

2008 Master of Science, University of California, San Diego

PUBLICATION

"Impact of Membrane Fusion and Proteolysis on SpoIIQ Dynamics and Interaction with SpoIIIAH" The Journal of Biological Chemistry, vol 282. 2576-2586, November 2006.

FIELDS OF STUDY

Major Field: Biology

Studies in endospore formation

Professor Kit Pogliano

ABSTRACT OF THE THESIS

SpoIVFB regulation during *Bacillus subtilis* sporulation:
Evidence for a morphological checkpoint governing protease activity

by

Kristina Ann Coleman

Master of Science in Biology

University of California, San Diego, 2008

Professor Kit Pogliano, Chair

To ensure the future existence of its progeny in times of starvation or other stress, *Bacillus subtilis* undergoes a process called sporulation. The resultant spore is capable of surviving extreme heat, irradiation, strong acids, and desiccation. This developmental pathway begins with an asymmetric cell division giving rise to two cells of unequal size, the smaller of which is known as the forespore. The larger mother cell begins a phagocytosis-like process called engulfment, where its membranes track around the

smaller forespore eventually enclosing it. The completion of engulfment serves as a morphological checkpoint to activate σ^G, which leads to the eventual activation of σ^K. The mother cell transcription factor σ^K is activated by SpoIVFB, an intramembrane protease that requires the σ^G produced SpoIVB protein for its activity. My thesis research demonstrates that SpoIVFB activity, and thus σ^K activation, are governed by two independent checkpoints: the previously identified forespore checkpoint under the control of σ^G, and a separate checkpoint regulated by the completion of engulfment. My research demonstrates that SpoIVFB protein levels are not directly proportional to σ^K activity, supporting the hypothesis that SpoIVFB activity is regulated.

CHAPTER I

Introduction

A. Environmental stress: sensing and responding

The ability to sense the environment is one that is indispensable for bacteria that live in changing environments. Without the capacity to sense nutrients, ionic strength, osmotic activity, and possible toxic compounds, bacteria would be ill-equipped to survive in our many complex ecosystems. When environmental conditions become unfavorable, bacteria sense these changes and are able to turn on genes to produce proteins and metabolites to help protect themselves against adverse surroundings.

The most common mechanism utilized by bacteria to sense environmental stress is two-component signal transduction. This system includes a membrane-bound histidine kinase that senses the environment, and a response regulator that triggers a cellular response [9, 10]. After sensing environmental change through its sensor domain, the histidine kinase domain is autophosphorylated [11]. The phosphate group is transferred to the response regulator, changing its conformation, and allowing it to bind to promoter regions of downstream genes [12]. This enables transcription of genes to deal with the specific environmental condition.

Many bacteria respond to difficult environments by entering stationary phase and lowering their metabolic activity. Other bacteria, such as *Pseudomonas aeruginosa* are able to protect themselves by forming biofilms [13], producing catalase [14], or expressing betalactamases [15] after extended treatment with hydrogen peroxide, and beta-lactam antibiotics, respectively. *Bacilli* and *Clostridia* are bacteria that are capable of surviving the most extreme conditions for extended periods of time. By forming an endospore, these bacteria encapsulate their genetic material within a highly protective, specialized cell capable of enduring nutritional deficit and severe environments

Bacillus subtilis is the conventional model for studying endospore formation in a laboratory setting. This investigation discusses work done predominantly in this species. The information garnered by studying the mother cell and forespore's divergent morphological and physiological changes will give the field of developmental biology insight as to how more complex systems might function.

B. The last resort: sporulation stimuli and the phosphorelay system

Starvation is the main sporulation stimulus, but high population density is also a crucial factor. With increasing cell density, quorum sensing peptides are secreted into the medium. When these peptides reach a critical concentration, they are sensed by cell surface receptors, giving the bacteria information about their population density [17]. A phosphorelay is activated, however, neither starvation nor high cell density cause a commitment to sporulation [17]. In fact, since sporulation is a lengthy and energetically costly process, the bacteria seem to use it only as a last resort, and have many other survival mechanisms and proteins dedicated to inhibiting or delaying sporulation [20].

It is well known that sporulation is induced by nutrient limitation and could be specifically caused by cells lacking sources of carbon, nitrogen, or phosphorus. It is currently believed that guanine nucleotides, GDP and GTP, are possible intracellular gauges for nutrient availability [17, 21]. When nutrients are scarce, GTP levels drop. It has been suggested that a repressor of early stationary phase and sporulation genes, CodY [22, 23], binds GTP in the cell and, once in this active state, causes repression. When nutrients are lacking and cause GTP levels to decrease, CodY is no longer active and sporulation can be initiated [17].

To respond to varying extracellular signals including nutrient limitation, *Bacillus subtilis* utilizes five histidine kinases, KinA-KinE [24]. These sensor kinases transfer phosphate to Spo0A indirectly through two intermediates, Spo0F and Spo0B (Figure 1). Microarray analysis has shown that more than 10% of all *B. subtilis* genes are directly or indirectly under the control of Spo0A [25], while phosphorylated Spo0A is a vital positive regulator of sporulation. Low levels of phosphorylated Spo0A (Spo0A~P) are produced while the cells are still in exponential phase but nutrients are limited. The primary task of Spo0A~P at this point is to repress *abrB*, a gene that encodes a repressor of many stationary phase genes [17].

Many of the genes repressed by AbrB encode proteins useful for other survival mechanisms of the cell including motility, chemotaxis, degradation of macromolecules, and import of alternate nutrients [17]. Alternate survival mechanisms include uptake of foreign DNA and transformation, and producing antibiotics to eliminate competition and utilize resultant nutrients [20]. The initial function of Spo0A~P indeed seems to aid in maintaining cell growth and hinders the onset of sporulation.

The phosphorelay intermediate Spo0F is phosphorylated by histidine kinases, and then auto-dephosphorylated by Rap proteins (Figure 1). This ensures that Spo0A will be minimally phosphorylated and only conservatively activate stationary phase genes. As nutrients become increasingly scarce, extracellular signals increase, thus amplifying the rate of phosphorylation of the intermediates. Eventually Rap proteins no longer act on Spo0F~P [26, 27] and high levels of Spo0A~P result. The increased levels of Spo0A~P act as a positive regulator for genes necessary for sporulation [17].

In a last ditch effort to further postpone the commitment to sporulation, it has been shown that cells early in sporulation secrete sporulation delaying and killing factors (to which they themselves are immune) that delay sporulation in and cause lysis of sister cells [19, 20]. The cannibal cells can then use the nutrients to facilitate further growth or support eventual sporulation.

C. Morphological changes of early engulfment

The first step in sporulation calls for chromosome condensation and an asymmetric cell division where, instead of dividing midcell, a septum forms at one-third the cell length close to the cell pole. This forms two cells of unequal size: a smaller cell deemed the forespore, and a larger compartment called the mother cell (Figure 2A). The condensed chromosome is then pumped into the forespore by the SpoIIIE protein (Figure 3B) [20]. Following this, the septum thins and the mother cell begins to migrate around the forespore (Figure 2B), beginning engulfment, a process resembling phagocytosis (Figure 3C,D). After engulfing the forespore, the mother cell membranes fuse at the cell pole, an event mediated by SpoIIIE (Figure 3F) [28].

Two distinct, complementary models have been proposed for the mechanism of engulfment. The first model is based on evidence that SpoIID and SpoIIP are highly active peptidoglycan hydrolases and are in a complex with SpoIIM at the septum [29-30, 64]. This data, and the failure to identify other proteins that are essential for engulfment, but dispensable for viability, led to the model that SpoIID and SpoIIP (anchored to the membrane by SpoIIM) hydrolyze the cell wall between the mother cell and forespore,

thereby pulling the mother cell membranes around the forespore. In this model, membrane migration is driven by cell wall hydrolysis [30].

The second proposed contribution to membrane migration is a ratchet-type mechanism consisting of a zipper-like interaction between two interacting membrane proteins, SpoIIQ and SpoIIIAH [7, 31]. Since SpoIIQ is produced in the forespore while SpoIIIAH is produced in the mother cell, the only place where they can interact is at the septum. This interaction is essential for the septal localization of many other sporulation proteins, including SpoIVFA and SpoIVFB, which are required for σ^K activation, the topic of my thesis research. Broder and Pogliano [31] found that when peptidoglycan is enzymatically removed, engulfment is still completed. Since this case involves no cell wall to hydrolyze, it is impossible that SpoIID is driving this migration, and indeed, the DMP proteins are dispensable for this process. However, the SpoIIQ and IIIAH proteins are essential for protoplast engulfment. It is shown that during engulfment, SpoIIQ makes a stationary structure, working with SpoIIIAH as a ratchet, locking in forward membrane migration and preventing reversal [31]. The Q-AH zipper is not normally required for engulfment in intact cells, but is required when DMP activity is reduced, or in the absence of SpoIIB. It is believed that the Q-AH zipper can mediate DMP localization in the absence of SpoIIB by recruiting FA and SpoIVFB to the septum [29]. Engulfment is essential for the survival of the individual sporulating cell, which is terminally differentiated at the time of engulfment. Thus, it is under strong selective pressure. It is reasonable to believe that the cell would employ two distinct systems to ensure the completion of engulfment.

D. Intercellular communication

Intercellular communication between the forespore and mother cell is a critical component for proper sporulation in *Bacillus subtilis*. Communication between these two cells governs the activity of four transcription factors that activate consecutively in either the forespore or the mother cell after the completion of two key morphological events (Figure 4). The first event is polar septation, which activates a forespore transcription factor, σ^F. The σ^F transcription factor is required for σ^E activation in the mother cell compartment. The second morphological event is the completion of engulfment, which allows σ^G (which is synthesized by the previous forespore transcription factor, σ^F) to become active in the forespore. The σ^G factor is required for the activation of the final transcription factor, σ^K, in the mother cell. The temporal order is due in large part to the dependency of mother cell transcription factors on forespore transcription factors. Thus, the activation of each sigma factor is dependent on its predecessor and on specific morphological events of sporulation.

The first sigma factor, σ^F, is synthesized prior to the formation of the polar septum, but is held inactive until after septation by an anti-sigma factor, SpoIIAB, which binds to σ^F, and prevents its interaction with RNA polymerase. The anti-sigma factor SpoIIAB is a protein kinase that can also phosphorylate and inactivate an anti-anti sigma factor, SpoIIAA. The completion of polar septation allows activation of the SpoIIE phosphatase, which dephosphorylates SpoIIAA. The anti-anti sigma factor SpoIIAA can then bind and inactivate the anti-sigma factor SpoIIAB. Free from its inhibitor, σ^F is now able to activate gene transcription [20, 55-56]. The σ^F factor transcribes about forty-eight genes, including *spoIIIG*, the gene for σ^G [57]. The σ^G factor is a forespore-specific, late

sporulation transcription factor that is present, but held inactive until after the completion of engulfment. The σ^F factor controls another gene, *spoIIR*, which makes the protein, SpoIIGA, a membrane protease that cleaves pro-σ^E into active σ^E. Although pro-σ^E is present in the cell before the septum forms, it is activated only in the mother cell, in part because it is degraded in the forespore compartment [20]. The transcription factor, σ^E, controls 262 genes including genes necessary for the activation of the final transcription factors, σ^G and σ^K, which are activated following engulfment [59-61].

The final transcription factors depend on the completion of engulfment. Much less is known about the mechanism by which the forespore transcription factor, σ^G, is controlled than about the mother cell transcription factor, σ^K. In addition to inhibiting σ^F, some findings suggest that the SpoIIAB anti-sigma factor also prevents σ^G activity until after engulfment, when it is deactivated by SpoIIAA [62]. Other findings suggest that an independent mechanism may hold σ^G inactive until after engulfment, and that SpoIIAB only plays a minor role, if any role at all [63]. The mother cell and forespore genes, *spoIIIA* and *spoIIIJ*, respectively, encode membrane proteins and are necessary for σ^G activation following engulfment [65-67]. Although many regulators of σ^G activation have been discovered, the mechanisms by which they, in concert with the completion of engulfment, effect σ^G activation remain unknown. The σ^G transcription factor regulates over 100 genes [68] including genes required for the activation of σ^K, the late mother cell-specific transcription factor [57,69].

E. Activation of σ^K

Engulfment is essential for both σ^G and σ^K activation, but the mechanism by which the cell senses the completion of engulfment is still unknown. It has recently been shown that inactivation of the σ^F-directed *csfB* locus leads to premature activation of σ^G [83]. In the absence of CsfB, σ^G becomes active after septation, rather than after the completion of engulfment. This is believed to be independent of the SpoIIIA-SpoIIIJ pathway, which is involved in σ^G activation following the completion of engulfment [65-67]. Mutations in *spoIIIA* and *spoIIIJ* arrest sporulation after engulfment, but before activation of σ^G. It was thought that these genes code for products that release σ^G from inhibition by SpoIIAB [66]. The workings of *spoIIIA* and *spoIIIJ* have recently been thrown back into mystery by the new data that suggests that SpoIIAB is either redundant or has no function in the inhibition of σ^G [63]. Even though it is still unknown how engulfment regulates σ^G, it is known that engulfment is necessary for its activation and that of σ^K as well.

The engulfment-dependent activation of σ^G is necessary for the activation of σ^K, a late mother cell transcription factor. Pro-σ^K, the inactive precursor of σ^K, is present before the completion of engulfment and tethered in the outer forespore membrane [70]. Following engulfment, σ^G upregulates production of *spoIVB*, which encodes a protein involved in a signal transduction cascade responsible for eventual activation of σ^K. Subsequently, σ^K activates genes necessary for formation of the protein spore coat and eventual lysis of the mother cell [61]. SpoIVFB, an intramembrane zinc metalloprotease, cleaves pro-σ^K into active σ^K, which is released into the mother cell, activating gene transcription [69].

Activation of σ^K by SpoIVFB is an example of regulated intramembrane proteolysis (RIP). RIP is a means of signal transduction by which transmembrane proteins are cleaved by membrane-bound proteases. RIP is a widespread mechanism that has been observed from bacteria to humans and other animals [84]. RIP is mediated by a group of membrane-bound proteases, deemed I-Clips (Intramembrane-cleaving proteases) [78]. SpoIVFB belongs to a subset of I-Clips, the site-2 proteases, or S2P, and is a zinc metalloprotease [79,80]. Zinc metalloproteases are characterized by an active site HExxH motif within a transmembrane segment [78,79]. SpoIVFB also has a second conserved NPDG domain. Both domains are important for σ^K cleavage (Figure 6) [78-80]. [80].

In other organisms, S2Ps serve varying functions. In spite of this, the mechanism by which they work is the same, and the proteins are recognized by their conserved active site domains. *Vibrio cholerae* and *Mycobacterium tuberculosis* S2P proteins YaeL and Rv2869c, respectively, control important virulence genes [78]. Human S2P is shown to cleave sterol regulatory element-binding proteins (SREBPs) which then initiate transcription of genes in the cholesterol and fatty acid biosynthetic pathways. S2P also regulates the unfolded protein response (UPR) in the endoplasmic reticulum [85]. MmpA, a *Caulobacter crescentus* S2P, is important for the preservation of cell asymmetry, a factor needed for assembly of pili and holdfast at the proper cell pole [86]. These cases illustrate the diversity of S2Ps and the widespread prevalence of RIP as a means of signal transduction.

During engulfment, SpoIVFB is held in a complex with SpoIVFA, and BofA, which inhibits SpoIVFB activity (Figure 5). In the absence of BofA, SpoIVFB is

uninhibited and can thus activate σ^K without the need for SpoIVB or σ^G activity. SpoIVFA is responsible for proper interaction between BofA and SpoIVFB, and also mediates their localization to the outer forespore membrane [71] via an interaction with the Q-AH zipper [41, 87]. SpoIVFB is thought to be inhibited by BofA through its provision of a metal ligand that blocks SpoIVFB's active site [72]. Elimination of BofA bypasses the normal requirement for the previous activation of the forespore transcription factor, σ^G, for the activation of σ^K, which I will refer to as the forespore checkpoint.

The forespore checkpoint for σ^K activity depends on the activation of SpoIVFB by two serine proteases. The first and most critical protease is SpoIVB, which is upregulated by σ^G, and secreted from the forespore into the intermembrane space between the forespore membranes (Figure 5) [73-74]. A small amount of SpoIVB is produced during engulfment by σ^F directed gene expression, but it is believed to be held inactive by a protein called BofC [75]. After secretion into the intermembrane space and the completion of engulfment, SpoIVB cleaves SpoIVFA, relieving its BofA-mediated inhibition [74-75]. Another protease, CtpB, thought to be produced by both cells, is found in the intramembrane space and is believed to cleave both SpoIVFA and BofA [73, 76-77]. Deleting CtpB delays σ^K activation by about thirty minutes, suggesting that CtpB is required for proper timing of σ^K activation. When SpoIVB is unable to cleave SpoIVFA, CtpB has been shown to be sufficient for σ^K activation after a delay [73, 77]. Following its release from BofA inhibition, SpoIVFB cleaves pro-σ^K into active σ^K (Figure 5).

While the forespore checkpoint has been well-characterized, recent work suggests that it is not the only mechanism governing the activity of σ^K. Specifically, when *bofA* is

deleted, SpoIVFB, and thus σ^K, can be activated without σ^G, thereby bypassing the forespore checkpoint [81,82]. If engulfment-defective mutants fail to activate σ^K simply because they fail to activate σ^G, then deleting *bofA* should bypass the requirement for σ^G and thus allow for σ^K activation. However, Jiang et al have found that when engulfment is blocked by the absence of SpoIID or SpoIIP, a *bofA* mutation is not sufficient to allow σ^K activation [41]. This suggests that the ability of SpoIVFB to activate σ^K is coupled independently to both σ^G activity, via the forespore checkpoint, and the completion of engulfment, deemed the engulfment checkpoint. The mechanism by which engulfment effects the activation of SpoIVFB is as yet unknown. Indeed, a recent paper has called into question this finding, claiming that the absence of σ^K activation in these strains is due to a further decrease in the levels of the σ^K-processing enzyme, SpoIVFB, when compared with SpoIVFB levels in a mutant lacking only *bofA* [88].

My thesis research has been directed at elucidating the mechanisms by which σ^K activity is regulated, with two main focuses. First, I investigated mechanisms by which SpoIVB protease activity is regulated. Second, I investigated the mechanisms by which SpoIVFB activity is regulated. Understanding the regulation of σ^K by the cell will provide valuable insight for sporulation and developmental biology in general. This system is useful for providing knowledge of regulated intramembrane proteolysis that can be applied to very distantly related organisms and extremely complex systems.

F. Maturation and release of the spore

Activation of late engulfment-dependent gene expression allows many changes to occur within the forespore. Multiple forms of protection are imparted to it by the mother

cell. Mature spores are resistant to toxic compounds, heat, desiccation, enzymes, and radiation [32]. One of the major reasons for such strong defenses is that the forespore's DNA is protected from damage by a coating of α/β type small, acid-soluble proteins (SASPs) [33-36]. SASPs are believed to protect the DNA from ionizing radiation [37] in addition to providing a source of amino acids upon spore germination [20]. One of the most important safeguards of the spore is its DNA repair enzymes. Upon exposure to radiation, DNA bipyrimidine photoproducts, more commonly known as spore photoproduct, are formed [36,39].

The spore contains multiple mechanisms in order to rapidly repair its DNA upon germination. Nucleotide excision, homologous recombination under control of *recA*, and most importantly, spore photoproduct lyase (SP lyase) are modes by which the spore can repair UV-induced DNA damage. It has been shown recently that SP lyase seems to have the greatest impact on removing spore photoproduct upon germination [39]. To further strengthen its defenses, the forespore takes up calcium and dipicolonic acid (DPA), synthesized in the mother cell, becoming dehydrated and mineralized. DPA helps protect the spore from wet heat, dry heat, hydrogen peroxide, and desiccation [40].

A modified cell wall, the spore cortex, is formed outside of the spore's plasma membrane [42]. Outside of the cortex, the mother cell forms a protective protein coat with both inner and outer layers, that will protect the spore from harmful lytic enzymes, such as lysozyme (Figure 2C) [42,43]. The coat is believed to be a permeability barrier of sorts, excluding large toxic molecules from accessing the spore, yet allowing small molecules, such as nutrient molecules, to reach sensors beneath the coat [44]. It is believed that the spore inner membrane, which separates the spore core from the cortex,

functions similarly, and is a proton permeability barrier for the spore core [45]. All of these protective barriers are then surrounded by the final layer, the exosporium [46].

After the spore is imparted with its defensive barriers, the mother cell lyses, releasing the mature spore (Figure 2D). Mature spores may remain dormant, even in severe environments, for many years or more [47,48]. *Bacillus subtilis* spores have even been isolated from an over 90-year-old dried milk powder found in Antarctica [47]. Although surviving for so many years is an incredible feat in itself, spores still must be able to germinate upon encountering nutrients and favorable environmental conditions. Luckily, mechanisms that allow the spore to respond to germinants, lyse its cortex, and to rehydrate are built into the spore in the final stages of sporulation [49]. When nutrient germinants bind to receptors in the spore, this causes the release of DPA and calcium, followed by an influx of water [51]. This triggers the hydrolysis of the spore cortex peptidoglycan, degradation of the spore coat [52], and outgrowth of the spore [50,51]. There is also evidence suggesting that a combination of high temperature and high pressure can induce spore germination [38]. Within a few minutes after germination, the cell begins RNA and protein synthesis [53], and is able to divide completely within two hours [54].

G. Figures

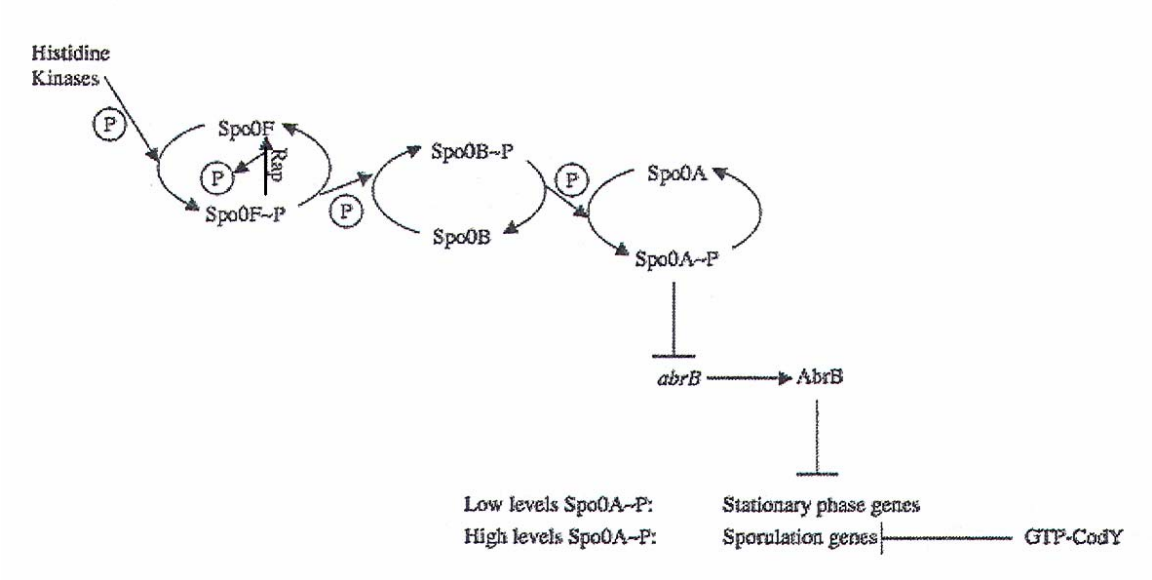

Figure 1. The Spo0A phosphorelay
While in exponential growth, AbrB and active GTP-CodY repress stationary phase and sporulation genes. When one of five histidine kinases (KinA-KinE) receives an extracellular signal, such as low nutrients or high population density, it autophosphorylates. The phosphate is transferred to an intermediate, Spo0F, which is either auto-dephosphorylated by Rap proteins or is allowed to transfer the phosphate on to a second intermediate, Spo0B. The phosphate is then transferred to Spo0A, and Spo0A~P represses *abrB*, a gene encoding a repressor of stationary phase genes. When environmental conditions worsen, more phosphates are transferred, and greater levels of Spo0A~P accumulate. This eventually leads to the activation of genes necessary for sporulation.

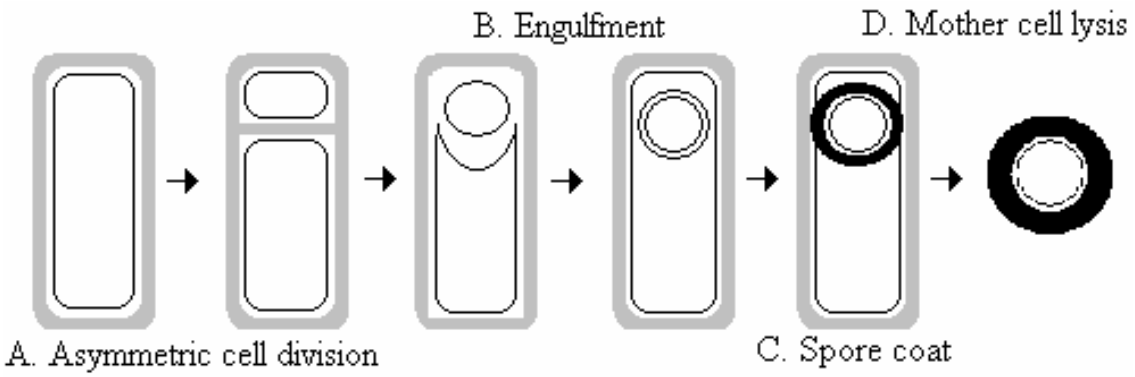

Figure 2. Sporulation
(A) Sporulation begins with a polar, asymmetric cell division forming a larger mother cell and smaller forespore. (B) In a phagocytosis-like process, the mother cell engulfs the forespore and its membranes fuse. (C) Following membrane fusion, the mother cell forms a protective protein coat around the forespore. (D) After maturation of the forespore, the mother cell lyses, releasing the mature spore. After this stage, when growth conditions are once again favorable, the spore can germinate and resume vegetative growth.

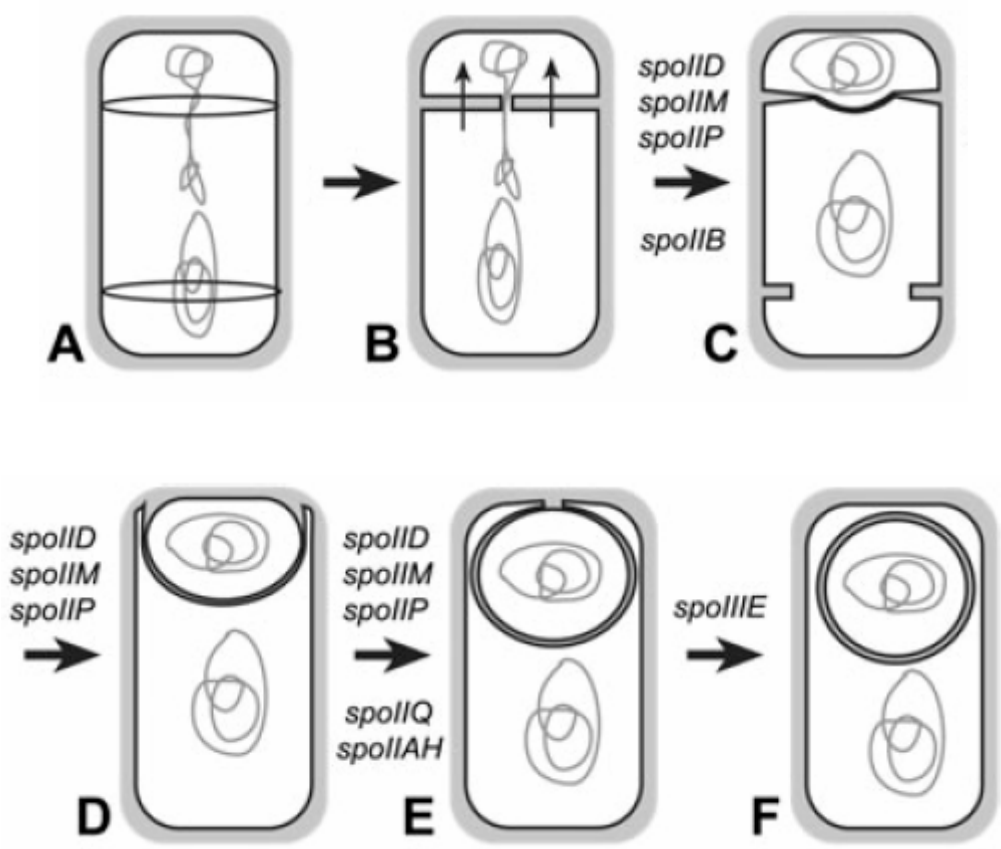

Figure 3. Engulfment
(A,B) The sporulating cell divides asymmetrically, forming the smaller forespore and larger mother cell. (B) The chromosome is pumped into the forespore by SpoIIIE. (C) SpoIID hydrolyzes septal peptidoglycan, pulling along the mother cell membranes. SpoIIM anchors D to the membrane. DMP utilizes SpoIIB for septal localization. (D,E) The mother cell membranes migrate around the forespore. This can be accomplished by two different mechanisms: the DMP module and the Q-AH module. (F) The membranes meet and fuse at the cell pole. Fusion requires the SpoIIIE DNA translocase. Used with permission from [29].

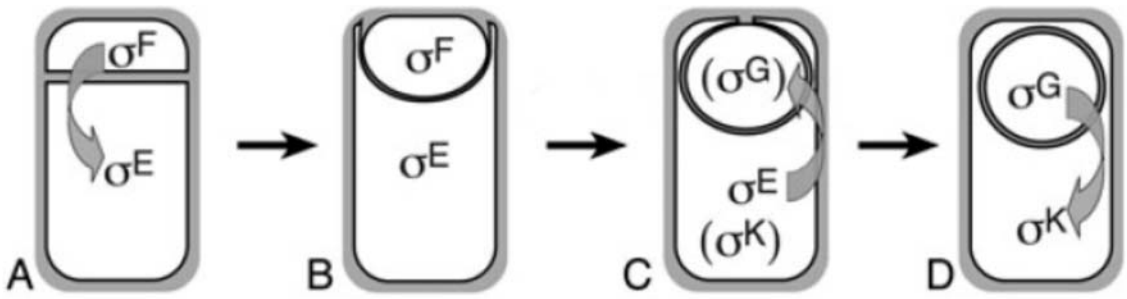

Figure 4. Transcription factor activation during sporulation
(A) σ^F in the forespore is activated first. (A,B) Genes are activated that allow for σ^E activation in the mother cell. (C) σ^G and σ^K are present in their respective compartments, but remain inactive until after engulfment. (D) σ^G initiates the forespore checkpoint which leads to σ^K activation in the mother cell. Used with permission from [41].

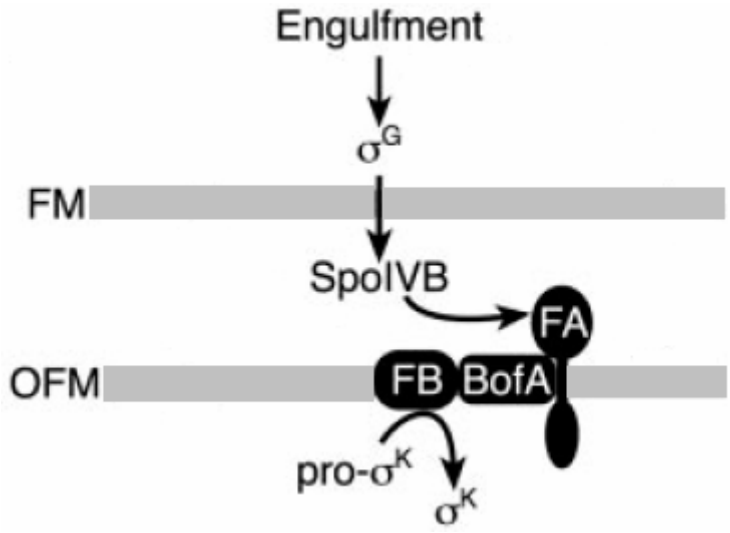

Figure 5. The forespore checkpoint
After engulfment, σ^G leads to upregulation of *spoIVB* causing high levels of SpoIVB protein to accumulate. SpoIVB is secreted into the intramembrane space (between the mother cell and forespore) and cleaves SpoIVFA. This cleavage relieves the BofA-mediated inhibition of SpoIVFB. SpoIVFB then executes regulated intramembrane proteolysis (RIP) of pro- σ^K into active σ^K, which is released into the mother cell. (It is believed that after cleavage of FA by SpoIVB, another protease, CtpB, cleaves FA and BofA). Modified with permission from [26].

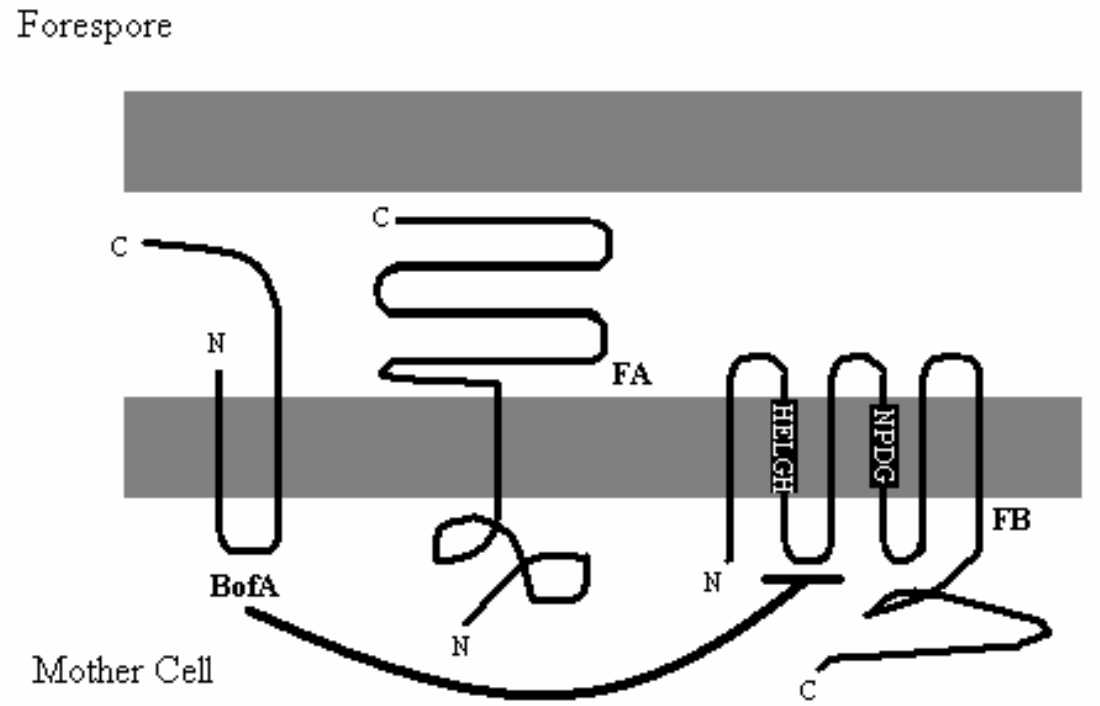

Figure 6. The BofA/SpoIVFA/FB Complex
While in a complex localized by SpoIVFA, BofA inhibits the zinc metalloprotease, SpoIVFB. A member of the S2P family, SpoIVFB has two conserved, transmembrane domains. The HExxH motif is conserved throughout zinc metalloproteases. Here, HELGH and NPDG are active-site domains and are responsible for the regulated intramembrane proteolysis of σ^K by SpoIVFB. (Not shown: pro- σ^K is also tethered in the outer forespore membrane).

H. References

1. Londono-Vallejo, J. A., Frehel, C., and Stragier, P. (1997) SpoIIQ, a forespore-expressed gene required for engulfment in *Bacillus subtilis*. *Mol. Microbiol.* **24,** 29-39.

2. Oke, V., Shchepetov, M., and Cutting, S. (1997) SpoIVB has two distinct functions during spore formation in *Bacillus subtilis*. *Mol. Microbiol.* **23,** 223-230.

3. Youngman, P., Perkins, J. B., and Losick, R. (1984) A novel method for the rapid cloning in *Escherichia coli* of *Bacillus subtilis* chromosomal DNA adjacent to Tn917 insertions. *Mol. Gen. Genet* **195,** 424-433.

4. Sterlini, J. M., and Mandelstam, J. (1969) Commitment to sporulation in *Bacillus subtilis* and its relationship to development of actinomycin resistance. *Biochem. J.* **113,** 29-37.

5. Miller, J. H. (1972) *Experiments in Molecular Genetics*. Cold Spring Harbor, New York, Cold Spring Harbor Laboratory Press.

6. Pogliano, K., Hofmeister, A. E., and Losick, R. (1997) Disappearance of the sigma E transcription factor from the forespore and the SpoIIE phosphatase from the mother cell contributes to establishment of cell-specific gene expression during sporulation in *Bacillus subtilis*. *J. Bacteriol.* **179,** 3331-3341.

7. Blaylock, B., Jiang, X., Rubio, A., Moran, C. P., Jr., and Pogliano, K. (2004) Zipper-like interaction between proteins in adjacent daughter cells mediates protein localization. *Genes Dev.* **18,** 2916-2928.

8. Perez, A. R., Abanes-De Mello, A., and Pogliano, K. (2000) SpoIIB localizes to active sites of septal biogenesis and spatially regulates septal thinning during engulfment in *Bacillus subtilis*. *J. Bacteriol.* **182,** 1096-1108.

9. Mascher, T. (2006) Intramembrane-sensing histidine kinases: a new family of cell envelope stress sensors in *Firmicutes* bacteria. *FEMS Microbiol. Lett* **264,** 133-144.

10. Murata, N., and Suzuki, I. (2006) Exploitation of genomic sequences in a systematic analysis to access how cyanobacteria sense environmental stress. *J Exp Bot.* **57,** 235-47.

11. Stock, A. M., Robinson, and V. L., Goudreau, P. N. (2000) Two-component signal transduction. *Annu Rev Biochem*. **69,** 183-215.

12. Aguilar, P.S., Hernandez-Arriaga, A. M., Cybulski, L.E., Erazo, A. C., and de Mendoza, D. (2001) Molecular basis of thermosensing: a two-component signal transduction thermometer in *Bacillus subtilis*. *EMBO J.* **20,** 1681-1691.

13. Fux, C. A., Costerton, J. W., Stewart, P. S., and Stoodley, P. (2005) Survival strategies of infectious biofilms. *Trends Microbiol.* **13,** 34-40.

14. Stewart, P. S., Roe, F., Rayner, J., Elkins, J. G., Lewandowski, Z., Ochsner, U. A., and Hassett, D. J. (2000) Effect of catalase on hydrogen peroxide penetration into *Pseudomonas aeruginosa* biofilms. *Appl Environ Microbiol.* **66,** 836-838.

15. Bagge, N., Hentzer, M., Andersen, J. B., Ciofu, O., Givskov, M., and Hoiby, N. (2004) Dynamics and spatial distribution of beta-lactamase expression in *Pseudomonas aeruginosa* biofilms. *Antimicrob Agents Chemother.* **48,** 1168-1174.

16. Rayner, M. G., Zhang, Y., Gorry, M. C., Chen, Y., Post, J. C., and Ehrlich, G. D. (1998) Evidence of bacterial metabolic activity in culture-negative otitis media with effusion. *JAMA* **279,** 296-299.

17. Sonenshein, A. L. (2000) Control of sporulation initiation in *Bacillus subtilis*. *Curr Opin Microbiol.* **3,** 561-566.

18. Stephenson, K., and Hoch, J. A. (2002) Evolution of signalling in the sporulation phosphorelay. *Mol. Microbiol.* **46,** 297-304.

19. Gonzalez-Pastor, J. E., Hobbs, E. C., and Losick, R. (2003) Cannibalism by sporulating bacteria. *Science* **301,** 510-513.

20. Errington, J. (2003) Regulation of endospore formation in *Bacillus subtilis*. *Nat Rev Microbiol.* **1,** 117-126.

21. Lopez, J. M., Marks, C. L., and Freese, E. (1979) The decrease of guanine nucleotides initiates sporulation of *Bacillus subtilis*. *Biochim Biophys Acta* **587,** 238-252.

22. Slack, F. J., Serror, P., Joyce, E., and Sonenshein, A. L. (1995) A gene required for nutritional repression of the *Bacillus subtilis* dipeptide permease operon. *Mol. Microbiol.* **15,** 689-702.

23. Serror, P., and Sonenshein, A. L. (1996) Interaction of CodY, a novel *Bacillus subtilis* DNA-binding protein, with the dpp promoter region. *Mol. Microbiol.* **20,** 843-852.

24. Jiang, M., Shao, W., Perego, M., and Hoch, J. A. (2000) Multiple histidine kinases regulate entry into stationary phase and sporulation in *Bacillus subtilis*. *Mol. Microbiol.* **38,** 535-542.

25. Fawcett, P., Eichenberger, P., Losick, R., and Youngman, P. (2000) The transcriptional profile of early to middle sporulation in *Bacillus subtilis*. *Proc. Natl Acad. Sci.* **97,** 8063-8068.

26. Core, L., and Perego, M. (2003) TPR-mediated interaction of RapC with ComA inhibits response regulator-DNA binding for competence development in *Bacillus subtilis*. *Mol. Microbiol.* **49,** 1509-1522.

27. Perego, M., Hanstein, C. G., Welsh, K. M., Djavakhishvili, T., Glaser, P., and Hoch, J. A. (1994) Multiple protein-aspartate phosphatases provide a mechanism for the integration of diverse signals in the control of development in *B. subtilis*. *Cell* **79,** 1047-1055.

28. Liu, N. J., Dutton, R. J., and Pogliano, K. (2006) Evidence that the SpoIIIE DNA translocase participates in membrane fusion during cytokinesis and engulfment. *Mol. Microbiol.* **59,** 1097-1113.

29. Aung, S., Shum, J., Abanes-De Mello, A., Broder, D. H., Fredlund-Gutierrez, J., Chiba, S., and Pogliano, K. (2007) Dual localization pathways for the engulfment proteins during *Bacillus subtilis* sporulation. *Mol. Microbiol.* **65,** 1534-1546.

30. Abanes-De Mello, A., Sun, Y. L., Aung, S., and Pogliano, K. (2002) A cytoskeleton-like role for the bacterial cell wall during engulfment of the *Bacillus subtilis* forespore. *Genes Dev.* **16,** 3253-3264.

31. Broder, D. H., and Pogliano, K. (2006) Forespore engulfment mediated by a ratchet-like mechanism. *Cell* **126,** 917-928.

32. Lee, K. S., Bumbaca, D., Kosman, J., Setlow, P., and Jedrzejas, M. J. (2008) Structure of a protein-DNA complex essential for DNA protection in spores of *Bacillus* species. *Proc Natl Acad Sci USA* **105,** 2806-2811.

33. Setlow, P. (2006) Spores of *Bacillus subtilis*: their resistance to and killing by radiation, heat, and chemicals. *J Appl Microbiol* **101,** 514-525.

34. Setlow, P. (2007) I will survive: DNA protection in bacterial spores. *Trends Microbiol* **15,** 172-180.

35. Nicholson, W. L., Schuerger, A. C., Setlow, P. (2005) The solar UV environment and bacterial spore UV resistance: Considerations for Earth-to-Mars transport by natural processes and human spaceflight. *Mutat Res* **571,** 249-264.

36. Nicholson, W. L., Munakata, N., Horneck, G, Melosh, H. J., and Setlow, P. (2000) Resistance of bacterial endospores to extreme terrestrial and extraterrestrial environments. *Microbiol. Mol. Biol. Rev.* **64,** 548-572.

37. Moeller, R., Setlow, P., Horneck, G., Berger, T., Reitz, G., Rettberg, P., Doherty, A. J., Okayasu, R., and Nicholson, W. L. (2008) Roles of the major, small, acid-soluble spore proteins and spore-specific and universal DNA repair mechanisms in resistance of *Bacillus subtilis* spores to ionizing radiation from X rays and high-energy charged-particle bombardment. *J. Bacteriol.* **190,** 1134-1140.

38. Lee, J. K., Movahedi, S., Harding, S. E., Mackey, B. M., and Waites, W. M. (2007) Effect of small, acid-soluble proteins on spore resistance and germination under a combination of pressure and heat treatment. *J. Food Prot.* **70,** 2168-2171.

39. Moeller, R., Douki, T., Cadet, J., Stackebrandt, E., Nichohlson, W. L., Rettberg, P., Reitz, G., and Horneck, G. (2007) UV-radiation-induced formation of DNA bipyrimidine photoproducts in *Bacillus subtilis* endospores and their repair during germination. *Int Microbiol.* **10,** 39-46.

40. Setlow, B., Atluri, S., Kitchel, R., Koziol-Dube, K., and Setlow, P. (2006) Role of dipicolonic acid in resistance and stability of spores of *Bacillus subtilis* with or without DNA-protective alpha/beta-type small acid-soluble proteins. *J. Bacteriol.* **188,** 3740-3747.

41. Jiang, X., Rubio, A., Chiba, S., and Pogliano, K. (2005) Engulfment-related proteolysis of SpoIIQ: evidence that dual checkpoints control σ^K activity. *Mol. Microbiol.* **58,** 102-115.

42. Takamatsu, H., and Watabe, K. (2002) Assembly and genetics of spore protective structures. *Cell Mol. Life Sci.* **59,** 434-444.

43. Henriques, A. O., and Moran, C. P., Jr. (2000) Structure and assembly of the bacterial endospore coat. *Methods*. **20,** 95-110.

44. Driks, A. (2002) Maximum shields: the assembly and function of the bacterial spore coat. *Trends Microbiol.* **10,** 251-254.

45. Kazakov, S., Bonvouloir, E., and Gzaryan, I. (2008) Physicochemical Characterization of Natural Ionic Microreservoirs: *Bacillus subtilis* Dormant Spores. *J. Phys. Chem B.* **112,** 2233-2244.

46. Waller, L. N., Fox, N., Fox, K. F., Fox, A., and Price, R. L. (2004) Ruthenium red staining for ultrastructural visualization of a glycoprotein layer surrounding the spore of *Bacillus anthracis* and *Bacillus subtilis*. *J. Microbiol. Methods* **58,** 23-30.

47. Cano, R. J., and Borucki, M. K. (1995) Revival and identification of bacterial spores in 25- to 40-million-year-old Dominican amber. *Science* **268,** 1060-1064.

48. Ronimus, R. S., Rueckert, A., and Morgan, H. W. (2006) Survival of thermophilic spore-forming bacteria in a 90+ year old milk powder from Ernest Shackelton's Cape Royds Hut in Antarctica. *J. Dairy Res.* **73,** 235-243.

49. Moir, A. Corfe, B. M., and Behravan, J. (2002) Spore germination. *Cell Mol. Life Sci.* **59,** 403-409.

50. Moir, A. (2003) Bacterial spore germination and protein mobility. *Trends Microbiol* **11,** 452-454.

51. Setlow, P. (2003) Spore germination. *Curr Opin Microbiol.* **6,** 550-556.

52. Atrih, A., Zollner, P., Allmaier, G., Williamson, M. P., and Foster, S. J. (1998) Peptidoglycan structural dynamics during germination of *Bacillus subtilis* 168 endospores. *J. Bacteriol.* **180,** 4603-4612.

53. Garrick-Silversmith, L., and Torriani, A. (1973) Macromolecular syntheses during germination and outgrowth of *Bacillus subtilis* spores. *J. Bacteriol.* **114,** 507-516.

54. Santo, L. Y., and Doi, R. H. (1974) Ultrastructural analysis during germination and outgrowth of *Bacillus subtilis* spores. *J. Bacteriol.* **120,** 475-481.

55. Clarkson, J., Campbell, I. D., and Yudkin, M. D. (2004) Physical evidence for the induced release of the *Bacillus subtilis* transcription factor, sigma(F), from its inhibitory complex. *J. Mol. Biol.* **340,** 203-209.

56. Duncan, L., Alper, S., and Losick, R. (1996) SpoIIAA governs the release of the cell-type specific transcription factor sigma F from its anti-sigma factor SpoIIAB. *J. Mol. Biol.* **260,** 147-164.

57. Wang, S. T., Setlow, B., Conlon, E. M., Lyon, J. L., Imamura, D., Sato, T., Setlow, P., Losick, R., and Eichenberger, P. (2006) The forespore line of gene expression in *Bacillus subtilis*. *J. Mol. Biol.* **358,** 16-37.

58. Fujita, M., and Losick, R. (2003) The master regulator for entry into sporulation in *Bacillus subtilis* becomes a cell-specific transcription factor after asymmetric division. *Genes Dev.* **17,** 1166-1174.

59. Silvaggi, J. M., Popham, D. L., Driks, A., Eichenberger, P., and Losick, R. (2004) Unmasking novel sporulation genes in *Bacillus subtilis*. *J. Bacteriol.* **186,** 8089-8095.

60. Eichenberger, P., Jensen, S. T., Conlon, E. M., van Ooij, C., Silvaggi, J., Gonzalez-Pastor, J. E., Fujita, M., Ben-Yehuda, S., Stragier, P., Liu, J. S., and Losick, R. (2003) The sigmaE regulon and the identification of additional sporulation genes in *Bacillus subtilis*. *J. Mol. Biol.* **327,** 945-972.

61. Eichenberger, P., Fujita, M., Jensen, S. T., Conlon, E. M., Rudner, D. Z., Wang, S. T., Ferguson, C., Haga, K., Sato, T., Liu, J. S., and Losick, R. (2004) The program of gene transcription for a single differentiating cell type during sporulation in *Bacillus subtilis*. *PLoS Biol.* **2,** e328.

62. Evans, L., Clarkson, J., Yudkin, M. D., Errington, J., and Feucht, A. (2003) Analysis of the interaction between the transcription factor sigmaG and the anti-sigma factor SpoIIAB of *Bacillus subtilis*. *J. Bacteriol.* **185,** 4615-4619.

63. Serrano, M., Neves, A., Soares, C. M., Moran, C. P., Jr., and Henriques, A. O. (2004) Role of the anti-sigma factor SpoIIAB in regulation of sigmaG during *Bacillus subtilis* sporulation. *J. Bacteriol.* **186,** 4000-4013.

64. Chastanet, A., and Losick, R. (2007) Engulfment during sporulation in *Bacillus subtilis* is governed by a multi-protein complex containing tandemly acting autolysins. *Mol. Microbiol.* **64,** 139-152.

65. Hilbert, D. W., and Piggot, P. J. (2004) Compartmentalization of gene expression during *Bacillus subtilis* spore formation. *Microbiol. Mol. Biol. Rev.* **68,** 234-262.

66. Serrano, M., Corte, L., Opdyke, J., Moran, C. P., Jr., and Henriques, A. O. (2003) Expression of SpoIIIJ in the prespore is sufficient for activation of σ^G and for sporulation in *Bacillus subtilis*. *J. Bacteriol.* **185,** 3905-3917.

67. Kellner, E. M., Decatur, A., and Moran, C. P., Jr. (1996) Two-stage regulation of an anti-σ factor determines developmental fate during bacterial endospore formation. *Mol. Microbiol.* **21,** 913-924.

68. Fujita, M., and Losick, R. (2002) An investigation into the compartmentalization of the sporulation transcription factor sigmaE in *Bacillus subtilis*. *Mol. Microbiol.* **43,** 27-38.

69. Prince, H., Zhou, R., and Kroos, L. (2005) Substrate requirements for regulated intramembrane proteolysis of *Bacillus subtilis* pro-sigmaK. *J. Bacteriol.* **187,** 961-971.

70. Zhang, B., Hofmeister, A., and Kroos, L. (1998) The prosequence of pro-sigmaK promotes membrane association and inhibits RNA polymerase core binding. *J. Bacteriol.* **180,** 2434-2441.

71. Rudner, D. Z., and Losick, R. (2002) A sporulation membrane protein tethers the pro-sigmaK processing enzyme to its inhibitor and dictates its subcellular localization. *Genes Dev* **16,** 1007-1018.

72. Zhou, R., and Kroos, L. (2004) BofA protein inhibits intramembrane proteolysis of pro-sigmaK in an intercompartmental signaling pathway during *Bacillus subtilis* sporulation. *Proc. Natl. Acad. Sci. USA* **101,** 6385-6390.

73. Campo, N, and Rudner, D. Z. (2007) SpoIVB and CtpB are both forespore signals in the activation of the sporulation transcription factor sigmaK in *Bacillus subtilis*. *J Bacteriol.* **189,** 6021-6027.

74. Hoa, N. T., Brannigan, J. A., and Cutting, S. M. (2002) The *Bacillus subtilis* signaling protein SpoIVB defines a new family of serine peptidases. *J. Bacteriol.* **184,** 191-199.

75. Wakeley, P. R., Dorazi, R., Hoa, N. T., Bowyer, J. R., and Cutting, S. M. (2000) Proteolysis of SpoIVB is a critical determinant in signaling of Pro-sigmaK processing in *Bacillus subtilis*. *Mol. Microbiol.* **36,** 1336-1348.

76. Zhou, R., and Kroos, L. (2005) Serine proteases from two cell types target different components of a complex that governs regulated intramembrane proteolysis of pro-sigmaK during *Bacillus subtilis* development. *Mol. Microbiol.* **58,** 835-846.

77. Campo, N., and Rudner, D. Z. (2006) A branched pathway governing the activation of a developmental transcription factor by regulated intramembrane proteolysis. *Mol Cell* **23,** 25-35.

78. Makinoshima, H., and Glickman, M. S. (2006) Site-2 proteases in prokaryotes: regulated intramembrane proteolysis expands to microbial pathogenesis. *Microbes Infect.* **8,** 1882-1888.

79. Yu, Y. T., and Kroos, L. (2000) Evidence that SpoIVFB is a novel type of membrane metalloprotease governing intercompartmental communication during *Bacillus subtilis* sporulation. *J. Bacteriol.* **182,** 3305-3309.

80. Rudner, D. Z., Fawcett, P., and Losick, R. (1999) A family of membrane-embedded metalloproteases involved in regulated proteolysis of membrane-associated transcription factors. *Proc Natl Acad Sci USA* **96,** 14765-14770.

81. Ricca, E., Cutting, S., and Losick, R. (1992) Characterization of *bofA*, a gene involved in intercompartmental regulation of pro-sigma K processing during sporulation in *Bacillus subtilis*. *J. Bacteriol.* **174,** 3177-3184.

82. Cutting, S., Oke, V., Driks, A., Losick, R., Lu, S., and Kroos, L. (1990) A forespore checkpoint for mother cell gene expression during development in *B. subtilis*. *Cell* **62,** 239-250.

83. Chary, V. K., Xenopoulos, P., and Piggot, P. J. (2007) Expression of the sigmaF-directed *csfB* locus prevents premature appearance of sigmaG activity during sporulation of *Bacillus subtilis*. *J. Bacteriol.* **189,** 8754-8757.

84. Brown, M. S., Ye, J., Rawson, R. B., and Goldstein, J. L. (2000) Regulated intramembrane proteolysis: a control mechanism conserved from bacteria to humans. *Cell* **100,** 391-398..

85. Lee, K., Tirasophon, W., Shen, X., Michalak, M., Prywes, R., Okada, T., Yoshida, H., Mori, K., and Kaufman, R. J. (2002) IRE1-mediated unconventional mRNA splicing and S2P-mediated ATF6 cleavage merge to regulate XPB1 in signaling the unfolded protein response. *Genes Dev.* **16,** 452-466.

86. Chen, J. C., Viollier, P. H., and Shapiro, L. (2005) A membrane metalloprotease participates in the sequential degradation of a *Caulobacter* polarity determinant. *Mol. Microbiol.* **55,** 1085-1103.

87. Doan, T., Marquis, K. A., and Rudner, D. Z. (2005) Subcellular localization of a sporulation membrane protein is achieved through a network of interactions along and across the septum. *Mol Microbiol.* **55,** 1767-1781.

88. Doan, T., and Rudner, D. Z. (2007) Perturbations to engulfment trigger a degradative response that prevents cell-cell signaling during sporulation in *Bacillus subtilis*. *Mol. Microbiol.* **64,** 500-511.

CHAPTER II

Impact of membrane fusion and proteolysis on SpoIIQ dynamics and interaction with SpoIIIAH

THE JOURNAL OF BIOLOGICAL CHEMISTRY VOL. 282, NO. 4, pp. 2576–2586, January 26, 2007

Impact of Membrane Fusion and Proteolysis on SpoIIQ Dynamics and Interaction with SpoIIIAH*[S]

Received for publication, June 23, 2006, and in revised form, October 10, 2006 Published, JBC Papers in Press, November 22, 2006, DOI 10.1074/jbc.M606056200

Shinobu Chiba[1], **Kristina Coleman, and Kit Pogliano**[2]

From the Division of Biological Sciences, University of California San Diego, La Jolla, California 92093-0377

The onset of engulfment-dependent gene expression during *Bacillus subtilis* sporulation requires the forespore membrane protein SpoIIQ, which recruits mother cell proteins involved in late gene expression to the outer forespore membrane. Engulfment activates the late forespore transcription factor σ^G, which produces high levels of the secreted SpoIVB protease that is required for activation of the late mother cell transcription factor σ^K. Engulfment also triggers the proteolytic cleavage of SpoIIQ, an event that depends on the SpoIVB protease but not on σ^G activity. To determine if SpoIVB directly cleaves SpoIIQ and to determine if this event participates in the onset of late gene expression, we purified SpoIVB, SpoIIQ, and SpoIVFA (another SpoIVB substrate). SpoIVB directly cleaved SpoIIQ at the same site *in vitro* and *in vivo* and cleaved SpoIVFA in at least three different locations. SpoIIQ cleavage depends on membrane fusion, but not on σ^G activity, suggesting that the ability of SpoIVB to cleave substrates is regulated by membrane fusion. We isolated SpoIVB-resistant SpoIIQ proteins by random mutagenesis of codons at the cleavage site and demonstrated that SpoIIQ processing is dispensable for spore formation and for activation of late forespore and mother cell gene expression. Fluorescence recovery after photobleaching analysis demonstrated that membrane fusion releases SpoIIQ from an immobile complex, an event that could allow SpoIVB to cleave SpoIIQ. We propose that this membrane fusion-dependent reorganization in the complex, rather than SpoIIQ proteolysis itself, is necessary for the onset of late transcription.

Endospore formation in *Bacillus subtilis* and its relatives depends on engulfment, a phagocytosis-like process that mediates a dramatic rearrangement of the sporangium from two adjacent daughter cells, to an endospore in which the forespore lies within the cytoplasm of the larger mother cell (see Fig. 1; reviewed by Refs. 1 and 2). Engulfment is critical for sporulation, because it allows spore assembly to occur in a protected environment. It also serves as a morphological checkpoint for activation of the late forespore and mother cell transcription factors σ^G and σ^K, respectively (reviewed by Refs. 1–4). The endospore-forming bacteria must therefore have some mechanism to sense the completion of engulfment and to couple this morphological event to the onset of late gene expression.

The forespore transcription factor σ^G is the first to become active after engulfment, but it remains unclear how σ^G is held inactive during engulfment or activated after engulfment. More is known about the regulation of the second late transcription factor, σ^K, which becomes active in the mother cell (summarized in Fig. 1*B* and reviewed by Refs. 1–4). The σ^K factor is initially synthesized as an inactive pro-protein containing a hydrophobic leader sequence, which functions as a covalently attached anti-sigma factor (5). This leader sequence is removed by the intramembrane protease SpoIVFB, which cleaves pro-σ^K within the membrane to release active σ^K (6–8). This processing event shares many characteristics with Regulated Intramembrane Proteolysis (RIP),[3] a widespread signal transduction mechanism in which extracellular signals are transduced to a protease that cleaves its substrate within the plane of the membrane to release an active transcription factor (reviewed by Refs. 9 and 10). As is typical of RIP systems, the intramembrane protease SpoIVFB is inactive until it receives an extracellular signal. In the case of SpoIVFB, the signal is the prior activation of the late forespore-specific transcription factor σ^G (11), which produces higher levels of the SpoIVB protease (12). This protease disrupts an inhibitory complex between the SpoIVFB intramembrane protease and two other proteins, SpoIVFA, which is necessary for complex assembly and localization (13), and BofA, which inhibits SpoIVFB activity (Fig. 1*B*) (7, 11, 13). BofA is likely the main inhibitor of the SpoIVFB intramembrane protease, because it can inhibit SpoIVFB activity in an ectopic expression system (7), and because its genetic inactivation allows σ^K to become active in the absence of σ^G activity and in the absence of the SpoIVB signal transduction protease (11). The SpoIVB protease cleaves SpoIVFA and relieves BofA-mediated inhibition of SpoIVFB (12, 14–16). This pathway results in the indirect coupling of σ^K activity to

* This work was supported in part by National Institutes of Health Grant GM 57045. The costs of publication of this article were defrayed in part by the payment of page charges. This article must therefore be hereby marked "*advertisement*" in accordance with 18 U.S.C. Section 1734 solely to indicate this fact.

[S] The on-line version of this article (available at http://www.jbc.org) contains supplemental Figs. S1–S3 and Tables S1 and S2.

[1] Supported by a Japan Society for the Promotion of Science Research Fellowship for Young Scientists.

[2] To whom correspondence should be addressed: Division of Biological Sciences, University of California San Diego, 9500 Gilman Drive, La Jolla, CA 92093-0377. Tel.: 858-822-1314; Fax: 858-822-1431; E-mail: kpogliano@ucsd.edu.

[3] The abbreviations used are: RIP, regulated intramembrane proteolysis; FRAP, fluorescence recovery after photobleaching; PBS, phosphate buffered saline; GFP, green fluorescent protein; AMS, 4-acetamido-4′-maleimidylstilbene-2;2′-disulfonic acid; KLH, Keyhole limpet hemocyanin; GST, glutathione *S*-transferase; BSA, bovine serum albumin; t_0, t_1, t_2 . . . , time of sporulation, with the number indicating hours after the initiation of sporulation by resuspension; FM, forespore membrane; OFM, outer forespore membrane.

engulfment, by virtue of its dependence on the prior activation of σ^G.

Recent evidence suggests that activation of σ^K is also directly coupled to the completion of engulfment in two distinct manners (17). First, although the genetic elimination of BofA allows σ^K to become active in the absence of σ^G and SpoIVB, it does not allow σ^K activity in engulfment defective mutants (11, 17). Thus, the failure of these mutants to activate σ^G is not the only reason for the failure to activate σ^K. This suggests that σ^K activation is directly governed by engulfment via a pathway that does not depend on BofA, the known inhibitor of SpoIVFB intramembrane protease activity. We therefore previously proposed the existence of two distinct checkpoints for σ^K activity (17): the previously described forespore checkpoint that couples σ^K activity to σ^G activity via the BofA inhibitor (11) and the engulfment checkpoint that couples σ^K activity to the completion of engulfment via a BofA-independent mechanism (Fig. 1*B*) (17). Second, engulfment also appears likely to govern the activity of the SpoIVB protease that participates in the forespore checkpoint. This was first suggested by the observation that SpoIVB is synthesized both before engulfment by the early forespore transcription factor σ^F and after engulfment by the late forespore transcription factor σ^G (18). Additional support for the regulation of SpoIVB protease activity came from observations that the forespore membrane protein SpoIIQ is subject to a proteolytic processing event that depends on both engulfment and on the SpoIVB protease (17, 19). However, SpoIIQ processing occurs with apparently identical kinetics in wild-type strain or in a strain with a mutation in the gene encoding σ^G (*spoIIIG*). Thus, if SpoIVB directly cleaves SpoIIQ then its activity or access to substrates must be regulated by engulfment.

SpoIIQ proteolysis could be involved in engulfment-dependent gene expression, because this forespore membrane protein plays several key roles in this stage of sporulation. First, SpoIIQ is essential for the engulfment-dependent activation of σ^G (20, 21), although its precise role in this process remains unclear. Second, SpoIIQ participates in engulfment, providing a secondary mechanism that is necessary for membrane migration when the activity of the primary engulfment machinery is compromised (22). This secondary engulfment mechanism requires the interaction between the extracellular domains of SpoIIQ and that of the mother cell membrane protein SpoIIIAH (Fig. 1*B*) (22, 23). This interaction can readily be detected by several biochemical methods such as co-immunoprecipitation (23), affinity chromatography (23, 24), and sucrose density gradient analysis (Fig. 5). Third, SpoIIQ is required for the localization of mother cell membrane proteins needed for both σ^G and σ^K activation to the outer forespore membrane that is the site of intracellular signal transduction (17, 23, 24). Specifically, the interaction between SpoIIQ and SpoIIIAH prevents SpoIIIAH from diffusing away from the outer forespore membrane (23, 24), where it is required for σ^G activity. SpoIIIAH and SpoIIQ together are needed to localize the σ^K-processing machinery, SpoIVFA and SpoIVFB, to the outer forespore membrane, although it is unclear if SpoIIQ or SpoIIIAH directly interact with SpoIVFA or SpoIVFB (17, 24). Interestingly, SpoIIQ, SpoIIIAH, and SpoIVFB all localize to foci surrounding the forespore (Fig. 4*B*) (17, 19, 23). These foci might represent synapse-like sites for intracellular signal transduction, perhaps allowing transcription in both cells to be coordinately regulated by engulfment. It remains unclear how the completion of engulfment is sensed, and if SpoIIQ serves only as a scaffold to localize these signal transduction proteins or if it also participates in signal transduction.

SpoIIQ proteolysis could affect its interaction with proteins involved in σ^G and σ^K activation, and therefore provides a potential mechanism by which late transcription might be coupled to engulfment. To determine if this is the case, and to determine if SpoIVB directly cleaves SpoIIQ, we further characterized SpoIIQ proteolysis. Specifically, we demonstrated that purified SpoIVB directly cleaves SpoIIQ, mapped the sites at which SpoIIQ is cleaved *in vivo* and *in vitro*, and isolated protease-resistant mutants. These mutants had no effect on σ^G or σ^K activity or spore formation, demonstrating that SpoIIQ processing is dispensable for sporulation. SpoIIQ proteolysis requires the membrane fusion event that is the final step of engulfment. Finally, fluorescence recovery after photobleaching (FRAP) demonstrates that the mobility of SpoIIQ dramatically increases after membrane fusion (in the absence of proteolysis), indicating that SpoIIQ is released from an essentially immobile complex after fusion. This reorganization in the SpoIIQ complex might control both proteolysis and signal transduction.

EXPERIMENTAL PROCEDURES

Strain and Plasmid Construction—B. subtilis strains (Table 1) were constructed by transformation (25). Plasmids (supplemental Table S1) were constructed by standard cloning methods and site-directed mutagenesis (26). Following introduction into the *B. subtilis* chromosome, recombinants were checked for their antibiotic resistance, the inactivation of *amyE*, and the loss of any additional drug resistance markers on the plasmid backbone. Primers used for plasmid construction are in supplemental Table S2. Plasmid pCH507 (*amyE*::P_{spoIIQ}*gfp*(Δ2–6)-*spoIIQ*Ω*cat*) was constructed by deleting the five codons that are derived from the *spoIIQ* gene and redundantly exist at the 5′ region of gfp on pAR47 (*amyE*::P_{spoIIQ}*gfp-spoIIQ*Ω*cat* (19)) by site-directed mutagenesis (26) using a primer, SP1. Plasmids encoding either *spoIIQ*, *gfp-spoIIQ*, or *gst-spoIIQ* derivatives were constructed by site-directed mutagenesis using either pCH505 (*amyE*::P_{spoIIQ}*spoIIQ*), pCH507 (*amyE*::P_{spoIIQ}*gfp*(Δ2–6)-*spoIIQ*), or pGEX-SpoIIQ (*gst-spoIIQ*$^{43–283}$ (23)) as the template. Primer SP2 was used for pCH510 (*amyE*::P_{spoIIQ}*spoIIQ-his*$_6$Ω*cat*). The plasmids encoding *spoIIQ* cleavage site mutants (V72, G73, or K74) were constructed by using either SP3, SP4, or SP5 (respectively), which had a random mixture of bases in the target codon. pCH550 (*spoIIQ*$^{1–72}$) was also isolated by this random mutagenesis. The DNA sequence of the resulting products was confirmed prior to transformation into *B. subtilis*. Plasmids encoding mono-Cys mutants of *spoIIQ* were constructed by site-directed mutagenesis using the template plasmid pCH505 (*spoIIQ*) and primers either SP10 (pCH528; A62C), SP11 (pCH530; D64C), SP12 (pCH531; D68C), SP13 (pCH532; V70C), SP14 (pCH533; E71C), SP15 (pCH534; V72C), SP16 (pCH535; G73C), or SP17 (pCH536; K74C), respectively.

TABLE 1
B. subtilis strains and plasmids used in this study

Strain	Genotype	Source
PY79	Wild type	(39)
KP575	Δ*spoIIQ::spc*	(21)
KP701	*sspB-lacZΩcat::tet*	This study
KP856	*spoIIIAH-flagΩcat*	(23)
KP857	*spoIIIAH-flagΩcat*, Δ*spoIIQ::spc*	(23)
KP953	Δ*spoIIQ::spc*, *thrC::cotD-lacZΩmls*	(17)
KP6012	*amyE::spoIIIE-gfpΩcat*, Δ*spoIIIE::spc*	(33)
KP6111	*amyE::spoIIIE124::i31-gfpΩcat*, Δ*spoIIIE::spc*	(33)
AR232	Δ*spoIIQ::spc*, *sspB-lacZΩcat::tet*	This study
XJ220	*thrC::cotD-lacZΩmls*	This study
XJ401	Δ*spoIIIAH*, *trpC2*	This study
XJ412	*spoIIQ-flagΩcat*	This study
SCB3	Δ*spoIIQ::spc*, *amyEΩcat*	This study
SCB4	Δ*spoIIQ::spc*, *amyE::P*$_{spoIIQ}$*spoIIQΩcat*	This study
SCB6	Δ*spoIIQ::spc*, *amyE::P*$_{spoIIQ}$*gfp*(Δ2–6)-*spoIIQΩcat*	This study
SCB9	Δ*spoIIQ::spc*, *amyE::P*$_{spoIIQ}$*spoIIQ-his*$_6$*Ωcat*	(17)
SCB15	Δ*spoIIQ::spc*, *spoIIIGΔ1*, *spoIIIG-lacZΩcat::erm*, *amyE::P*$_{spoIIQ}$*spoIIQΩcat*	This study
SCB18	Δ*spoIIQ::spc*, *sspB-lacZΩcat::tet*, *amyE::P*$_{spoIIQ}$*spoIIQΩcat*	This study
SCB21	Δ*spoIIQ::spc*, *thrC::cotD-lacZΩmls*, *amyE::P*$_{spoIIQ}$*spoIIQΩcat*	This study
SCB43	Δ*spoIIQ::spc*, *amyE::P*$_{spoIIQ}$*spoIIQA62CΩcat*	This study
SCB45	Δ*spoIIQ::spc*, *amyE::P*$_{spoIIQ}$*spoIIQD64CΩcat*	This study
SCB46	Δ*spoIIQ::spc*, *amyE::P*$_{spoIIQ}$*spoIIQD68CΩcat*	This study
SCB47	Δ*spoIIQ::spc*, *amyE::P*$_{spoIIQ}$*spoIIQV70CΩcat*	This study
SCB48	Δ*spoIIQ::spc*, *amyE::P*$_{spoIIQ}$*spoIIQE71CΩcat*	This study
SCB49	Δ*spoIIQ::spc*, *amyE::P*$_{spoIIQ}$*spoIIQV72CΩcat*	This study
SCB50	Δ*spoIIQ::spc*, *amyE::P*$_{spoIIQ}$*spoIIQG73CΩcat*	This study
SCB51	Δ*spoIIQ::spc*, *amyE::P*$_{spoIIQ}$*spoIIQK74CΩcat*	This study
SCB62	Δ*spoIIQ::spc*, *amyE::P*$_{spoIIQ}$*spoIIQV72RΩcat*	This study
SCB63	Δ*spoIIQ::spc*, *amyE::P*$_{spoIIQ}$*spoIIQV72YΩcat*	This study
SCB64	Δ*spoIIQ::spc*, *amyE::P*$_{spoIIQ}$*spoIIQV72NΩcat*	This study
SCB65	Δ*spoIIQ::spc*, *amyE::P*$_{spoIIQ}$*spoIIQV72SΩcat*	This study
SCB66	Δ*spoIIQ::spc*, *amyE::P*$_{spoIIQ}$*spoIIQV72AΩcat*	This study
SCB67	Δ*spoIIQ::spc*, *amyE::P*$_{spoIIQ}$*spoIIQV72IΩcat*	This study
SCB68	Δ*spoIIQ::spc*, *amyE::P*$_{spoIIQ}$*spoIIQV72HΩcat*	This study
SCB69	Δ*spoIIQ::spc*, *amyE::P*$_{spoIIQ}$*spoIIQV72KΩcat*	This study
SCB70	Δ*spoIIQ::spc*, *amyE::P*$_{spoIIQ}$*spoIIQV72EΩcat*	This study
SCB71	Δ*spoIIQ::spc*, *amyE::P*$_{spoIIQ}$*spoIIQV72MΩcat*	This study
SCB72	Δ*spoIIQ::spc*, *amyE::P*$_{spoIIQ}$*spoIIQG73VΩcat*	This study
SCB73	Δ*spoIIQ::spc*, *amyE::P*$_{spoIIQ}$*spoIIQG73EΩcat*	This study
SCB74	Δ*spoIIQ::spc*, *amyE::P*$_{spoIIQ}$*spoIIQ1–72Ωcat*	This study
SCB75	Δ*spoIIQ::spc*, *amyE::P*$_{spoIIQ}$*spoIIQG73LΩcat*	This study
SCB76	Δ*spoIIQ::spc*, *amyE::P*$_{spoIIQ}$*spoIIQG73PΩcat*	This study
SCB77	Δ*spoIIQ::spc*, *amyE::P*$_{spoIIQ}$*spoIIQG73TΩcat*	This study
SCB78	Δ*spoIIQ::spc*, *amyE::P*$_{spoIIQ}$*spoIIQG73IΩcat*	This study
SCB79	Δ*spoIIQ::spc*, *amyE::P*$_{spoIIQ}$*spoIIQG73SΩcat*	This study
SCB80	Δ*spoIIQ::spc*, *amyE::P*$_{spoIIQ}$*spoIIQK74EΩcat*	This study
SCB81	Δ*spoIIQ::spc*, *amyE::P*$_{spoIIQ}$*spoIIQK74IΩcat*	This study
SCB83	Δ*spoIIQ::spc*, *amyE::P*$_{spoIIQ}$*spoIIQK74RΩcat*	This study
SCB84	Δ*spoIIQ::spc*, *amyE::P*$_{spoIIQ}$*spoIIQK74AΩcat*	This study
SCB85	Δ*spoIIQ::spc*, *amyE::P*$_{spoIIQ}$*spoIIQK74NΩcat*	This study
SCB86	Δ*spoIIQ::spc*, *amyE::P*$_{spoIIQ}$*spoIIQK74SΩcat*	This study
SCB87	Δ*spoIIQ::spc*, *amyE::P*$_{spoIIQ}$*spoIIQK74PΩcat*	This study
SCB88	Δ*spoIIQ::spc*, *amyE::P*$_{spoIIQ}$*spoIIQK74DΩcat*	This study
SCB89	Δ*spoIIQ::spc*, *amyE::P*$_{spoIIQ}$*spoIIQK74GΩcat*	This study
SCB108	Δ*spoIIQ::spc*, *sspB-lacZΩcat::tet*, *amyE::P*$_{spoIIQ}$*spoIIQV72CΩcat*	This study
SCB109	Δ*spoIIQ::spc*, *sspB-lacZΩcat::tet*, *amyE::P*$_{spoIIQ}$*spoIIQV72MΩcat*	This study
SCB110	Δ*spoIIQ::spc*, *sspB-lacZΩcat::tet*, *amyE::P*$_{spoIIQ}$*spoIIQG73VΩcat*	This study
SCB111	Δ*spoIIQ::spc*, *sspB-lacZΩcat::tet*, *amyE::P*$_{spoIIQ}$*spoIIQG73EΩcat*	This study
SCB114	Δ*spoIIQ::spc*, *thrC::cotD-lacZΩmls*, *amyE::P*$_{spoIIQ}$*spoIIQV72CΩcat*	This study
SCB115	Δ*spoIIQ::spc*, *thrC::cotD-lacZΩmls*, *amyE::P*$_{spoIIQ}$*spoIIQV72MΩcat*	This study
SCB116	Δ*spoIIQ::spc*, *thrC::cotD-lacZΩmls*, *amyE::P*$_{spoIIQ}$*spoIIQG73VΩcat*	This study
SCB117	Δ*spoIIQ::spc*, *thrC::cotD-lacZΩmls*, *amyE::P*$_{spoIIQ}$*spoIIQV73EΩcat*	This study
SCB138	Δ*spoIIQ::spc*, *amyE::P*$_{spoIIQ}$*gfp*(Δ2–6)-*spoIIQV72YΩcat*	This study
SCB139	Δ*spoIIQ::spc*, *amyE::P*$_{spoIIQ}$*gfp*(Δ2–6)-*spoIIQV72EΩcat*	This study
SCB223	Δ*spoIIQ::spc*, *thrC::cotD-lacZΩmls*, *amyE::Ωcat*, *bofA::cat::tet*, *spoIIIG::neo*	This study
SCB224	Δ*spoIIQ::spc*, *thrC::cotD-lacZΩmls*, *amyE::P*$_{spoIIQ}$*spoIIQ*, *bofA::cat::tet*, *spoIIIG::neo*	This study
SCB225	Δ*spoIIQ::spc*, *thrC::cotD-lacZΩmls*, *amyE::P*$_{spoIIQ}$*spoIIQV72CΩcat*, *bofA::cat::tet*, *spoIIIG::neo*	This study
SCB227	Δ*spoIIQ::spc*, *thrC::cotD-lacZΩmls*, *amyE::P*$_{spoIIQ}$*spoIIQV72MΩcat*, *bofA::cat::tet*, *spoIIIG::neo*	This study
SCB228	Δ*spoIIQ::spc*, *thrC::cotD-lacZΩmls*, *amyE::P*$_{spoIIQ}$*spoIIQG73VΩcat*, *bofA::cat::tet*, *spoIIIG::neo*	This study
SCB229	Δ*spoIIQ::spc*, *thrC::cotD-lacZΩmls*, *amyE::P*$_{spoIIQ}$*spoIIQV73EΩcat*, *bofA::cat::tet*, *spoIIIG::neo*	This study

pCH687 (*gst-spoIVFA*$^{101–264}$*-FLAG*) was constructed as follows: *spoIVFA* was amplified from PY79 chromosomal DNA using primers SP6 and SP7, digested by BamHI, and then cloned into pDG1662. A FLAG tag was introduced at the C-terminal end of *spoIVFA* by site-directed mutagenesis using SP8. A BamHI site was further introduced between the 100th and 101st codons by site-directed mutagenesis using primer SP9. A BamHI fragment encoding the C-terminal extracytoplasmic region was cloned into the same site of pGEX4T-3 (Amersham Biosciences).

Sporulation Conditions—Sporulation was induced by resuspension at 37 °C (27), with t_n being the hours after the onset of

sporulation. For small scale sporulations, the cells were resuspended in 2 ml of the sporulation media and cultured with rotating in test tubes (small scale culture for Fig. 3*A*). For larger scale sporulations, the cells were resuspended in 15 ml (for other Western blotting, β-galactosidase activity assay, and microscopy) or 200 ml (for immunopurification of SpoIIQ-FLAG derivatives in Fig. 2*B*) and shaken in flasks. Sporulation efficiency was determined as described (28). β-Galactosidase assays were performed as described (29, 30).

Co-immunoprecipitation and Western Blotting—Sporulating cells were harvested and washed with SMM buffer (0.5 M sucrose, 20 mM $MgCl_2$, and 20 mM maleic acid, pH 6.5), resuspended in the same buffer and treated with 1 mg/ml lysozyme at 37 °C for 10 min. The spheroplasts were harvested by centrifugation and resuspended in ice-cold buffer A (20 mM HEPES-NaOH, 150 mM NaCl, and 1 mM EDTA, pH 7.6) with 1 mM phenylmethylsulfonyl fluoride, 1 μg/ml leupeptin, and 1 μg/ml pepstatin and then treated with 0.5% *n*-dodecyl β-D-maltoside (Sigma) on ice for 30 min. The insoluble fraction was removed by ultracentrifugation with a Beckman TLA120-2[d] rotor (40,000 rpm, 30 min), and the supernatant was incubated with anti-FLAG M2 affinity gel (Sigma) overnight at 4 °C with gentle rolling. The affinity gel was washed twice with buffer A containing 0.5% *n*-dodecyl β-D-maltoside, and the bound proteins were eluted by SDS-loading buffer (without reducing agent) at 42 °C. Proteins in the cell lysate and in the flow-through containing unbound protein were precipitated by 5% trichloroacetic acid for 20 min on ice, washed by acetone, and then solubilized in SDS loading buffer. Proteins were analyzed by SDS-PAGE or Western blotting as described previously (17, 23). 1:5,000 dilutions of anti-SpoIIQ (17), anti-SpoIIIAH (see below), anti-GFP (Roche Applied Science), and anti-FLAG M2 antibodies (Sigma) were used to probe derivatives of SpoIIQ, GFP-SpoIIQ, and SpoIIIAH-FLAG, respectively.

Sucrose Density Gradient Ultracentrifugation—Sucrose density gradient ultracentrifugation was performed essentially as described (31), with the following modifications. Sporulating cell lysates were prepared by the same procedure as described above for co-immunoprecipitation, except that buffer B (20 mM HEPES-NaOH, 300 mM KCl, and 1 mM EDTA, pH 7.6) was used instead of buffer A. The lysates were loaded on top of 5-ml sucrose gradient beds (5–20% sucrose, 20 mM HEPES-NaOH, 300 mM KCl, and 1 mM EDTA, pH7.6). Proteins were separated by ultracentrifugation in a Beckman MLS50 rotor (4 °C, 43,000 rpm, 16 h) and collected into 17–18 fractions. Purified proteins catalase (226 kDa), adolase (146 kDa, Amersham Biosciences), bovine serum albumin (68 kDa), and lysozyme (14.3 kDa, Sigma) were used as the protein standards.

AMS Modification of Monocysteine Derivatives of SpoIIQ—For AMS treatment, whole cell proteins were solubilized in SDS-loading buffer, containing 1 mM Tris(2-carboxyethyl) phosphine instead of 2 mM dithiothreitol. The pH of the SDS-loading buffer changed by addition of Tris(2-carboxyethyl) phosphine was adjusted to pH 6.8 by adding the proper volume of 0.5 M Tris-HCl (pH 6.8). Samples were treated with 2 mM AMS (4-acetamido-4′-maleimidylstilbene-2,2′-disulfonic acid) at 37 °C for 1 h and then analyzed by Western blotting.

In Vivo Proteolysis Assay of SpoIIQ Derivatives—A whole cell trichloroacetic acid precipitation was prepared from 1 ml of culture to which trichloroacetic acid was added (to 5% final concentration). The cells were collected by centrifugation, and the pellet was washed with 0.75 ml of 1 M Tris-HCl (pH 8) and treated with 1 mg/ml lysozyme in 60 μl of buffer C (33 mM Tris-HCl, 40% sucrose, 1 mM EDTA, pH 8). Proteins were then solubilized by SDS-loading buffer with 2 mM dithiothreitol and analyzed by Western blotting.

Purification of SpoIVB, SpoIIQ, and SpoIVFA—BL21(DE3)/pZR53 (SpoIVB-His_6) was grown in LB ampicillin (100 μg/ml) media, and expression of SpoIVB-His_6 was induced by 1 mM isopropyl 1-thio-β-D-galactopyranoside for 1 h at 30 °C. Cells were washed by buffer D (20 mM Tris-HCl (pH 8.0), 150 mM NaCl) and disrupted by sonication. After removing debris by centrifugation, cell lysate was subjected to nickel affinity column (Sigma) equilibrated in buffer D. The column was washed with buffer D plus 20 mM imidazole and eluted with 300 mM imidazole in the same buffer. Eluted protein was then dialyzed in buffer D, loaded on Hi-Trap Q (Amersham Biosciences) anion-exchange chromatography column previously equilibrated in buffer D. Flow-through fractions that include SpoIVB-His_6 were collected and then loaded onto a Hi-Trap SP (Amersham Biosciences) cation-exchange chromatography column previously equilibrated in buffer D. SpoIVB-His_6 was eluted by a sodium chloride gradient (0–1 M) in buffer D.

GST-SpoIVFA and GST-SpoIIQ were expressed in BL21 (DE3). Expression was induced by the addition of 1 mM isopropyl 1-thio-β-D-galactopyranoside for 2–3 h at 37 °C. Cells were washed with phosphate-buffered saline (PBS), suspended in PBS/1 mM dithiothreitol/1 mM EDTA, and disrupted by sonication. Cell lysate was loaded on a glutathione-Sepharose column (Amersham Biosciences) previously equilibrated in PBS, washed with PBS, and eluted with 50 mM Tris-HCl (pH 8.0) containing 10 mM glutathione. GST-SpoIVFA$^{101-264}$-FLAG was dialyzed by buffer D and further purified by using a Sephacryl S-200 column (Amersham Biosciences). All proteins were dialyzed in buffer D, and concentration was determined by a Bradford protein assay (Sigma).

In Vitro Protease Assay and Amino Acid Sequence Analysis—Purified substrates (240 ng/μl) were incubated in buffer D at 37 °C in 0–4 h in the presence or absence of 30 ng/μl purified SpoIVB-His_6. The reaction was stopped with SDS-loading buffer, and the products were analyzed by SDS-PAGE and Coomassie staining. Bands were excised from polyvinylidene difluoride membrane and subjected to N-terminal sequencing.

Microscopy and Image Analysis—For GFP visualization, live cells were stained with 4′,6′-diamidino-2-phenylindole (0.2 μg/ml, Molecular Probes) and FM4-64 (5 μg/ml, Molecular Probes) as described previously (32). Images were collected with an Applied Precision Spectris microscope with a QLM laser module (described in Ref. 33). Photobleaching was performed and quantified as described (22), using a 0.02- to 0.05-s pulse of a 488 nm argon laser at 50% power. Subsequent GFP images were collected at 30-s intervals for 5 min for GFP-SpoIIQ and V72Y or as quickly as possible for smoothly localized GFP-SpoIIQV72Y. Exposure times were limited to 1.5–2.5 s. These experiments were quantified as previously described (22).

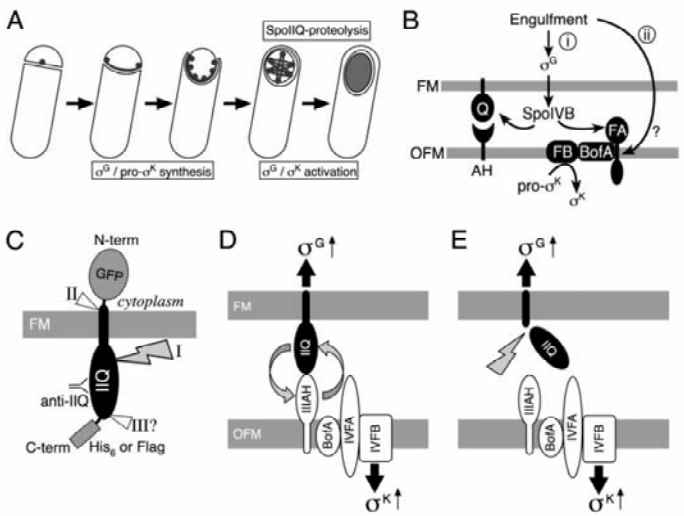

FIGURE 1. ***B. subtilis* engulfment, SpoIIQ proteolysis, and σ^G and σ^K activation.** *A*, after septation, the larger mother cell engulfs the smaller forespore, which is ultimately completely enclosed in the mother cell cytoplasm. GFP-SpoIIQ (*dark gray*) assembles foci at the septal midpoint and migrates around the forespore with the engulfing membrane, assembling a helical or hexagonal structure in the forespore (19). After engulfment, SpoIIQ is cleaved to release the N-terminal GFP fragment into the forespore cytoplasm (17, 19). The forespore transcription factor σ^G and the mother cell transcription factor σ^K are synthesized during engulfment and activated after engulfment (reviewed by Ref. 1). *B*, the interacting proteins SpoIIQ (*Q*) and SpoIIIAH (*AH*) are required for activation of σ^G and recruit the BofA-SpoIVFA-SpoIVFB complex necessary for activation of σ^K to the outer forespore membrane (*OFM*) (17, 24). Activation of σ^K is governed by two checkpoints: the forespore checkpoint (i) in which σ^G activation allows the production of high levels of SpoIVB (11), which cleaves SpoIVFA to relieve SpoIVFB from inhibition by BofA, and the engulfment checkpoint (ii) in which σ^K activity is coupled to engulfment by a BofA-independent mechanism (17). SpoIVB is also required to process SpoIIQ (17). *C*, SpoIIQ traverses the forespore membrane (*FM*), with a cytoplasmic N terminus that is the site of the GFP fusion. The extracellular C-terminal domain was used as the antigen for polyclonal antibodies (anti-IIQ) (17) while His_6 and FLAG tags were fused to the extreme C terminus. Three proteolysis events are indicated by roman numerals (*I–III*). The first initiating proteolysis event (*I*) requires SpoIVB serine protease (*lightning bolt*), and allows a subsequent cleavage within the membrane or in the cytoplasm (*II*). There might also be a third cleavage event (*III?*) near the C terminus of the protein that releases the His_6 and FLAG tags. *D* and *E*, models for the role of SpoIIQ in engulfment-dependent gene expression. *D*, the "pre-proteolytic activation model," in which full-length SpoIIQ is required for σ^G and σ^K activity; *E*, "post-proteolytic activation model," in which SpoIIQ proteolysis mediates intracellular signal transduction.

Briefly, the images were corrected for photobleaching during image collection, and the fluorescence intensity of the bleached and unbleached regions were quantified throughout the experiment, and corrected for bleaching during image acquisition. The small size of the forespore results in a small and variably sized pool of unbleached GFP-SpoIIQ from which recovery can occur. We therefore calculated the theoretical equilibration point between the bleached and unbleached regions, which is represented as a *dashed line*.

Immunofluorescence and Preparation of Anti-SpoIIIAH Antibody—Anti-SpoIIIAH polyclonal antiserum was made by injection of the KLH-conjugated chemically synthesized antigen peptide, CDLFTTYRLDLEDARSKEREE, into rabbits (subcontracted to Sigma Genosys). This peptide was chosen for its hydrophilicity and corresponds to amino acids 104–123 of SpoIIIAH plus an N-terminal Cys for conjugation to KLH. Immunofluorescence microscopy was performed as described (34).

RESULTS

Identification of in Vivo Cleavage Site of SpoIIQ—Previous results demonstrated that both N- and C-terminal proteolytic products of SpoIIQ, GFP-SpoIIQ, and SpoIIQ-His_6 were soluble, suggesting that the protein was cleaved on both sides of the membrane (Fig. 1*C*) (17). The ability to completely block SpoIIQ proteolysis with *spoIVB* mutations suggested that SpoIIQ proteolysis is initiated by the secreted SpoIVB protease, which releases the extracellular domain from the membrane, and allows a subsequent cytoplasmic (or perhaps intramembrane) proteolysis that releases the N-terminal GFP tag into the cytoplasm (Fig. 1*C*) (17). There might also be a third proteolysis event near the C terminus of SpoIIQ (Fig. 1*C*), based on our analysis of SpoIIQ-His_6. This protein shows two proteolytic products (Fig. 2*A*) in immunoblot experiments with anti-SpoIIQ antibodies, one slightly larger than that of native SpoIIQ (which reacts with His_6-specific antibodies) and one identical in size to that of native SpoIIQ (and that does not react with His_6-specific antibodies).

To further characterize the SpoIVB-dependent proteolysis event that appears to initiate SpoIIQ degradation we used two independent methods to identify the site at which SpoIIQ was cleaved in intact cells. First, we immunoprecipitated SpoIIQ-FLAG from whole cell lysates and extracted a band of ~25 kDa that appeared only when SpoIIQ-FLAG was expressed (Fig. 2*B*, *lane 2*). The major signal from the amino acid sequencing analysis was GKSMEN (corresponding to amino acids 73–78 of SpoIIQ), suggesting that extracellular cleavage occurs between Val-72 and Gly-73. Second, we constructed a series of SpoIIQ derivatives with individual cysteines introduced between codons 62 and 74 and used AMS modification (35) to determine if the cysteine residue was present in the C-terminal degradation product, which confirmed that in intact cells proteolysis occurred between Val-72 and Gly-73 (supplemental Fig. S1).

Purified SpoIVB Cleaves SpoIIQ—To determine if SpoIVB (a serine protease) directly cleaves SpoIIQ, we tested if purified SpoIVB cleaved purified GST-SpoIIQ *in vitro*, using GST-SpoIVFA (a known SpoIVB substrate), GST and α- and β-casein as control proteins. SpoIVB was able to cleave GST-SpoIIQ and GST-SpoIVFA with similar kinetics (Fig. 2*C*),

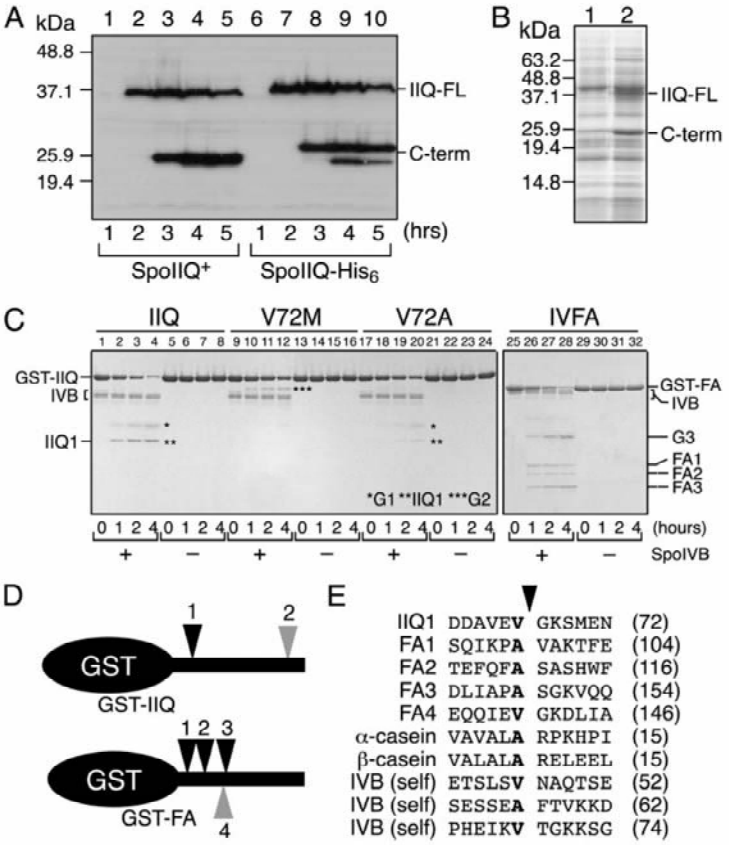

FIGURE 2. **Identification of SpoIVB cleavage sites in SpoIIQ and SpoIVFA.** *A, in vivo* proteolysis of SpoIIQ (PY79) and SpoIIQ-His_6 (SCB9) analyzed by Western blot using anti-SpoIIQ polyclonal antiserum at various times of sporulation. Full-length SpoIIQ (*IIQ-FL*) migrates at ~37 kDa, the C-terminal product (*C-term*) at ~26 kDa. *B*, SpoIIQ-FLAG (*lane 2*, XJ412) and the negative control strain PY79 (*lane 1*) were immunoprecipitated with anti-FLAG antibodies, and visualized by Coomassie staining. The bands indicated by *C-term* in *lane 2* and *lane 1* were extracted and subject to N-terminal amino acid sequencing. *C, in vitro* proteolysis of GST-SpoIIQ, various mutant derivatives, and GST-$SpoIVFA^{101-264}$-FLAG by purified SpoIVB-His_6. Purified GST-$SpoIIQ^{43-283}$ and GST-SpoIVFA were incubated at 37 °C for 4 h in the presence or absence of purified SpoIVB-His_6 and visualized by Coomassie staining. *IIQ1* and *FA1–3* are C-terminal cleavage products of SpoIIQ and SpoIVFA, respectively. *G1–3* are fragments containing GST released from the N terminus. *D*, cleavage sites are indicated by *arrowheads*. *Gray arrowhead 2* indicates the estimated position of the second C-terminal cleavage in SpoIIQ; *gray arrowhead 4* indicates cleavage at FA4 (15). *E*, amino acid alignment of SpoIVB-dependent cleavage sites in SpoIIQ, SpoIVFA, SpoIVB (22), and α- and β-casein. *Arrowhead* indicates position of cleavage. The numbers of amino acids before the cleavage site are in *parentheses*.

whereas GST was stable during the incubation (data not shown). The degradation products of GST-SpoIIQ and GST-SpoIVFA were excised and subjected to N-terminal amino acid sequencing. GST-SpoIIQ was cleaved once to yield a GST-containing product (G1) and a product with an N-terminal sequence starting at Gly-73 of SpoIIQ (IIQ1). Thus, purified SpoIVB cleaves SpoIIQ between Val-72 and Gly-73, the same position at which SpoIIQ is cut in intact cells. SpoIVB cleaved GST-SpoIVFA and itself in three locations (Fig. 2*E*) (36). A comparison of the SpoIVB cleavage sites of these three proteins and α- and β-casein demonstrated that in each case SpoIVB cut after either alanine (in the case of SpoIVFA, caseins, and one site in SpoIVB) or valine (in the case of SpoIIQ and two sites in SpoIVB), with little other primary sequence similarity in the surrounding region. A similar analysis by another group also identified these three sites in SpoIVFA (15). Using mass spectrometry analysis, they also observed cleavage at an EVGK motif within SpoIVFA that is identical to the site of proteolysis in SpoIIQ (15). Cleavage at this site depended on cleavage at the most C-terminal cleavage site. This explains why our N-terminal sequencing analysis failed to detect cleavage at EVGK, because we sequenced only the larger C-terminal products, which will have the same N terminus with or without cleavage at EVGK. The 8-amino acid internal product of cleavage at these sites is too small to be detected by SDS-PAGE.

Isolation of Cleavage-defective SpoIIQ Proteins—The above results demonstrate that SpoIIQ is directly cleaved by the SpoIVB serine protease that is essential for σ^K activation. To determine if SpoIIQ proteolysis was essential for sporulation, we used site-directed mutagenesis to randomize codons 72, 73, and 74 of wild-type *spoIIQ* ("Experimental Procedures"), isolating 26 different amino acid substitutions at these sites. The mutations were introduced into *B. subtilis* and screened for defects in SpoIIQ proteolysis using small scale sporulations (in test tubes) and anti-SpoIIQ Western blots from extracts prepared 5 h after the initiation of sporulation (t_5, Fig. 3*A*). Under these conditions, sporulation is slowed, likely due to decreased aeration, but wild-type SpoIIQ was cleaved by t_5 (Fig. 3*A*, *lanes 1* and *28*). Of the 29 mutants tested (including three Cys substitutions, supplemental Fig. S1), 14 were cleavage-defective, and 15 were permissive. At amino acid 72 only V72A and V72C allowed proteolysis (Fig. 3*A*, *lanes 2–11*, supplemental Fig. S1), demonstrating that Val-72 plays a crucial role in substrate recognition. In contrast, many substitutions at amino acids 73 and 74 allowed proteolysis (Fig. 3*A*, *lanes 12–27*), although introduction of negatively charged amino acids (Glu or Asp) or proline inhibited proteolysis. Alignment of the N-terminal regions of SpoIIQ from various *Bacillus* species (Fig. 3*C*) demonstrated that each had

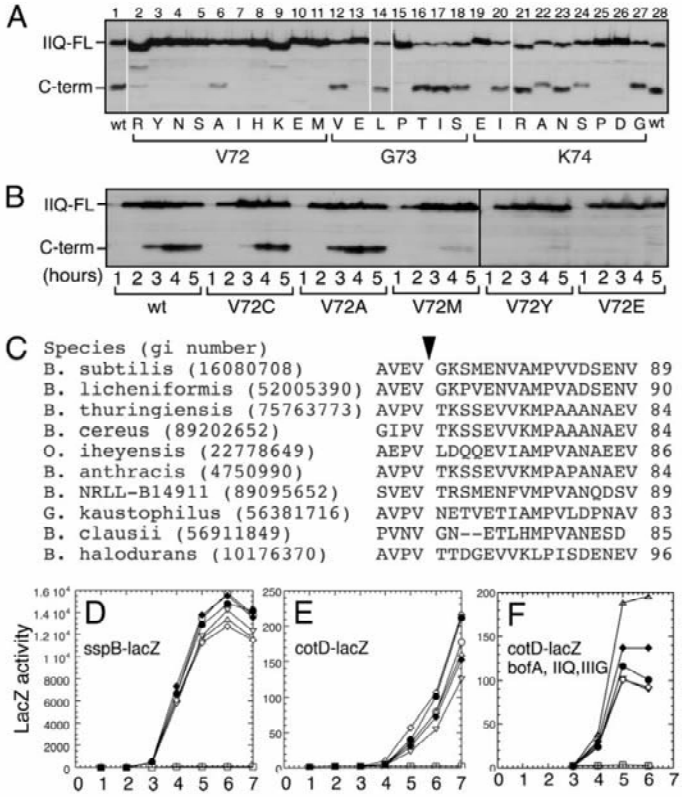

FIGURE 3. **Protease sensitivity and σ^G and σ^K activity of SpoIIQ cleavage site-mutants.** *A*, proteolysis in small-scale cultures. Sporulation was induced by resuspension in a 2-ml culture in test tubes, and samples were prepared after 5 h at 37 °C for Western blot analysis with anti-SpoIIQ. Amino acids introduced at Val-72 (*lanes 2–11*), Gly-73 (*lanes 12–18*), and Lys-74 (*lanes 19–27*) are indicated. *B*, time course of proteolysis in large scale cultures. IIQ-FL and C-term indicate full-length SpoIIQ and C-terminal cleavage products. *C*, alignment of predicted cleavage sites of SpoIIQ from various *Bacillus* sp. The *arrowhead* indicates cleavage site of *B. subtilis* SpoIIQ. D–F, affect of various *spoIIQ* mutations on σ^G and σ^K activity. All strains contained the *lacZ* fusion indicated in each panel, and the *spoIIQ* mutation indicated by the following symbols (*circles*, *spoIIQ*$^+$; *squares*, Δ*spoIIQ*; *triangles*, wt; *inverted triangles*, V72C; *solid diamonds*, V72M; *open diamonds*, G73V; *solid circles*, G73E). In addition, all strains with a *spoIIQ* derivative at *amyE* also contained a *spoIIQ* null mutation. *D*, to assay σ^G activity, strains KP701, AR232, SCB18, SCB108, SCB109, SCB110, and SCB111 were used. *E*, for σ^K activity, XJ220, KP953, SCB21, SCB114, SCB115, SCB116, and SCB117 were used. *F*, the cleavage site mutants also supported σ^K activity in strains lacking *spoIIIG* and *bofA*. Strains contained the indicated *spoIIQ* mutations plus *bofA* and *spoIIIG* (SCB223, SCB224, SCB225, SCB227, SCB228, and SCB229).

valine at the predicted SpoIVB cleavage site and permissive substitutions at positions corresponding to Gly-73 and Lys-74 of *B. subtilis* SpoIIQ (aside from *Geobacter* and *Oceanobacillus iheyensis*, which had a non-permissive substitution at position 74). Thus, valine appears to be conserved at the cleavage site of SpoIIQ proteins that are sufficiently closely related to allow a reliable alignment of their N-terminal domain.

We more precisely followed degradation of three cleavage-defective mutants and two permissive mutants using larger scale sporulations (Fig. 3*B*). Each of the cleavage-defective mutants showed very slow and inefficient degradation, with little accumulation of the C-terminal product and no notable decrease in the levels of full-length SpoIIQ even after 5 h of sporulation. In contrast the permissive mutants showed normal or slightly slower (V72C) degradation (Fig. 3*B*), accumulating a stable C-terminal breakdown product. To determine if these proteins were equally resistant or sensitive to *in vitro* proteolysis by purified SpoIVB, we introduced the cleavage-defective substitution V72M and the permissive substitution V72A into GST-SpoIIQ. As expected, V72M was resistant to SpoIVB cleavage at the usual cleavage site, although it generated a larger proteolysis product that might correspond to cleavage at a more C-terminal SpoIVB cleavage (*G2* in Fig. 2*C*). We could find no evidence that SpoIVB cleaved V72M at this site *in vivo*, because no intermediate size product was observed in whole cell extracts (Fig. 3*B*). Interestingly, V72A, which is permissive for proteolysis in intact cells, was degraded *in vitro* more slowly than wild-type SpoIIQ (Fig. 2*C*).

Effects of SpoIIQ Cleavage Mutants on σ^G and σ^K Activity—Both SpoIIQ proteolysis and activation of σ^G and σ^K depend on engulfment, raising the possibility that SpoIIQ proteolysis might mediate extracellular signal transduction via an RIP-like mechanism (post-proteolytic model in Fig. 1*E*). However, full-length SpoIIQ also acts during engulfment to recruit mother cell membrane proteins required for σ^G and σ^K activation to the septum (17, 23, 24), raising the possibility that an event that occurs before proteolysis might mediate signal transduction (pre-proteolytic model in Fig. 1*D*). To distinguish between these models, we compared the levels of σ^G and σ^K activity (using *sspB-lacZ* and *cotD-lacZ*, respectively) in strains carrying mutations that block (V72M and G73E) or allow (V72C and G73V) SpoIIQ proteolysis. These mutants showed σ^G and σ^K activities nearly identical to wild type (Fig. 3, *D* and *E*). Thus, the proteolysis-defective mutants have no effect on σ^G or σ^K activity, suggesting that SpoIIQ proteolysis is not essential for engulfment-dependent gene expression, in keeping with the pre-proteolytic model.

The activation of σ^K is governed by two checkpoints, the prior activation of σ^G (the forespore checkpoint) (11) and a separate checkpoint governed by the completion of engulfment (the engulfment checkpoint). The forespore checkpoint can be

TABLE 2
Sporulation efficiency of *spoIIQ* mutants

Strain	Genotype	Cleavage	Spore titer
PY79	*spoIIQ*$^+$	+	2.7×10^8
SCB3	Δ*spoIIQ::spc, amyE::cat*		0
SCB4	Δ*spoIIQ::spc, amyE::*$_{pspoIIG}$*spoIIQΩcat*	+	2.5×10^8
SCB50	Δ*spoIIQ::spc, amyE::*$_{pspoIIG}$*spoIIQV72CΩcat*	+	2.6×10^8
SCB71	Δ*spoIIQ::spc, amyE::*$_{pspoIIG}$*spoIIQV72MΩcat*	−	2.0×10^8
SCB72	Δ*spoIIQ::spc, amyE::*$_{pspoIIG}$*spoIIQG73VΩcat*	+	1.7×10^8
SCB73	Δ*spoIIQ::spc, amyE::*$_{pspoIIG}$*spoIIQG73EΩcat*	−	2.0×10^8
SCB83	Δ*spoIIQ::spc, amyE::*$_{pspoIIG}$*spoIIQK74RΩcat*	+	1.8×10^8
SCB80	Δ*spoIIQ::spc, amyE::*$_{pspoIIG}$*spoIIQK74EΩcat*	−	1.9×10^8

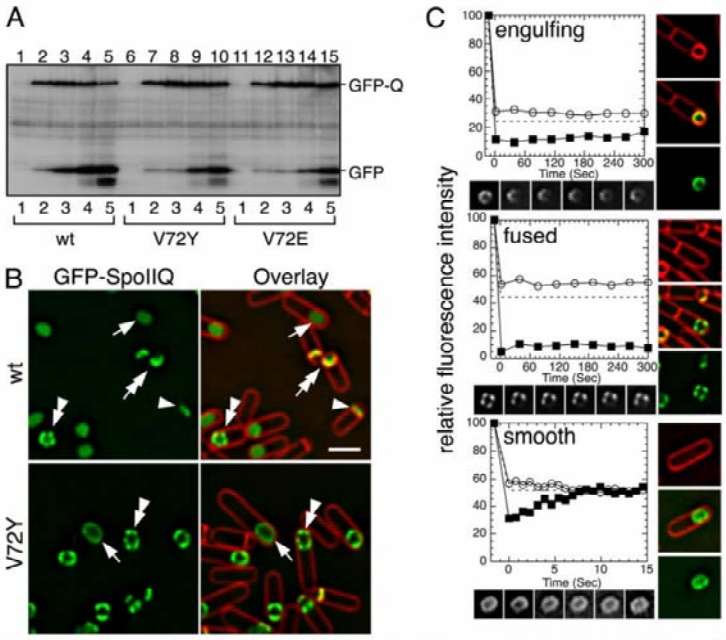

FIGURE 4. **Altered proteolysis, localization, and dynamics of cleavage-defective GFP-SpoIIQ.** *A*, proteolysis of GFP-SpoIIQ (SCB6) V72Y (SCB138) and V72E (SCB139), analyzed by Western blots with anti-GFP. "*GFP-Q*" and "*GFP*" indicate full-length and N-terminal GFP degradation product of GFP-SpoIIQ. *B*, localization of GFP-SpoIIQ (*wt*) and GFP-SpoIIQ (*V72Y*) 4 h after the initiation of sporulation (t_4). Membranes were stained with FM4-64 (*red*). *Arrowheads* indicate septal localization of GFP-SpoIIQ (*green*); *double arrows*, GFP-SpoIIQ migrating with mother cell membrane; *double arrowheads*, helical structure. Membrane fusion (indicated by exclusion of FM4-64 from the forespore membranes, *arrow* and *double arrowhead*) occurs before proteolysis, which releases GFP into the cytoplasm (*arrow*). After fusion, V72Y remains membrane-bound but localizes smoothly around the forespore (*arrow*). *C*, FRAP analysis of GFP-SpoIIQV72Y at t_3 performed and quantified as described under "Experimental Procedures." Images of GFP (*green*) and FM4-64 (*red*)-stained membranes of cells before bleaching are to the *right* of each *graph*. Images *below* each plot show the GFP fluorescence during the experiment; the *second panel* shows the cell just after bleaching. Recovery kinetics were quantified and plotted to show the mean pixel intensity of the bleached (*filled square*) and unbleached (*empty circle*) regions and the theoretical pixel intensity value following equilibration between these regions (*dashed line*). Wild-type GFP-SpoIIQ shows very little recovery (see supplemental Fig. S2 and Ref. 22).

bypassed by a *bofA* mutation, which allows σ^K activity in the absence of σ^G (37), but the *bofA* mutation does not bypass either engulfment or the requirement for SpoIIQ and SpoIIIAH for σ^K activity (17). We tested whether cleavage-defective SpoIIQ supported σ^K activation in a *bofA* mutant lacking σ^G, by introducing the cleavage-defective or -permissive mutants into a cell that has null mutations in *spoIIIG* (encoding σ^G), *bofA* and *spoIIQ*. Again, both cleavage-defective and cleavage-permissive mutations supported σ^K activation in these assays, with a slight reduction in activity seen in both classes of mutations at late times (Fig. 3*F*).

Thus, SpoIVB-mediated proteolysis of SpoIIQ is dispensable for both σ^G and σ^K activity, as well as for the production of heat-resistant spores (Table 2). These results suggest that either SpoIIQ proteolysis is normally dispensable for sporulation or that cytoplasmic proteolysis does not depend on SpoIVB-mediated extracellular proteolysis.

Cytoplasmic Cleavage of SpoIIQ Depends on Extracytoplasmic Cleavage—The absence of smaller breakdown products in SpoIIQ proteins resistant to SpoIVB-mediated extracellular proteolysis (Fig. 3) and in the absence of SpoIVB (17) suggests that, in intact cells, cytoplasmic proteolysis occurs after extracellular proteolysis. To further test this hypothesis, we introduced the cleavage-resistant mutations V72Y and V72E into GFP-SpoIIQ and tested whether the cytoplasmic cleavage occurred to release the N-terminal GFP tag into the cytoplasm. Western blot analysis demonstrated that GFP-SpoIIQ was partially stabilized by these mutations, with a decreased amount of the N-terminal GFP-containing breakdown product relative to wild type at t_3 (Fig. 4*A*). Prior studies have demonstrated that GFP-SpoIIQ is more permissive for proteolysis than native SpoIIQ. Unlike the wild-type protein, GFP-SpoIIQ is not completely stabilized by the absence of either SpoIVB or SpoIIIAH (17). This proteolysis might occur during sample preparation, because fluorescence microscopy demonstrated that, similar to GFP-SpoIIQ in the *spoIVB* and *spoIIIAH* mutants (17), the proteolysis-resistant mutant V72Y remained membrane-bound after engulfment, with little cytoplasmic GFP fluorescence (Fig. 4*B*). Together

with the ability of mutations at the site of extracellular cleavage to completely stabilize native SpoIIQ (with no slightly smaller breakdown products, Fig. 3), these results suggest that cytoplasmic cleavage of SpoIIQ normally depends on its extracellular cleavage by SpoIVB (Fig. 1*C*).

This mechanism of SpoIIQ proteolysis shows similarity to that of RIP, in which degradation of a signal transduction protein is typically initiated by an extracellular cleavage that allows a second intracellular or intramembrane cleavage by a second protease. However, despite the observation that SpoIIQ proteolysis is governed by the same morphological checkpoint (engulfment) and protease (SpoIVB) as late mother cell gene expression, we found no evidence that it participates in intracellular signal transduction.

Release of SpoIIQ from an Immobile Complex after Engulfment—We reasoned that the completion of engulfment might mediate a rearrangement in the complex between SpoIIQ and its mother cell ligand SpoIIIAH or its unidentified tether (19, 23) and that this rearrangement might allow both SpoIIQ proteolysis and signal transduction. If this is the case, then SpoIIQ might show different diffusion kinetics before and after the membrane fusion event that is the final step of engulfment. Indeed, a FRAP analysis of the diffusion kinetics of wild-type GFP-SpoIIQ during and after engulfment demonstrated that SpoIIQ is relatively immobile during engulfment with somewhat increased mobility after engulfment (22). However, wild-type SpoIIQ is degraded after engulfment, so this could reflect loss of the extracellular domain rather than release from a complex. We therefore performed a FRAP analysis of the protease-resistant mutant V72Y. During engulfment, V72Y showed the same restricted mobility as wild-type SpoIIQ (supplemental Fig. S2) (22), with equilibration between the bleached and unbleached regions requiring at least 200 s (supplemental Fig. S2) (22). After engulfment, V72Y showed both the punctate localization seen in wild type before proteolysis, and a smooth localization pattern not observed in wild type (Fig. 4*B*), unless it is expressed in the absence of SpoIVB (17). These two patterns each had distinct FRAP results (Fig. 4*C*): sporangia with punctate localization showed low mobility (equilibration times or $t_{eq} \geq 240$ s), whereas those with smooth localization showed a high mobility ($t_{eq} \leq 10$ s) similar that of forespore-expressed $MalF^{TM1-2}$-GFP ($t_{eq} \leq 6$ s) (22). We obtained essentially the same results with another cleavage-defective SpoIIQ protein (V72E), and wild-type SpoIIQ in the proteolysis-defective *spoIVB* strain (supplemental Fig. S2).

Thus after membrane fusion, protease-resistant SpoIIQ is released from a punctate or helical structure in which it is essentially immobile, attaining a rapid diffusion rate similar to a non-localized protein. This event could allow both RIP and intracellular signal transduction necessary for engulfment-dependent gene expression in the forespore and the mother cell.

Reduced Interaction between the Extracellular Proteolysis Product of SpoIIQ and SpoIIIAH—We were interested in determining if the proteolytic products of SpoIIQ interacted with its mother cell ligand SpoIIIAH. We therefore used non-denaturing sucrose density gradient analysis (31) to compare the apparent molecular weight of full-length SpoIIQ, its C-terminal degradation product, and SpoIIIAH. Full-length SpoIIQ and

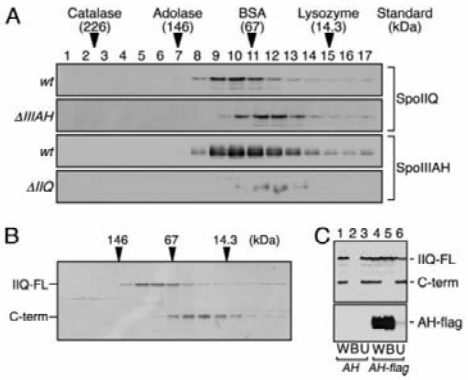

FIGURE 5. **The C-terminal fragment of SpoIIQ shows reduced interaction with SpoIIIAH.** *A* and *B*, sucrose density gradient analysis to assess the apparent molecular masses of proteins in whole cell lysates from t_2 (*A*) and $t_{3.5}$ (*B*). Fractions were collected from the bottom (*lane 1*) to the top (*lane 17*) of the gradient. SpoIIIAH-FLAG (*AH-flag*) and full-length SpoIIQ (*IIQ-FL*) and the C-terminal cleavage product (*C-term*) were visualized by Western blot with anti-FLAG or anti-SpoIIQ antibodies, respectively. *Arrowheads* indicate positions of proteins used as size standards. *A*, at early times of sporulation (t_2), full-length SpoIIQ and SpoIIIAH-FLAG are present in the same fractions (~100 kDa). In the absence of one, the other migrates at a lower apparent molecular mass (~40 kDa). *B*, at later times ($t_{3.5}$), full-length SpoIIQ migrates at ~100 kDa, whereas the C-terminal proteolytic product migrates at a lower apparent molecular mass. *C*, co-immunoprecipitation of SpoIIQ with SpoIIIAH-FLAG. Whole cell lysates from strains PY79 (*spoIIIAH*; *lanes 1–3*) and KP856 (*spoIIIAH-flag*; *lanes 4–6*) were immunoprecipitated with anti-FLAG M2 antibody. *W*, *B*, and *U* indicate whole cell lysate, bound, and unbound protein fractions, respectively.

SpoIIIAH were present in the same fractions (Fig. 5*A*), with apparent molecular masses of ~100 kDa, significantly higher than their predicted molecular masses of 31 kDa and 24 kDa, respectively. The high molecular weight was likely a consequence of the interaction between SpoIIQ and SpoIIIAH, because both proteins had a reduced apparent molecular mass in strains lacking the other protein (~40 kDa). The level of SpoIIIAH was reduced in the absence of SpoIIQ (Fig. 5*A*, supplemental Fig. S3*D*), suggesting that SpoIIQ protects SpoIIIAH from proteolysis.

Samples harvested after SpoIIQ proteolysis commenced demonstrated that, although the differences in molecular mass between full-length SpoIIQ and its C-terminal product is only ~8 kDa (31 kDa *versus* 23 kDa), these two proteins showed strikingly different apparent sizes, with full-length SpoIIQ behaving as a ~100 kDa protein, and the C-terminal product as a ~30 kDa protein (Fig. 5*B*). This suggests a reduced interaction between the C-terminal fragment of SpoIIQ and SpoIIIAH. We confirmed this hypothesis by immunoprecipitating SpoIIIAH-FLAG and probing the eluate with anti-SpoIIQ antibody. While full-length SpoIIQ was efficiently co-precipitated with SpoIIIAH-FLAG, the C-terminal fragment of SpoIIQ was not precipitated (Fig. 5*C*). Together these results indicate that if there is any interaction between the C-terminal degradation product of SpoIIQ and SpoIIIAH, the affinity is too low to be detected by either sucrose density gradient analysis or co-immunoprecipitation.

SpoIVB-mediated SpoIIQ proteolysis occurs after V72, leaving the N-terminal transmembrane segment and almost 30

amino acids outside the cell that might interact with SpoIIIAH. In an attempt to determine if this region interacted with SpoIIIAH, we expressed the N-terminal fragment of SpoIIQ$^{1-72}$ and used immunofluorescence and Western blotting to determine if it was able to recruit SpoIIIAH to the sporulation septum and protect it from proteolysis. SpoIIIAH localization and stability was reduced in the SpoIIQ$^{1-72}$ strain. This might be due to the rapid degradation of the N-terminal fragment, because GFP fusions to the first 60 or 72 amino acids of SpoIIQ were quickly degraded to soluble GFP (data not shown), as is the N-terminal cleavage product of full-length GFP-SpoIIQ (which fails to accumulate). This suggests that the N-terminal product of SpoIVB cleavage is too unstable to sustain an interaction with SpoIIIAH. Thus, SpoIIQ appears to make a high affinity interaction with SpoIIIAH only before proteolysis, raising the possibility that premature degradation of SpoIIQ might compromise its ability to recruit SpoIIIAH and other proteins to the sporulation septum.

SpoIIQ Proteolysis Occurs in a Membrane Fusion-dependent Manner—Although SpoIVB is synthesized during engulfment (18), three lines of evidence indicate that SpoIVB-mediated proteolysis of SpoIIQ occurs only after engulfment. First, cell biological studies of GFP-SpoIIQ degradation demonstrate that the N-terminal GFP moiety is released from the membrane only in sporangia that have completed membrane fusion, demonstrating that cytoplasmic proteolysis occurs only after fusion (19). Second, Western blot analysis of native SpoIIQ (with anti-SpoIIQ antiserum) demonstrates that low levels of SpoIIQ proteolysis is first observed at 2.5 h of sporulation (Fig. 5*C*), consistent with observations that membrane fusion is first completed in a few sporangia just before 2 h of sporulation (at 105 min (32)). Finally, proteolysis of native SpoIIQ does not occur in *spoIID* or *spoIIP* mutants, which block engulfment prior to the onset of membrane migration (17).

We were interested in determining if SpoIIQ proteolysis was regulated by membrane migration or by the membrane fusion event that is the final step of engulfment. To address this question, we made use of a *spoIIIE* mutant that completes membrane migration but not membrane fusion (and which translocates DNA (33)). The membrane fusion-defective mutant abolished degradation of native SpoIIQ (Fig. 6*B*) and accumulated full-length SpoIIQ. These results indicate that SpoIVB-mediated degradation of SpoIIQ depends on the final step of engulfment, membrane fusion, in keeping with prior cell biological studies.

DISCUSSION

Our results demonstrate that SpoIIQ is directly cleaved by the SpoIVB protease that is also required for activation of the late mother cell transcription factor σ^K. Interestingly, both σ^K activation and SpoIIQ proteolysis depend on the phagocytosis-like process of engulfment (17, 38). We here provide evidence that SpoIIQ proteolysis more specifically depends on the final step of engulfment, membrane fusion, which releases the forespore into the mother cell cytoplasm. Although SpoIIQ proteolysis is not essential for sporulation, it in some ways provides a better model for SpoIVB-mediated proteolysis than the other identified SpoIVB substrate, SpoIVFA. Specifically, unlike

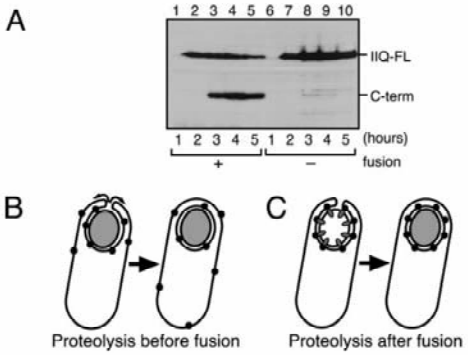

FIGURE 6. **SpoIIQ proteolysis depends on engulfment membrane fusion.** *A*, SpoIIQ proteolysis assessed by Western blot analysis of strains KP6012 (*gfp-spoIIIE*$^+$; *lanes 1–5*) and the membrane fusion-defective KP6111 (*gfp-spoIIIE*121; *lanes 6–10*). *B* and *C*, *schematics* depicting the potential importance of coupling SpoIIQ proteolysis to membrane fusion. *B*, if SpoIIQ proteolysis occurs before fusion, mother cell proteins that interact with SpoIIQ (such as SpoIIIAH) would be released from the septum and therefore be distributed throughout the mother cell membrane. *C*, if SpoIIQ proteolysis occurs after fusion, binding proteins cannot escape from the outer forespore membrane. Coupling SpoIIQ proteolysis to membrane fusion might therefore be necessary for the efficient localization of mother cell membrane proteins to the outer forespore membrane.

SpoIVFA, SpoIIQ proteolysis releases stable proteolysis products that can readily be detected by both immunoblot analysis and cell biological methods. SpoIIQ thereby provides a tractable system to investigate the mechanism by which SpoIVB activity is governed by the morphological checkpoint of engulfment.

The Checkpoint for SpoIIQ Proteolysis Might Retain the Active Signal Transduction Complex at the Septum—It remains unclear why SpoIIQ is subject to engulfment-dependent proteolysis, because we have failed to identify any phenotypic consequence of blocking SpoIIQ proteolysis. However, our results allow us to propose a reason for why it is important to delay SpoIIQ proteolysis until after the completion of membrane fusion. The interaction between SpoIIQ and SpoIIIAH is required to retain SpoIIIAH and SpoIVFB in the outer forespore membrane (17, 23, 24), where they are involved in intracellular signal transduction cascades that result in activation of late forespore and mother cell transcription factors. We have been unable to detect an interaction between the SpoIIQ proteolysis products and SpoIIIAH in living cells. Thus, if SpoIIQ were degraded prior to membrane fusion the decreased affinity of the interaction between SpoIIQ and SpoIIIAH might result in the release of SpoIIIAH and SpoIVFB from the outer forespore membrane (Fig. 6*B*), thereby compromising intracellular signal transduction. Thus, using membrane fusion as a checkpoint for SpoIIQ proteolysis might serve to maintain the interaction between SpoIIQ and SpoIIIAH and SpoIVFB until after engulfment, ensuring that proteins required for σ^G and σ^K activation localize exclusively to the outer forespore membrane where cell-to-cell communication occurs (Fig. 6*C*).

A Membrane Fusion-dependent Reorganization in the SpoIIQ-SpoIIIAH Complex—Our studies also suggest a membrane fusion-dependent rearrangement in the complex be-

tween SpoIIQ, SpoIIIAH, and other proteins involved in late forespore and mother cell gene expression. Specifically, our FRAP studies demonstrate that, although SpoIIQ is essentially immobile during engulfment (22), after membrane fusion it diffuses through the forespore membrane at rates nearly identical to a non-localized MalF-GFP protein (Fig. 4). This result is most easily interpreted as reflecting a remodeling of the interaction between SpoIIQ and its binding partner, SpoIIIAH (or another unidentified SpoIIQ-interacting protein), an event that could easily initiate intracellular signal transduction. It is therefore tempting to speculate that remodeling of the SpoIIQ complex provides a signal both for σ^G and σ^K activation and for SpoIIQ proteolysis, because this would explain both the coordinate regulation of these events by membrane fusion and the dispensable nature of SpoIIQ proteolysis.

Acknowledgments—We thank Ruanbao Zhou, Lee Kroos, and Charles Moran for providing strains and Dan Broder and Amber Dance for providing helpful comments on the manuscript.

REFERENCES

1. Errington, J. (2003) *Nat. Rev. Microbiol.* **1,** 117–126
2. Piggot, P. J., and Hilbert, D. W. (2004) *Curr. Opin. Microbiol.* **7,** 579–586
3. Rudner, D. Z., and Losick, R. (2001) *Dev. Cell* **1,** 733–742
4. Kroos, L., and Yu, Y. T. (2000) *Curr. Opin. Microbiol.* **3,** 553–560
5. Zhang, B., Hofmeister, A., and Kroos, L. (1998) *J. Bacteriol.* **180,** 92434–92441
6. Yu, Y. T., and Kroos, L. (2000) *J. Bacteriol.* **182,** 3305–3309
7. Zhou, R., and Kroos, L. (2004) *Proc. Natl. Acad. Sci. U. S. A.* **101,** 6385–6390
8. Rudner, D. Z., Fawcett, P., and Losick, R. (1999) *Proc. Natl. Acad. Sci. U. S. A.* **96,** 14765–14770
9. Ehrmann, M., and Clausen, T. (2004) *Annu. Rev. Genet* **38,** 709–724
10. Brown, M. S., Ye, J., Rawson, R. B., and Goldstein, J. L. (2000) *Cell* **100,** 391–398
11. Cutting, S., Oke, V., Driks, A., Losick, R., Lu, S., and Kroos, L. (1990) *Cell* **62,** 239–250
12. Cutting, S., Driks, A., Schmidt, R., Kunkel, B., and Losick, R. (1991) *Genes Dev.* **5,** 456–466
13. Rudner, D. Z., and Losick, R. (2002) *Genes Dev.* **16,** 1007–1018
14. Dong, T. C., and Cutting, S. M. (2003) *Mol. Microbiol.* **49,** 1425–1434
15. Campo, N., and Rudner, D. Z. (2006) *Mol. Cell* **7,** 25–35
16. Zhou, R., and Kroos, L. (2005) *Mol. Microbiol.* **58,** 835–846
17. Jiang, X., Rubio, A., Chiba, S., and Pogliano, K. (2005) *Mol. Microbiol.* **58,** 102–115
18. Gomez, M., and Cutting, S. M. (1996) *Microbiology* **142,** 3453–3457
19. Rubio, A., and Pogliano, K. (2004) *EMBO J.* **23,** 1636–1646
20. Sun, Y. L., Sharp, M. D., and Pogliano, K. (2000) *J. Bacteriol.* **182,** 2919–2927
21. Londono-Vallejo, J. A., Frehel, C., and Stragier, P. (1997) *Mol. Microbiol.* **24,** 29–39
22. Broder, D. H., and Pogliano, K. (2006) *Cell* **126,** 917–928
23. Blaylock, B., Jiang, X., Rubio, A., Moran, C. P., Jr., and Pogliano, K. (2004) *Genes Dev.* **18,** 2916–2928
24. Doan, T., Marquis, K. A., and Rudner, D. Z. (2005) *Mol. Microbiol.* **55,** 1767–1781
25. Dubnau, D., and Davidoff-Abelson, R. (1971) *J. Mol. Biol.* **56,** 209–221
26. Sawano, A., and Miyawaki, A. (2000) *Nucleic Acids Res.* **28,** 78
27. Sterlini, J. M., and Mandelstam, J. (1969) *Biochem. J.* **113,** 29–37
28. Abanes-De Mello, A., Sun, Y. L., Aung, S., and Pogliano, K. (2002) *Genes Dev.* **16,** 3253–3264
29. Miller, J. H. (1972) *Experiments in Molecular Genetics*, Cold Spring Harbor Laboratory, Cold Spring Harbor, NY
30. Pogliano, K., Hofmeister, A. E., and Losick, R. (1997) *J. Bacteriol.* **179,** 3331–3341
31. Saikawa, N., Akiyama, Y., and Ito, K. (2004) *J. Struct. Biol.* **146,** 123–129
32. Sharp, M. D., and Pogliano, K. (1999) *Proc. Natl. Acad. Sci. U. S. A.* **96,** 14553–14558
33. Liu, N. J., Dutton, R. J., and Pogliano, K. (2006) *Mol. Microbiol.* **59,** 1097–1113
34. Perez, A. R., Abanes-De Mello, A., and Pogliano, K. (2000) *J. Bacteriol.* **182,** 1096–1108
35. Kobayashi, T., Kishigami, S., Sone, M., Inokuchi, H., Mogi, T., and Ito, K. (1997) *Proc. Natl. Acad. Sci. U. S. A.* **94,** 11857–11862
36. Wakeley, P. R., Dorazi, R., Hoa, N. T., Bowyer, J. R., and Cutting, S. M. (2000) *Mol. Microbiol.* **36,** 1336–1348
37. Ricca, E., Cutting, S., and Losick, R. (1992) *J. Bacteriol.* **174,** 3177–3184
38. Rubio, A., Jiang, X., and Pogliano, K. (2005) *J. Bacteriol.* **187,** 5000–5002
39. Youngman, P., Perkins, J. B., and Losick, R. (1984) *Mol. Gen. Genet* **195,** 424–433

A. Contributions

As a secondary author and investigator of this paper, I made several contributions. First, I aided in transformation of strains that were used in this study. I induced sporulation on these strains by resuspension and collected samples for co-immunoprecipitation, Western blotting, and beta-galactosidase assays. I performed co-immunoprecipitation of SpoIIQ and SpoIIIAH-flag. I performed beta-galactosidase assays to test for σ^K and σ^G activity. I also purified SpoIVB protein. I performed Western blotting of purified SpoIVB and sequenced its self-cleavage products. I performed an *in vivo* proteolysis assay of SpoIIQ by SpoIVB and analyzed the results by Western blotting. I also performed *in vitro* protease assays with alpha and beta-casein and SpoIVB and sequenced the resultant cleavage products to discern SpoIVB's cleavage site preferences. I assisted writing of the paper via comments, insight, and corrections.

Chapter 2 consists, in full, of a reprint of material as it appears in The Journal of Biological Chemistry, Chiba, Shinobu; Coleman, Kristina; and Pogliano, Kit, JBC Papers in Press, 2007. The thesis author was a secondary author and investigator of this paper.

CHAPTER III

SpoIVFB regulation during *Bacillus subtilis* sporulation:

Evidence for a morphological checkpoint governing protease activity

A. Abstract

Sporulation of *Bacillus subtilis* is first characterized by an asymmetric cell division, a process that forms a larger compartment, the mother cell, and a smaller cell, the forespore, which becomes the spore. The SpoIVFB protease is required to activate the mother cell transcription factor, σ^K, allowing the formation of the protective spore coat. The forespore transcription factor, σ^G, leads to the activation of SpoIVFB. Via this pathway, deemed the forespore checkpoint, a protease is produced that cleaves SpoIVFA, thus relieving inhibition of SpoIVFB by BofA. Here, it will be shown that a second checkpoint, the engulfment checkpoint, also controls σ^K activity via SpoIVFB. Mutants in *spoIVF* have been characterized that can bypass either the forespore checkpoint, or the engulfment checkpoint. A mutant in *spoIVFA*, S80L, allows for σ^K activation in the absence of the forespore checkpoint. A *spoIVFB* mutant, S260G, allows SpoIVFB to bypass the engulfment checkpoint in the absence of BofA. It is believed that the forespore and engulfment checkpoints are separate pathways, since no mutants have yet been found that can bypass both checkpoints. Moreover, it will be shown that σ^K activation is independent of SpoIVFB protein levels.

B. Introduction

Sporulation in *Bacillus subtilis* is an informative model for many aspects of developmental biology. It offers knowledge of cell development and differentiation in a small scale, two-cell system, which can be applied when studying more complex mechanisms. Issues of intercellular communication, morphogenesis, and regulation of gene expression can be addressed utilizing the model of spore formation. When exposed to adverse conditions such as nutrient starvation, the cell eventually commits to an extreme developmental pathway to ensure its survival. The cell first switches from medial to polar, asymmetric cell division [1-4] forming a sporangium consisting of a smaller and larger compartment (Figure 1A, 1B). The septum between the larger mother cell and smaller forespore is degraded by a peptidoglycan hydrolase (Figure 1C) and the mother cell membranes migrate around those of the forespore (Figure 1D, 1E) [5,6]. The mother cell membranes fuse with the help of SpoIIIE, releasing the forespore into the mother cell cytoplasm (Figure 1F) [6-8]. The mother cell forms a protective protein coat around the forespore and then lyses, releasing a mature spore with resistances to heat, desiccation, chemicals, and UV radiation [9-12].

A sequence of cell-specific transcription factors are temporally and spatially regulated to coordinate gene expression and morphogenesis in both the mother cell and forespore [13-16]. The σ^F factor is activated in the forespore, followed by σ^E in the mother cell, following polar cell division. The σ^F transcription factor is activated first in the forespore [17]. It activates genes that allow for the activation of σ^E in the mother cell (Figure 2A) [18]. The σ^F factor upregulates the gene for forespore transcription factor, σ^G [18], which is held inactive until after engulfment (Figure 2C) [20]. Small amounts of

the intramembrane protease SpoIVB are also produced under control of σ^F before engulfment [19]. Once engulfment is completed, σ^G is activated, and high levels of SpoIVB are accumulated, thus beginning the forespore checkpoint for the activation of σ^K (Figure 2D).

i. σ^K activation via the forespore checkpoint

SpoIVFB cleaves pro- σ^K into active σ^K. It is unable to perform this task until after it is activated by a pathway that begins with σ^G activation. This activation pathway is known as the forespore checkpoint. SpoIVFB is held in a complex with SpoIVFA and BofA. This interaction seems to be mediated by FA [21]. BofA inhibits SpoIVFB and this inhibition is relieved by cleavage of SpoIVFA [22,23]. High levels of the serine protease, SpoIVB, are produced following engulfment due to upregulation by σ^G (Figure 3) [19]. SpoIVB is secreted into the intramembrane space where it then cleaves SpoIIQ and SpoIVFA [24-26]. Another protease, CtpB, thought to be produced by both cells, is found in the intramembrane space and is believed to cleave both FA and BofA (Figure 4) [23-25]. Once its inhibition is relieved, SpoIVFB cleaves pro-sigmaK into σ^K and coat production can commence within the mother cell.

ii. SpoIVFB and Regulated Intramembrane Proteolysis

Regulated intramembrane proteolysis (RIP) is a means of signal transduction by which transmembrane proteins are cleaved by membrane-bound proteases. SpoIVFB, an integral membrane protein, employs RIP to cleave and activate σ^K. RIP is a widespread mechanism that has been observed from bacteria to humans and other animals [28].

RIP proteases are divided into serine, aspartyl, or metalloprotease subfamilies which are identified by their conserved active site residues [27]. RIP is mediated by a group of membrane-bound proteases, deemed I-Clips (Intramembrane-cleaving proteases) [27]. SpoIVFB belongs to a subset of I-Clips, the site-2 proteases, or S2P, and is a zinc metalloprotease [29,30]. Zinc metalloproteases are characterized by an active site HExxH motif within a transmembrane segment [27,29]. SpoIVFB also has a second conserved NPDG motif (Figure 5) [30]. Both of these motifs are necessary for the activation of σ^K.

In other organisms, S2Ps serve varying functions. In spite of this, the mechanism by which they work is the same, and the proteins are recognized by their conserved active site domains. *Vibrio cholerae* and *Mycobacterium tuberculosis* S2P proteins YaeL and Rv2869c, respectively, control important virulence genes [27]. Human S2P is shown to cleave sterol regulatory element-binding proteins (SREBPs) which then initiate transcription of genes in the cholesterol and fatty acid biosynthetic pathways. The gene encoding the LDL-receptor is also directly upregulated by SREBPs, allowing cells to absorb cholesterol and fatty acids from external sources [31]. S2P also regulates the unfolded protein response (UPR) in the endoplasmic reticulum [32]. MmpA, a *Caulobacter crescentus* S2P, is important for the preservation of cell asymmetry, a factor needed for assembly of pili and holdfast at the proper cell pole [33]. S2Ps are even significant in plants. It has been demonstrated that AraSP (*Arabidopsis* SP), a plant S2P and metalloprotease, is necessary for chloroplast (specifically thylakoid) development, and may have a role in general plant development as well [34]. These cases illustrate the

diversity of S2Ps and the widespread prevalence of RIP as a means of signal transduction.

iii. The second checkpoint dispute

Engulfment is required for σ^G activation. Though the exact mechanism is unknown, there are some ideas as to how engulfment transmits a signal making the cell aware of its completion. In normal sporulation, σ^G is produced before engulfment is completed, but is held inactive [20]. Activation requires a σ^E signal from the mother cell and transcription directed by the forespore-specific, σ^F [38,39]. In recent studies, σ^G was expressed and activated in the forespore after septum formation without the requirements of σ^E or the completion of engulfment [40]. Ordinarily, σ^E is required for *spoIIIG* transcription and σ^G activation. This construct was made by deleting *spoIIIE* so that only the "origin-proximal" 30% of the chromosome would be pumped into the forespore. It is also necessary that *spoIIIG* be made part of this 30% of the chromosome so its transcription can be directed by σ^F. It was found that σ^G was expressed near wild type levels and that restoring σ^E activity did not affect these levels. These data suggest that σ^E does not function to control levels of σ^G, but rather to coordinate activation of σ^G with the completion of engulfment [40].

In the absence of BofA, SpoIVFB is uninhibited and can thus activate σ^K without the need for SpoIVB or σ^G activity. It is currently believed, however, that SpoIVFB activity is not regulated by the forespore checkpoint alone (Figure 4). It has been found that when *bofA* is deleted, SpoIVFB, and thus σ^K, can be activated without σ^G, bypassing the forespore checkpoint [36,37]. Jiang et al have found that when *spoIID* is mutated,

disabling engulfment, a *bofA* mutation is not sufficient for SpoIVFB and σ^K activation [35]. This suggests that the ability of SpoIVFB to activate σ^K is coupled independently to both σ^G activity, via the forespore checkpoint, and the completion of engulfment, deemed the engulfment checkpoint (Figure 4). The mechanism by which engulfment effects the activation of SpoIVFB is as yet unknown.

Another model by which engulfment controls activation of σ^K has been proposed by Doan and Rudner [41]. This model suggests that when engulfment is perturbed, a degradative response is activated to proteolytically clear all proteins secreted into the intermembrane space. They show that SpoIVB, a protease responsible for SpoIVFB activation, fails to accumulate when engulfment is blocked. They state that this is a reversible process, and that SpoIVB can accumulate when engulfment is restored, thus restoring SpoIVFB and σ^K activation [41]. They believe that in this way, at the level of SpoIVB, engulfment acts as a morphological checkpoint for σ^K activation (Figure 4A).

Doan and Rudner [41] go on to address the model of Jiang et al [35] where a *bofA* mutation is not sufficient to activate σ^K in the absence of engulfment. Doan and Rudner suggest that the reason for this phenotype is not due to an engulfment checkpoint regulating SpoIVFB activity, but rather to instability and a significant reduction of SpoIVFB protein [41]. They show that in a *bofA* deletion background, SpoIVFB levels are significantly reduced, but still yield activation of σ^K due to a small amount of constitutively active SpoIVFB [21]. They analyzed SpoIVFB levels in *bofA* bypass strains also lacking *spoIIQ* or *spoIID* and suggested that in these strains, SpoIVFB levels were further reduced [41]. They propose that the lack of σ^K activation in these strains is

simply due to further reduced SpoIVFB levels, and do not signify the existence of a second, engulfment, checkpoint regulating SpoIVFB activity.

Here, we describe mutants that can bypass either the forespore or the engulfment checkpoint, and provide further evidence for an engulfment checkpoint directly regulating SpoIVFB activity. As yet, no mutants have been found that are able to bypass both of these checkpoints, indicating their separate nature. It will also be shown that SpoIVFB protein levels do not directly correlate with σ^K activity, and that there is, indeed, no further reduction in SpoIVFB levels in strains lacking *bofA* as compared with those lacking both *bofA* and *spoIID*.

C. Results – Fusion activation

i. Constructing *spoIVFAB* mutants

If σ^K is controlled by two separate checkpoints, then it should be possible to isolate mutants that bypass one or the other checkpoint. Point mutants in both SpoIVFA and SpoIVFB were previously created and screened that can bypass the requirement for the forespore checkpoint and the engulfment checkpoint, respectively (performed by Amber Dance).

To identify bypass of engulfment (Boe) mutants, mutagenized *spoIVFAB* plasmid was transformed into a *Bacillus subtilis* strain incapable of engulfment. This strain was deficient in *spoIID*, necessary for engulfment, and also *bofA*, so as to bypass the forespore checkpoint. This strain also carried a null *spoIVFAB* mutation. To test for σ^K activation, a *cotD-lacZ* fusion was used under control of σ^K. About 40,000 point mutants were screened on DSM-X-gal plates and only one boe point mutant was found in *spoIVFB* (performed by Amber Dance). This mutant contained a serine to glycine change at amino acid 260, SpoIVFB-S260G.

Bypass of forespore (Bof) mutants were screened in the same way, but mutant plasmids were instead transformed into a strain lacking wild-type *spoIVFAB* and *spoIIIG*, the gene for σ^G. This strain also contained the *cotD-lacZ* fusion to assess σ^K activity. A Bof point mutation in *spoIVFA*, containing a serine to leucine change at amino acid 80, SpoIVFA-S80L, was obtained (performed by Amber Dance).

An attempt was made to find mutants that bypassed both checkpoints, Bob mutants. Chromosomal DNA from various Bof mutants was transformed into a strain lacking wild-type *spoIVFAB*, *spoIID*, and *spoIIIG*, and also containing the *cotD-lacZ*

fusion. No bob mutants were obtained (performed by Amber Dance). This supports the idea that the forespore and engulfment checkpoints are two distinct mechanisms for controlling SpoIVFB and σ^K activity.

ii. σ^K activation by wild-type SpoIVFAB in various backgrounds

It has been demonstrated that a *bofA* mutation bypasses the requirement for σ^G activity and for SpoIVB to activate σ^K [35]. However, in the absence of engulfment, a *bofA* mutation is not sufficient to activate σ^K, suggesting the existence of dual checkpoints, forespore, and engulfment. An engulfment-defective mutant in *spoIID* also fails to activate σ^K [41], but this is likely due to an engulfment checkpoint, and not simply because it lacks σ^G activity.

We have reproduced each of these prior results. Using a beta-galactosidase activity assay (Materials and Methods) to measure the activity of a *cotD-lacZ* fusion, we have assessed σ^K activity in strains containing wild-type SpoIVFAB in various backgrounds. The fusion is activated in the wild-type SpoIVFAB strain (Figure 6), but when engulfment is impaired by a mutation in *spoIID*, the fusion is not activated to adequate levels (Figure 8). Placing wild-type SpoIVFAB in a strain lacking *bofA* bypasses the requirement for σ^G, or the forespore checkpoint, and allows for activation of the *cotD-lacZ* fusion (Figure 7). Fusion activation levels in this *bofA* deletion do not reach those of wild-type SpoIVFAB in a wild-type background. Also reproducible is the result that, wild-type SpoIVFAB in an engulfment-impaired background, is unable to activate the fusion even in the absence of *bofA* (Figure 9). This result supports the idea that two independent checkpoints govern SpoIVFB and thus, σ^K activation.

It has been shown that the SpoIIQ protein plays an important role in engulfment and is essential for engulfment-dependent σ^G activation [42]. SpoIIQ interacts with mother cell protein, SpoIIIAH, tethering it to the forespore membrane where it is required for σ^G activation [43,43]. Mutants in SpoIIQ also lacking *bofA* fail to complete engulfment [35]. It is thus interesting to see whether σ^K would be activated in the absence of SpoIIQ. Doan and Rudner have shown that mutants in *spoIIQ* fail to activate σ^K [41]. We have observed the same result in our *spoIIQ* deletion strain containing wild-type SpoIVFAB (Figure 10). This strain fails to activate the *cotD-lacZ* fusion. The *cotD-lacZ* fusion is also not activated by wild-type SpoIVFAB in a strain lacking *spoIIQ* and *bofA* (Figure 11). Even though *bofA* is deleted, since this strain cannot complete engulfment, it lends support to the existence of an engulfment checkpoint governing the activation of SpoIVFB.

iii. Bypassing the forespore checkpoint: FA-S80L

The ability to bypass the forespore checkpoint for SpoIVFB activation was tested utilizing a mutant in SpoIVFA, FA-S80L. However, it was thought that this bof phenotype could be due to a disruption of the interactions between SpoIVFB and BofA. Since SpoIVFA mediates the localization of the BofA/FA/FB complex to the outer forespore membrane [23], mutating amino acids necessary for this interaction would result in a constitutively active SpoIVFB. It was shown that SpoIVFA-S80L was able to properly recruit SpoIVFB-GFP to the outer forespore membrane (Amber Dance). However, GFP-(Δ27)BofA [21] was mislocalized and expressed at low intensity (Amber Dance). With BofA missing, SpoIVFB would be uninhibited. This accounts for FA-

S80L's bof phenotype and suggests that amino acid 80 is in a region necessary for the proper localization and interaction of BofA and SpoIVFB (Amber Dance).

This mutant is useful in demonstrating the existence of dual checkpoints in SpoIVFB activation. FA-S80L in a wild-type background allows for early activation of the *cotD-lacZ* fusion at t4 (Figure 6). Activation levels also highly exceed those of wild-type SpoIVFAB at t5 in a similar background. This can be attributed to FA-S80L's bof phenotype: since BofA is absent, SpoIVFB is uninhibited and can activate the fusion earlier. In a strain lacking *bofA*, FA-S80L allows activation of the *cotD-lacZ* fusion to levels higher than that of wild-type SpoIVFAB in the same background (Figure 7). In an engulfment-deficient background, FA-S80L, like wild-type SpoIVFAB in the same background, fails to permit activation of the *cotD-lacZ* fusion to adequate levels (Figure 8). Since FA-S80L is a bof mutant, the forespore checkpoint is already bypassed. By not being able to activate the fusion in a *spoIID* mutant strain, the existence of a second, engulfment checkpoint, is further validated. This idea is tested again by examining *cotD-lacZ* fusion activation in a strain with FA-S80L, lacking *bofA* and engulfment. Like wild-type SpoIVFAB in the same background, the fusion is not activated (Figure 9). Without engulfment, bypassing the forespore checkpoint is not enough to effect activation of σ^K. The engulfment checkpoint is essential for this activation.

Activation of the *cotD-lacZ* fusion was also tested in an FA-S80L strain lacking *spoIIQ*. Unlike wild-type strains in the same background, the FA-S80L mutation allows for activation of the fusion (Figure 10). This can be attributed to FA-S80L's bof phenotype. Even though SpoIIQ is necessary for σ^G activation [42], and thus the forespore checkpoint, this is already bypassed by FA-S80L. Since this strain still engulfs,

bypass of the forespore checkpoint is enough and the fusion can be activated. FA-S80L, like wild-type SpoIVFAB in the same background, does not support the activation of the *cotD-lacZ* fusion in a strain lacking *spoIIQ* and *bofA* (Figure 11). Even though FA-S80L is able to bypass the forespore checkpoint, strains lacking *spoIIQ* and *bofA* are unable to engulf. Thus, since FA-S80L cannot bypass the requirement for engulfment, the fusion is not activated. Once again, evidence for the engulfment checkpoint is established by this model.

iv. Bypassing the engulfment checkpoint: FB-S260G

SpoIVFB and BofA localization to the forespore membrane is mediated by SpoIVFA. It was theorized that FB-S260G's boe phenotype could be due to mislocalization, separating it from its inhibitor, BofA. An uninhibited SpoIVFB would be constitutively active, thus giving us the resulting phenotype. Proper localization of SpoIVFB and BofA was examined. It was found that in the SpoIVFB-S260G strain, FB-S260G-GFP and GFP-(Δ27)BofA [21] localize normally (Amber Dance). Since SpoIVFA is required to mediate this localization, it is believed that SpoIVFA was present in this complex as well. Thus, the boe phenotype is due to a change in signaling, not to mislocalization or an uninhibited SpoIVFB.

SpoIVFB-S260G is able to activate σ^K in multiple different backgrounds. In a wild-type background, FB-S260G activates the *cotD-lacZ* fusion around t4 and activity increases over the next three hours (Figure 6). Activation levels are only slightly lower than those of wild-type SpoIVFAB. In a strain lacking *bofA*, FB-S260G activates the fusion at levels significantly higher than those of wild-type SpoIVFAB in the same

background (Figure 7). This can be attributed to the *bofA* deletion and FB-S260G's boe phenotype. Deleting *bofA* makes the SpoIVFB protein constitutively active. Since it already bypasses the engulfment checkpoint, fusion activation can reach even higher levels. In an engulfment-defective strain, FB-S260G is unable to activate the *cotD-lacZ* fusion and levels are similar to those of wild-type SpoIVFAB in the same strain (Figure 8). Even though FB-S260G has a boe phenotype, this is not enough to activate the fusion when engulfment is absent. This result is due to the fact that BofA-mediated inhibition of FB-S260G is still intact. Since it can bypass the engulfment checkpoint, but not the forespore checkpoint, the fusion is not activated. Most importantly, in a strain lacking both engulfment and *bofA*, FB-S260G is able to activate the *cotD-lacZ* fusion, a feat impossible for both wild-type SpoIVFAB and FA-S80L in the same background (Figure 9). These data show that FB-S260G can bypass the engulfment checkpoint, but not the forespore checkpoint, presenting further confirmation for two, distinct and separable checkpoints for SpoIVFB and σ^K activation.

These results are further supported by testing for *cotD-lacZ* fusion activity in *spoIIQ* mutant strains. In a strain lacking *spoIIQ*, FB-S260G, like wild-type SpoIVFAB in the same strain, is unable to activate the fusion (Figure 10). This is due to the fact that since SpoIIQ is necessary for σ^G activation, BofA-inhibition of SpoIVFB, and thus the forespore checkpoint, would remain intact. This prevents activation of the fusion by FB-S260G in spite of it being able to bypass the engulfment checkpoint. In a strain lacking *spoIIQ* and *bofA*, FB-S260G activates the *cotD-lacZ* fusion early after resuspension, by t3. Activation levels are also extremely high (Figure 11). As previously stated, strains lacking *spoIIQ* and *bofA* are unable to complete engulfment. Since BofA is not present,

allowing for bypass of the forespore checkpoint, and FB-S260G can bypass the engulfment checkpoint, fusion activity in this strain is quite high. The high levels of activity and early activation in this strain are likely due to FB-S260G being uninhibited in the absence of BofA, and also able to bypass engulfment. The presence of two checkpoints is only more strongly established by these results.

D. Results – SpoIVFB protein levels do not directly correlate with σ^K activity

i. SpoIVFB protein levels and σ^K activity

It has previously been shown that in strains lacking *bofA*, levels of SpoIVFB are significantly reduced compared to wild-type [21,41]. It is suggested that in these mutants, pro-σ^K processing is "delicately balanced:" that although SpoIVFB is constitutively active in the absence of *bofA*, there is barely enough SpoIVFB protein present to support activation of σ^K [41]. It is then reported that SpoIVFB levels are further reduced in strains lacking both *bofA* and either *spoIID* or *spoIIQ* [41]. This study thus supports the idea that the lack of σ^K activity in engulfment-impaired strains also lacking *bofA* is due to instability of the SpoIVFB protein, not due to the presence of an engulfment checkpoint preventing activation [41]. It is logical then to say that, if this hypothesis is true, σ^K activation should show a direct correlation with SpoIVFB protein levels. That is, lower protein levels would yield less σ^K activity, and higher protein levels would yield greater σ^K activity.

To test these preceding results and this hypothesis, SpoIVFB protein levels were analyzed in all strains mentioned in the above sections. To do this, Western blotting of each strain was performed (Materials and Methods). Membranes were probed with anti-

SpoIVFB antibodies followed by an anti-rabbit Cy5 fluorescent secondary antibody. The membranes were then scanned for fluorescence using a Typhoon scanner (Materials and Methods). Band intensity for different strains was quantified. It must be remembered that, since each membrane is different and there is normalization of intensity for each scanned membrane, intensity numbers shown in resultant graphs are only relative, not absolute. Thus, only strains in the same membrane can be compared.

ii. Wild-type SpoIVFB levels in various backgrounds

We tried to verify the result of Doan and Rudner [41] that perturbing engulfment in a strain lacking *bofA* causes an additional decrease in SpoIVFB protein levels. Our results directly contradict those of Doan and Rudner. We compared SpoIVFB levels in our SpoIID mutant (IID298), their mutant (Tn917), and another lab mutant in SpoIID (Δ*IID*), all in a background with wild-type SpoIVFAB where *bofA* is absent. These strains were compared with a strain lacking *bofA* only. SpoIVFB protein levels in all of the engulfment-minus and *bofA*-minus strains are actually **higher** than levels in a strain lacking *bofA* only (Figure 12). This includes the Doan and Rudner construct and another of our lab constructs. Our main engulfment-minus construct, IID298, also lacking *bofA*, even has slightly higher SpoIVFB levels than the other two constructs. This shows that the reason for σ^K not being activated in these strains, even though it is active in a *bofA* deletion, is not due to a further decrease in protein levels, but rather, due to the inability of wild-type SpoIVFB protein to bypass the engulfment checkpoint, even when constitutively active.

It has been observed that when *bofA* is present in an engulfment-defective strain, there is no reduction in SpoIVFB protein levels [41]. We compared SpoIVFB levels in each of the three SpoIID constructs listed above in the presence of *bofA*. In a normal Western blot utilizing ECL-plus and visualizing on x-ray film, SpoIVFB levels in the engulfment-defective strains appears exactly the same as those in a wild-type strain (data not shown). To double-check this finding, we utilized the Typhoon scanner once again and quantified the bands. It seems as though engulfment-defective mutants have slightly less SpoIVFB protein than wild-type (Figure 13). This result is most likely due to the Typhoon scanner being more sensitive and able to pick up more subtle differences in band intensities than can be noticed on x-ray film. In spite of this result, the difference in SpoIVFB levels in these strains is not significant. The Tn917 and ΔIID strains have lower SpoIVFB levels than the IID298 strain, which has levels slightly lower than wild-type (Figure 13). Since no engulfment-defective strain can activate σ^K in the presence of *bofA*, this difference in SpoIVFB levels is insignificant.

Since our IID298 construct is not significantly different than the Tn917 or ΔIID constructs, we went on to compare SpoIVFB protein levels in strains lacking *bofA* and either SpoIID or *spoIIQ* (*bofA* and *spoIIQ* double mutants cannot complete engulfment). (Henceforth, SpoIID mutants referred to are IID298). It is once again shown that SpoIVFB levels in an engulfment-defective strain also lacking *bofA* are higher than those in a strain lacking only *bofA* (Figure 14). Additionally, in a strain where both *bofA* and *spoIIQ* are absent, SpoIVFB levels are similar to levels in the strain lacking only *bofA* (Figure 14). These results directly contradict a finding by Doan and Rudner [41] that there is a further reduction in SpoIVFB levels in *bofA*-minus/ SpoIIQ-minus strains when

compared to the *bofA*-minus only strain [41]. Since the *bofA*-minus strain is capable of activating σ^K to nearly 50% of wild-type levels (Table 1) while having low levels of SpoIVFB protein, our results further show that levels of SpoIVFB are irrelevant. Processing of σ^K is not delicately balanced by SpoIVFB levels, but rather controlled by two, separate checkpoints. Strains lacking both *bofA* and SpoIID or SpoIIQ cannot activate σ^K because, although the forespore checkpoint is bypassed, they are unable to bypass the engulfment requirement for σ^K activation.

To further test our model, SpoIVFB levels were analyzed in strains lacking only SpoIID or SpoIIQ, in comparison with a *bofA* deletion. Consistent with our earlier results, it can be seen that SpoIVFB levels in a strain lacking *spoIID* are slightly lower than those in a wild-type background (Figure 15). Deleting *spoIIQ* appears to have a greater influence on SpoIVFB levels, as this strain has lower levels than both wild-type and SpoIID-minus (Figure 15). Since SpoIIQ has many functions, including IIIAH localization, and FA and SpoIVFB recruitment, in addition to being important for σ^K activation, it is logical that its deletion could lead to decreased levels of SpoIVFB. Once again, the *bofA* deletion strain has the lowest SpoIVFB levels, yet is the only strain that can activate σ^K. Wild-type SpoIVFB in strains lacking SpoIID or SpoIIQ is unable to bypass the forespore checkpoint in the presence of *bofA*, and is also inhibited by the engulfment checkpoint. This, and not SpoIVFB protein levels, explains their lack of σ^K activity.

iii. SpoIVFB levels: wild-type SpoIVFB versus FB-S260G and FA-S80L

Anticipating further assessment of SpoIVFB levels in strains containing mutants in SpoIVFA and SpoIVFB (in other backgrounds), we have also compared SpoIVFB levels in wild-type strains containing either wild-type SpoIVFB, FB-S260G, or FA-S80L.

In a wild-type background, a strain containing FB-S260G has slightly higher levels than wild-type at t4, but SpoIVFB levels are otherwise similar between these two strains (Figure 16). A strain containing FA-S80L has SpoIVFB levels similar to those in wild-type, but these levels plummet drastically after t3, resembling a *bofA* deletion strain (Figure 16). This can be accounted for by FA-S80L's bof phenotype. Since it bypasses the forespore checkpoint even in the presence of *bofA*, it has lower levels of SpoIVFB protein, but is still able to activate σ^K. A summary of each mutant in all various backgrounds is included in Table 1. SpoIVFB levels do not correlate directly with levels of σ^K activity. This can be seen by comparing the data in Table 1 with relative levels of SpoIVFB protein in each strain. Although FB-S260G has slightly higher levels of SpoIVFB protein than wild-type, σ^K activity is lower in this strain (137.6 units in FB-S260G versus 189.4 units in wild-type) (Table 1). If the Doan/Rudner [41] explanation for activity were correct, one would expect that higher SpoIVFB levels, thus a more stabilized protein, would yield an increase in σ^K activity. It can easily be seen that this is not the case. The converse is also untrue. A reduction in levels of SpoIVFB does not equate to a reduction in σ^K activity. SpoIVFB levels in a strain containing FA-S80L are drastically lower than those in wild-type (Figure 16). In spite of this, σ^K activity is drastically higher in FA-S80L than in wild-type (417.2 units in FA-S80L versus 189.4 units in wild-type) (Table 1). One might explain that this result is due to FA-S80L's bof phenotype: that since the SpoIVFB protein is unregulated, it can support σ^K activity. If

this were the only explanation, however, one would not expect such high levels of σ^K activity. In the presence of such low levels of SpoIVFB, Doan and Rudner would expect it to barely activate σ^K, much like it does in strains lacking *bofA*. It seems as though SpoIVFB activity may even be higher in the FA-S80L strain.

SpoIVFB levels were also measured in strains lacking *bofA* for each mutant. SpoIVFB levels in all strains, wild-type SpoIVFAB, FB-S260G, and FA-S80L in a *bofA* deletion seemed to follow the same trend, and were almost exactly the same (Figure 17). Each strain's SpoIVFB levels were significantly lower than those of wild-type. In spite of each strain having extremely low SpoIVFB levels, they all activate σ^K (Table 1). Units of activity in the *bofA* deletion background are: wild-type SpoIVFAB – 95.2, FB-S260G – 245.6, FA-S80L – 155.9 (Table 1). Since each strain has nearly identical levels of SpoIVFB, differences in σ^K activity must be due to each strain's respective phenotype, and thus due to separable checkpoints still in place. Wild-type SpoIVFAB is still controlled by the engulfment checkpoint, FB-S260G bypasses engulfment, and FA-S80L bypasses the forespore checkpoint. Each strain is also constitutively active due to the absence of BofA. In addition to being governed by dual checkpoints, it seems that each strain has differential SpoIVFB protein activity. This is most likely due to some inhibition mechanism that has been made obsolete by mutations in their respective amino acid residues.

iv. SpoIVFB levels: FB-S260G in various backgrounds

SpoIVFB levels were measured in strains containing the FB-S260G mutation in order to further prove the lack of any correlation between σ^K activity and SpoIVFB

levels. We compared FB-S260G strains lacking *bofA*, *spoIIQ*, or SpoIID. Of these strains, the *bofA*-minus strain is shown, once again, to have the lowest SpoIVFB levels (Figure 18). Deleting *bofA* significantly reduces SpoIVFB levels in a strain containing FB-S260G when compared to FB-S260G in a wild-type background. In spite of this, the *bofA* deletion strain is able to activate the *cotD-lacZ* fusion to very high levels (245.6 units) (Table 1). This is most likely due to the ability of this mutant to bypass the engulfment checkpoint, and that it is constitutively active in the absence of BofA.

In an engulfment-defective strain containing FB-S260G, SpoIVFB levels are only slightly lower than those in the wild-type FB-S260G strain (Figure 18). In spite of these higher levels of SpoIVFB protein (when compared to *bofA*-minus), this strain is still unable to activate the *cotD-lacZ* fusion (Table 1). This gives evidence for the separate nature of the two checkpoints governing SpoIVFB and σ^K activity. Even though this mutant is able to bypass the engulfment checkpoint, it cannot activate the *cotD-lacZ* fusion while *bofA* is still in place. Thus, the presence of the forespore checkpoint here is preventing activation of the *cotD-lacZ* fusion. A similar case can be seen in the FB-S260G strain lacking *spoIIQ*. While SpoIVFB levels in this strain start out close to those of wild-type FB-S260G, they decrease significantly after t3 to less than 50% of wild-type levels (Figure 18). Like the engulfment-defective FB-S260G strain, the SpoIIQ-minus strain also cannot activate the *cotD-lacZ* fusion (Table 1). It is likely that this result is not due to the decrease in SpoIVFB levels, but rather to the forespore checkpoint remaining intact and preventing activation of the fusion.

Strengthening the argument for an engulfment checkpoint that also governs SpoIVFB and σ^K activity are the FB-S260G mutants lacking both *bofA* and *spoIIQ* or

SpoIID. SpoIVFB levels in the FB-S260G strain lacking both *bofA* and engulfment are only slightly higher than levels in a mutant lacking only *bofA* (Figure 19). In an FB-S260G mutant lacking both *bofA* and *spoIIQ*, SpoIVFB levels are very slightly lower than the mutant lacking only *bofA* (Figure 19). All three of these strains have SpoIVFB levels that are significantly lower than levels in a wild-type strain containing FB-S260G. In spite of these extremely low SpoIVFB levels, these engulfment-defective, *bofA*-minus strains are able to activate the *cotD-lacZ* fusion. The FB-S260G strain lacking *bofA* and SpoIID activates the fusion to 44.4 units, while the strain lacking *bofA* and *spoIIQ* activates the fusion to 202.0 units (Table 1). Differences in activation between these two strains are mostly likely due to other effects of deleting *spoIIQ*. Since *spoIIQ* is important for engulfment and σ^G activation, it is possible that its deletion causes a disruption of multiple components of both the engulfment and forespore checkpoints. With both checkpoints inoperative and with SpoIVFB constitutively active (due to BofA's absence), the fusion can be activated to higher levels than in the mutant lacking *bofA* and SpoIID.

The key point to be taken from these results is that, even with extremely low SpoIVFB levels, the FB-S260G mutant can activate the *cotD-lacZ* fusion, and thus bypass the engulfment checkpoint in the absence of *bofA*. Since it is unable to bypass engulfment in the presence of *bofA*, it is thus shown to be a bypass of engulfment, and not a bypass of forespore mutant. This also lends greater credence to the notion that these are independently operating checkpoints. It is also shown that activation of σ^K is independent from SpoIVFB protein levels.

v. SpoIVFB levels: FA-S80L in various backgrounds

To further investigate the existence of dual checkpoints and the lack of a relationship between SpoIVFB levels and σ^K activity, SpoIVFB levels were measured in strains containing the FA-S80L mutation. First, we compared strains containing FA-S80L and lacking *bofA*, *spoIIQ*, or SpoIID. It was found that, when compared to FA-S80L in a wild-type background, SpoIVFB levels decrease slightly in a strain lacking SpoIID (Figure 20). Since this strain is unable to activate the *cotD-lacZ* fusion (Table 1), even though it has a bof phenotype and relatively high SpoIVFB levels, this result is most likely due to its inability to bypass the engulfment checkpoint. Like strains containing wild-type SpoIVFAB and FB-S260G, deleting *bofA* in an FA-S80L strain causes a significant decrease in SpoIVFB levels (Figure 20). In spite of these decreased levels, this strain is able to activate the *cotD-lacZ* fusion to 155.9 units. This result further shows the lack of correlation between SpoIVFB levels and σ^K activity. Unlike wild-type SpoIVFAB and FB-S260G, deleting *spoIIQ* in an FA-S80L mutant causes SpoIVFB levels to decrease to slightly lower than in a mutant where *bofA* is deleted (Figure 20). In this strain, BofA is present, but mislocalized. Even though *spoIIQ* is deleted, SpoIID, SpoIIM, and SpoIIP are still present to allow the cell to engulf. In this way, the *spoIIQ* deletion's primary effects are on the forespore checkpoint, affecting σ^G activation. In spite of extremely low SpoIVFB levels, the FA-S80L strain lacking *spoIIQ* is able to activate the *cotD-lacZ* fusion to 53.4 units (Table 1). This result shows that this strain is able to bypass the forespore checkpoint for σ^K activation, and that SpoIVFB levels are inconsequential.

SpoIVFB levels were tested in FA-S80L strains lacking *bofA* and either *spoIIQ* or SpoIID. Of these strains, the FA-S80L strain lacking *bofA* had the lowest SpoIVFB levels (Figure 21). Slightly higher SpoIVFB levels were observed in the FA-S80L strain lacking both *bofA* and *spoIIQ* (Figure 21). SpoIVFB levels were appreciably higher in the FA-S80L strain lacking both *bofA* and SpoIID. Although SpoIVFB levels are higher in the strains lacking both *bofA* and *spoIIQ* or SpoIID (as opposed to the strain lacking only *bofA*), neither of these strains is able to activate the *cotD-lacZ* fusion (Table 1). The implications of these results are two-fold: the FA-S80L mutant can only bypass the forespore checkpoint and not the engulfment checkpoint (as the double-mutant strains do not engulf). Also, higher SpoIVFB levels do not equate to higher levels of fusion activation.

E. Discussion and conclusion

The forespore pathway for the activation of σ^K and SpoIVFB has been well-characterized [19, 21-25]. Our results verify the existence of a second, distinct pathway that also governs SpoIVFB and σ^K activation: the engulfment checkpoint. If only one checkpoint existed, or if these two checkpoints were not separable, it should have been possible to isolate mutants that bypassed both checkpoints, and could activate σ^K without σ^G or engulfment. Previous studies show that this is not possible, and that mutants found can bypass the requirements for either σ^G or engulfment, but not for both. This indicates that the checkpoints function via different pathways. Also, we have found that σ^K activity does not correlate directly with SpoIVFB protein levels. If this were true, a decrease in SpoIVFB levels should always result in lower σ^K activity, and vice versa.

This was found to not always be true, as some strains which had low SpoIVFB levels exhibited high σ^K activity. Indeed, dual checkpoints, and not SpoIVFB levels, govern σ^K activity through regulation of the **activity** of SpoIVFB, and not only through its accumulation levels.

i. SpoIVFA is involved in receipt of the forespore signal

It has been shown that SpoIVFA is important for the localization of BofA and SpoIVFB, and for mediating the interaction between BofA and SpoIVFB (Figure 3) [21]. If FA and BofA are not present, the complex is mislocalized. It is possible that if mislocalized, SpoIVFB could be targeted for degradation, resulting in lower levels of SpoIVFB protein in strains lacking *bofA*, or containing a mutated SpoIVFA. Our results for mutants containing FA-S80L are consistent with such a hypothesis. Strains containing FA-S80L have lower levels of SpoIVFB. This is most likely due to mislocalization of the whole σ^K processing complex. Without proper recruitment to the outer forespore membrane, it is possible that rogue SpoIVFB protein is degraded. SpoIVFB protein that happens to find its way to its proper position, would be constitutively active without SpoIVFA to mediate its inhibition by BofA. It has been shown that SpoIVFA requires the presence of *bofA* to localize the complex [44]. Our hypothesis would also help explain such low SpoIVFB levels in strains lacking *bofA*. It is proposed that SpoIVFA is involved in the receipt of the forespore signal for σ^K activation. In our model, normal SpoIVFA mediates BofA inhibition of SpoIVFB and proper localization of the complex. The forespore signal leads to SpoIVB cleavage of SpoIVFA, and release of SpoIVFB inhibition. When SpoIVFA is mutated, or when *bofA*

is deleted, the entire complex mislocalizes, and improperly-positioned SpoIVFB is degraded. The SpoIVFB that does make it into the correct position is able to activate σ^K. It is thus thought that the forespore checkpoint regulates σ^K activation by relieving inhibition and controlling protein levels of SpoIVFB.

ii. SpoIVFB is involved in the receipt of the engulfment signal

Only one mutant was found to bypass the engulfment checkpoint for σ^K activity: FB-S260G. It is likely that the serine residue at position 260 is involved in receiving a signal sent through the engulfment pathway, activating SpoIVFB, or increasing its activity. SpoIVFB-S260G was found to be able to activate a *cotD-lacZ* fusion in the absence of both *bofA* and *spoIIQ* or SpoIID (even though these strains have low levels of SpoIVFB). Deleting *bofA* is necessary to bypass the forespore checkpoint. If BofA is present, SpoIVFB will be inhibited. By replacing the S260 residue with glycine, this mutant is able to bypass the engulfment requirement for activation. In the absence of *bofA* only, the FB-S260G mutant was found to have higher *cotD-lacZ* fusion activity than its wild-type SpoIVFAB counterpart in the same background. This suggests that by replacing the serine at position 260 with a glycine imparts the SpoIVFB protein with higher activity. Wild-type SpoIVFAB and FA-S80L in strains lacking both *bofA* and *spoIIQ* or SpoIID are unable to activate a *cotD-lacZ* fusion (even with similar SpoIVFB levels to those in FB-S260G in the same background). Even though the low levels of SpoIVFB in these strains are uninhibited, they still are unable to activate the fusion. This is assumed to be because the SpoIVFB protein has not been activated via an unknown engulfment checkpoint-dependent mechanism. It is thus concluded that the engulfment

checkpoint regulates σ^K activity by controlling specific activity of the SpoIVFB protein itself, through an unknown mechanism (Figure 4B).

In conclusion, SpoIVFB activity and thus σ^K activation are regulated by two independent checkpoints: The forespore checkpoint, which regulates SpoIVFB protein levels, and the engulfment checkpoint, which regulates SpoIVFB protein activity. These dual checkpoints assure that both the forespore and mother cell are prepared for σ^K activation.

F. Suggested future experiments

Utilizing the mutants from this study, it would be advantageous to see if mutating specific residues would result in the same bof or boe phenotypes previously described. Random mutagenesis on residue 80 of SpoIVFA should be performed to see if other mutants can be created with the same or stronger bof phenotype. It is also interesting to see if random mutagenesis can be performed on residue 260 of SpoIVFB to create any other boe mutants. These mutants can be used to further test the hypotheses put forth above.

It has been proposed that engulfment regulates σ^K activity not at the level of SpoIVFB, but at the level of SpoIVB. It is thought that perturbing engulfment causes the proteolytic clearance of SpoIVB and all secreted proteins, preventing activation of SpoIVFB, and thus σ^K [41]. It is important then, to test levels of the SpoIVB protein in each of the mutants we have characterized. If SpoIVFB and σ^K activation can be achieved without SpoIVB, further evidence for dual checkpoints will be garnered.

It has previously been shown that SpoIIQ is important for proper localization of SpoIIIAH and these two proteins also recruit SpoIVFA and SpoIVFB to the septum [35, 43-44]. It would be interesting then to see the effects of a SpoIIIAH deletion on SpoIVFB protein levels, SpoIVFA, SpoIVFB, and BofA localization, and σ^K activity. It would also be important to test SpoIVB levels in these strains, as SpoIVB is known to cleave SpoIIQ.

Each of these experiments would be useful to completely elucidate the mechanisms employed by the mother cell and the forespore to control SpoIVFB and σ^K activation.

G. Materials and Methods

i. Strain construction

B. subtilis strains (Appendix B) were constructed by transformation [45]. Chromosomal DNA from specific strains (wild-type or mutant in *spoIVFA* or *spoIVFB*) with a deletion of wild-type *spoIVFAB* was added to competent cells whose chromosome lacked wild-type *spoIVFAB* and contained the desired background (ex: IID298, Δ*bofA*, *cotD-lacZ*, Δ*spoIIQ*, etc). Following introduction into the *B. subtilis* chromosome, recombinants were checked for their antibiotic resistances, ability to form spores, activation of *cotD-lacZ*, and the inactivation of *amyE*.

ii. β-galactosidase activity assay

Sporulation was induced by resuspension at 37°C [46]. The cells were resuspended in 25 ml media (for Western blotting and β-galactosidase assay) and shaken in flasks. One ml samples were collected each hour at 1 through 7 hours after the onset of sporulation. Samples were processed and β-galactosidase assays were performed as described [47,48]. Data from repeated experiments were averaged and graphs were prepared using Microsoft Excel.

iii. Western Blotting

Bacterial cultures were induced to sporulate by resuspension. One ml samples were taken into 110µl 50% trichloroacetic acid (TCA) each hour at 1 through 7 hours after the onset of sporulation. Samples were prepared [48], heated for 10min at 42°C, and loaded on a 12.5% SDS-polyacrylamide gel. Proteins were transferred to PVDF

[49], blocked with 5% nonfat dry milk in PBS-0.5% Tween-20, and probed with a 1:1000 dilution of rabbit polyclonal anti-SpoIVFA (1:3000 when in conjunction with chemiluminescent secondary) or anti-SpoIVFB antibodies. Each membrane was probed with a secondary antibody of 1:3000 HRP-conjugated anti-rabbit IgG (visualized with ECL-plus [Amersham]), or 1:2000 anti-rabbit Cy5 fluorescent antibody (for protein level quantification).

iv. Quantification of SpoIVFB protein levels

Western blotting was performed as described above using an anti-rabbit Cy5 fluorescent secondary antibody. The membranes were then scanned using a Typhoon scanner and a setting specific for Cy5 fluorescence at 500PMT. The resulting image was quantified using ImageQuant software and the band intensity volume data was imported to Microsoft Excel. Membrane background values were subtracted from band intensity values for bands of each strain. Graphs were then made in Microsoft Excel using the intensity data. Upon scanning, the Typhoon scanner seems to normalize pictures according to the highest intensity band. In this way, it helps prevent over-exposure and maintain the intensity relationship between bands. Since each membrane is unique and has different background values, band intensities for varying strains can only be compared to strains that are on the same membrane. Thus, band intensity numbers are relative values, not absolute.

H. Figures and Tables

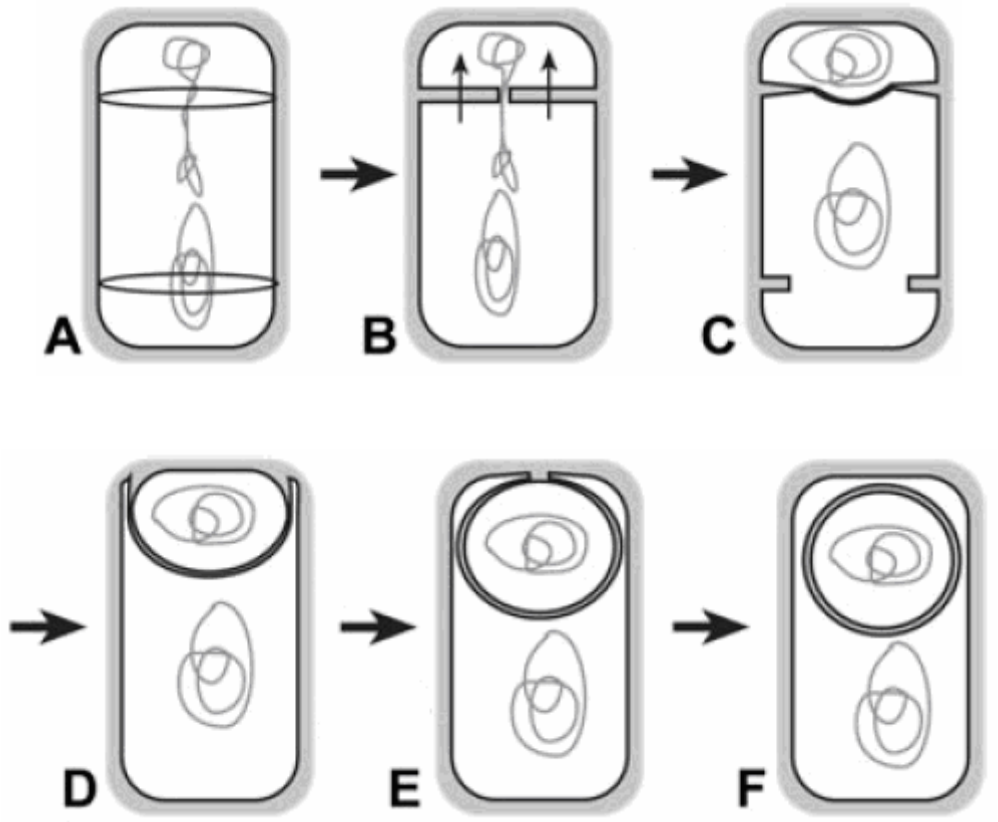

Figure 1. Sporulation
(A,B) The sporulating cell divides asymmetrically, forming the smaller forespore and larger mother cell. (B) The chromosome is pumped into the forespore. (C) SpoIID hydrolyzes septal peptidoglycan, pulling along the mother cell membranes. (D,E) The mother cell membranes migrate around the forespore. (F) The membranes meet and fuse at the cell pole. Following this is the formation of the spore coat and spore release from the lysed mother cell. Modified with permission from [5].

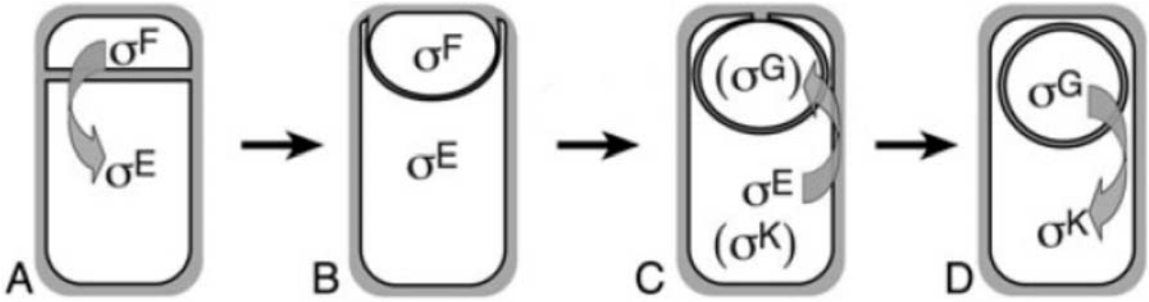

Figure 2. Transcription factor activation during sporulation
(A) σ^F in the forespore is activated first. (A,B) Genes are activated that allow for σ^E activation in the mother cell. (C) σ^G and σ^K are present in their respective compartments, but remain inactive until after engulfment. (D) σ^G initiates the forespore checkpoint which leads to σ^K activation in the mother cell. Used with permission from [35].

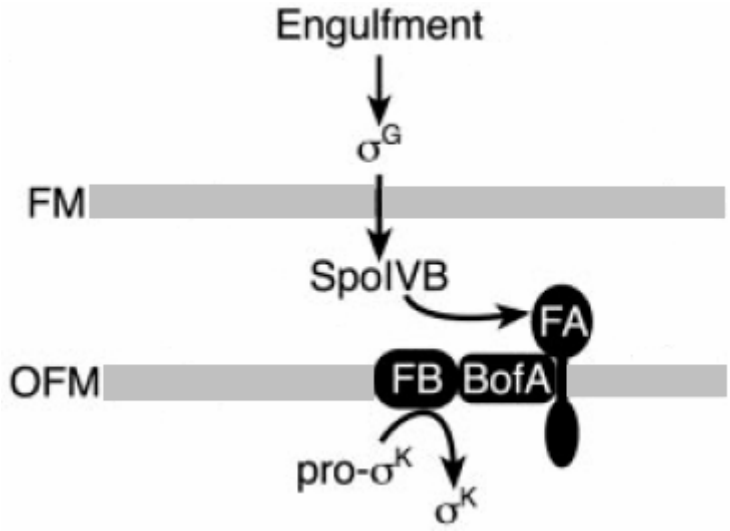

Figure 3. The forespore checkpoint
After engulfment, σ^G leads to upregulation of *spoIVB* causing high levels of SpoIVB protein to accumulate. SpoIVB is secreted into the intramembrane space (between the mother cell and forespore) and cleaves SpoIVFA. This cleavage relieves the BofA-mediated inhibition of SpoIVFB. SpoIVFB then executes regulated intramembrane proteolysis (RIP) of pro- σ^K into active σ^K, which is released into the mother cell. (It is believed that after cleavage of FA by SpoIVB, another protease, CtpB, cleaves FA and BofA). Modified with permission from [26].

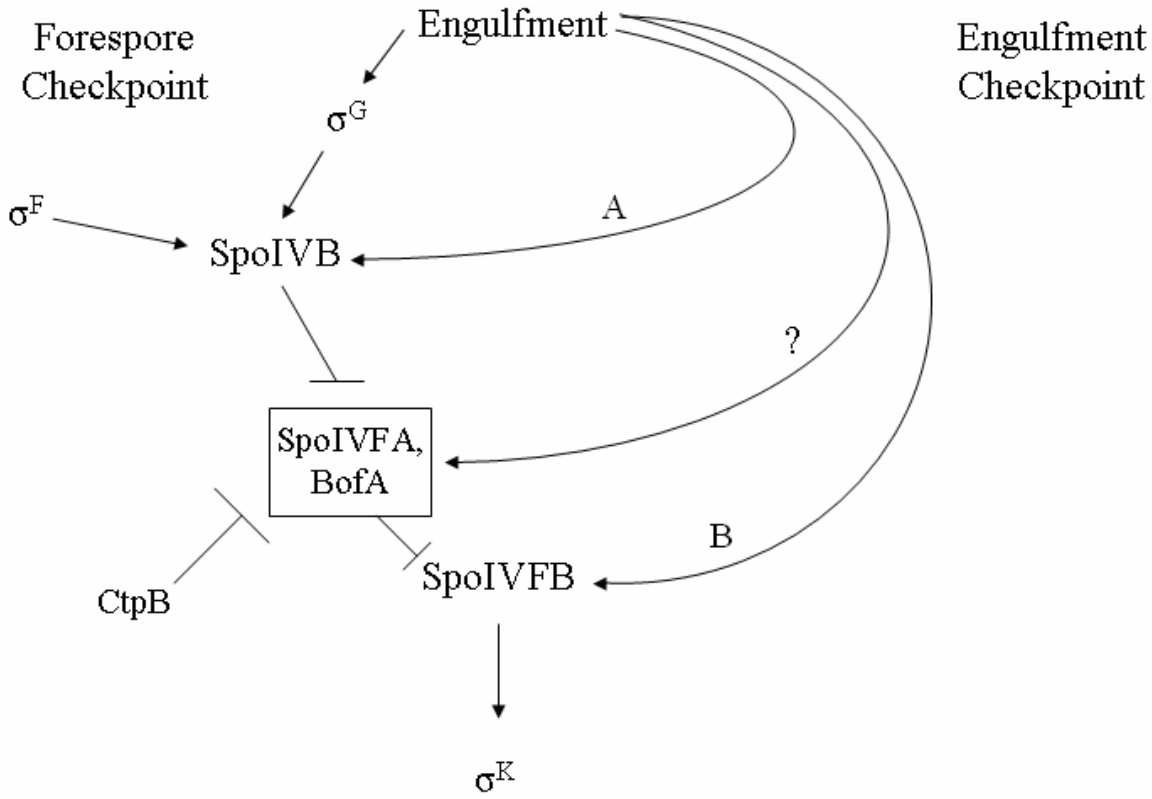

Figure 4. Two independent checkpoints
The forespore checkpoint is well characterized. It begins with σ^G activation, and SpoIVB production. Although low levels of SpoIVB are produced under control of σ^F, its levels are greatly increased under σ^G. SpoIVB cleaves SpoIVFA, relieving inhibition of SpoIVFB by BofA. It is also believed that CtpB cleaves FA and BofA. SpoIVFB then cleaves pro- σ^K into active σ^K which is released into the mother cell. (A) One engulfment model suggests that engulfment regulates σ^K processing by preventing accumulation of SpoIVB and other proteins secreted into the intramembrane space if engulfment is perturbed. (B) Another engulfment model proposes that engulfment regulates σ^K processing by regulating the SpoIVFB processing enzyme. (?) Amid so many models, it is possible that engulfment could regulate σ^K activity by directly or indirectly regulating SpoIVFA or BofA, two key components in SpoIVFB regulation. It is possible that mechanisms exist to support all three potential models of the engulfment checkpoint.

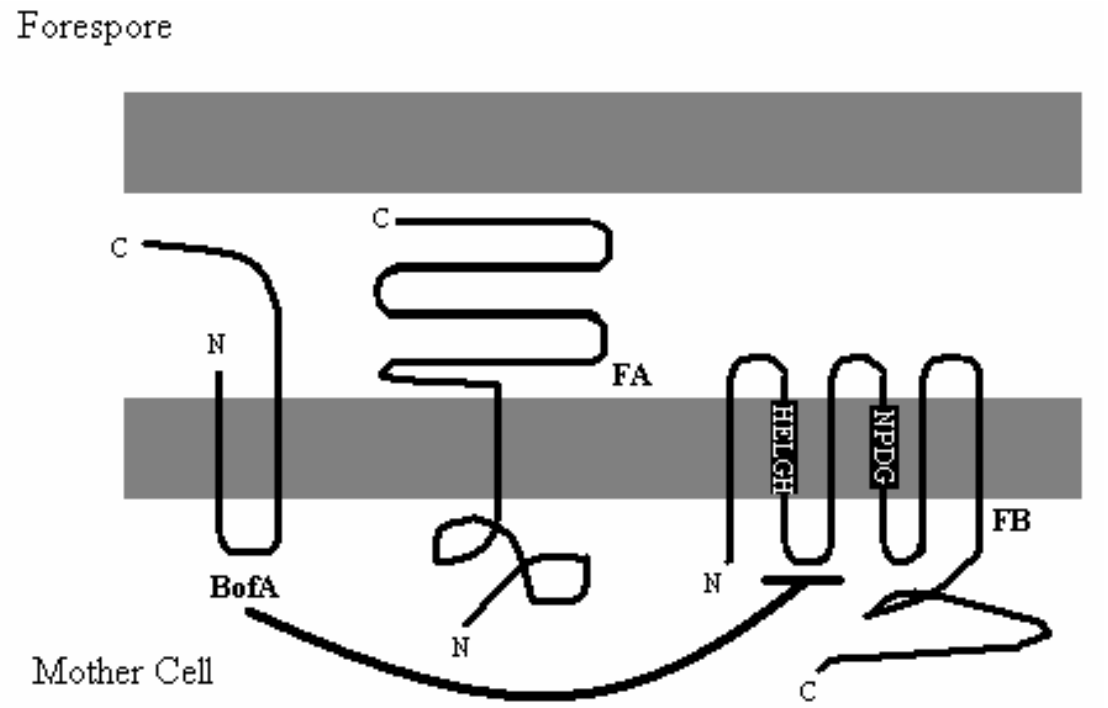

Figure 5. The BofA/SpoIVFA/FB Complex
While in a complex localized by SpoIVFA, BofA inhibits the zinc metalloprotease, SpoIVFB. A member of the S2P family, SpoIVFB has two conserved, transmembrane domains. The HExxH motif is conserved throughout zinc metalloproteases. Here, HELGH and NPDG are active-site domains and are responsible for the regulated intramembrane proteolysis of σ^K by SpoIVFB. (Not shown: pro- σ^K is also tethered in the outer forespore membrane).

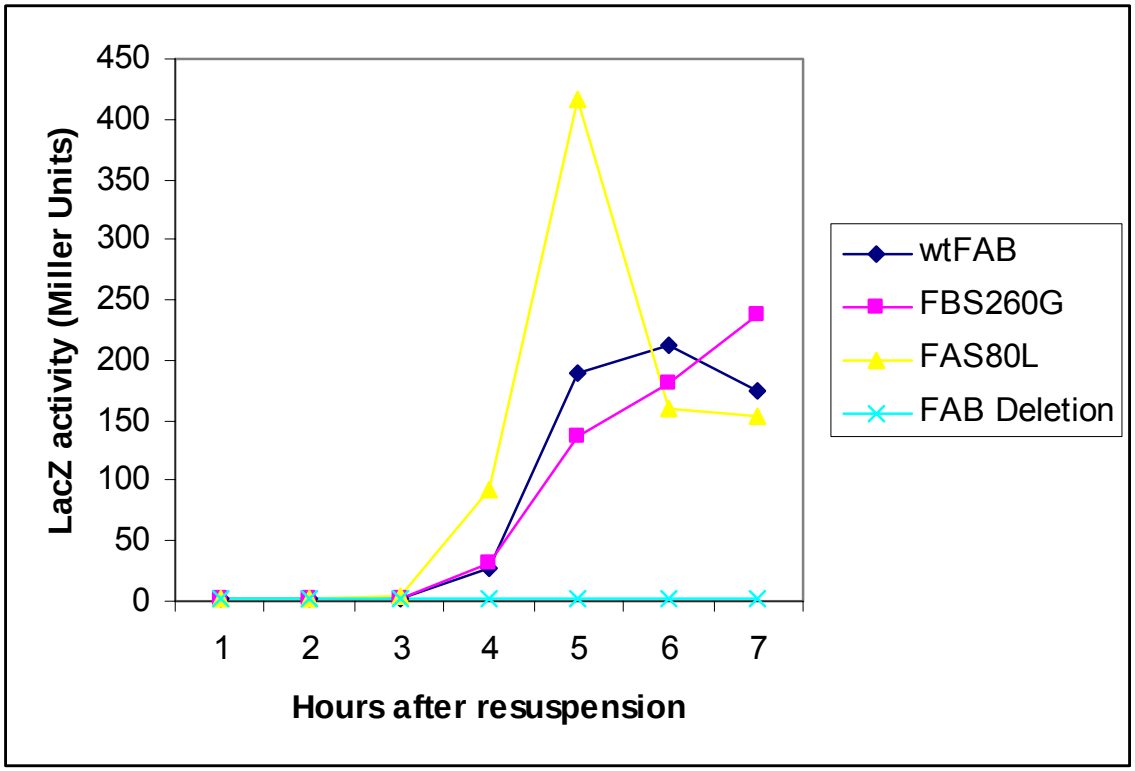

Figure 6. Activity of the *cotD-lacZ* fusion in a wild type background
Wild-type SpoIVFAB is able to activate the *cotD-lacZ* fusion in a wild-type background (diamonds). The FB-S260G mutant also activates the fusion in the same background but does not reach wild-type levels (squares). The FA-S80L mutant allows for early activation of the *cotD-lacZ* fusion at t4, and its levels highly exceed those of wild-type SpoIVFAB in a wild-type background at t5 (triangles). A *spoIVFAB* deletion mutant was used as a negative control showing no activity of the fusion (x's).

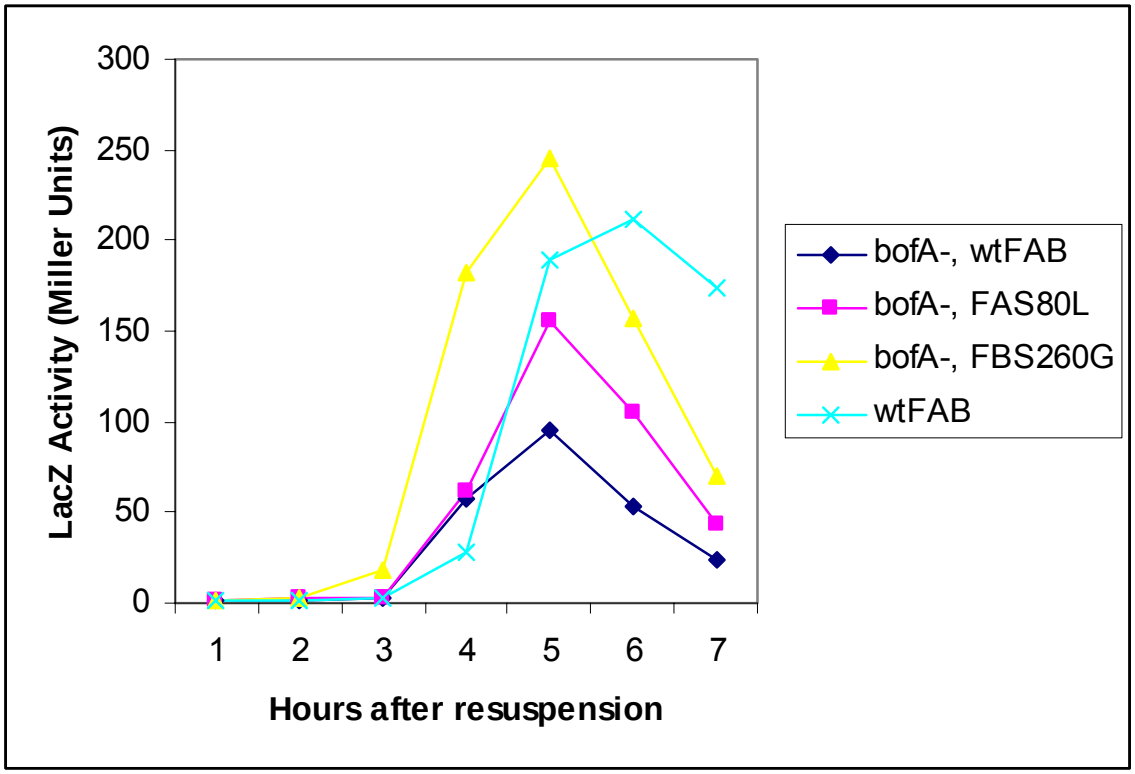

Figure 7. Activity of the *cotD-lacZ* fusion in a *bofA* deletion background
All three strains, wild-type SpoIVFAB (diamonds), FB-S260G (triangles), and FA-S80L (squares) are able to activate the *cotD-lacZ* fusion in the absence of *bofA*. At t5, activity of the fusion is greater than wild-type levels in the FB-S260G strain (both in the absence of *bofA*. Fusion activity at t5 in wild-type SpoIVFAB and FA-S80L (lacking *bofA*) does not reach wild-type levels. Wild-type SpoIVFAB is used for a comparison of fusion activity (x's).

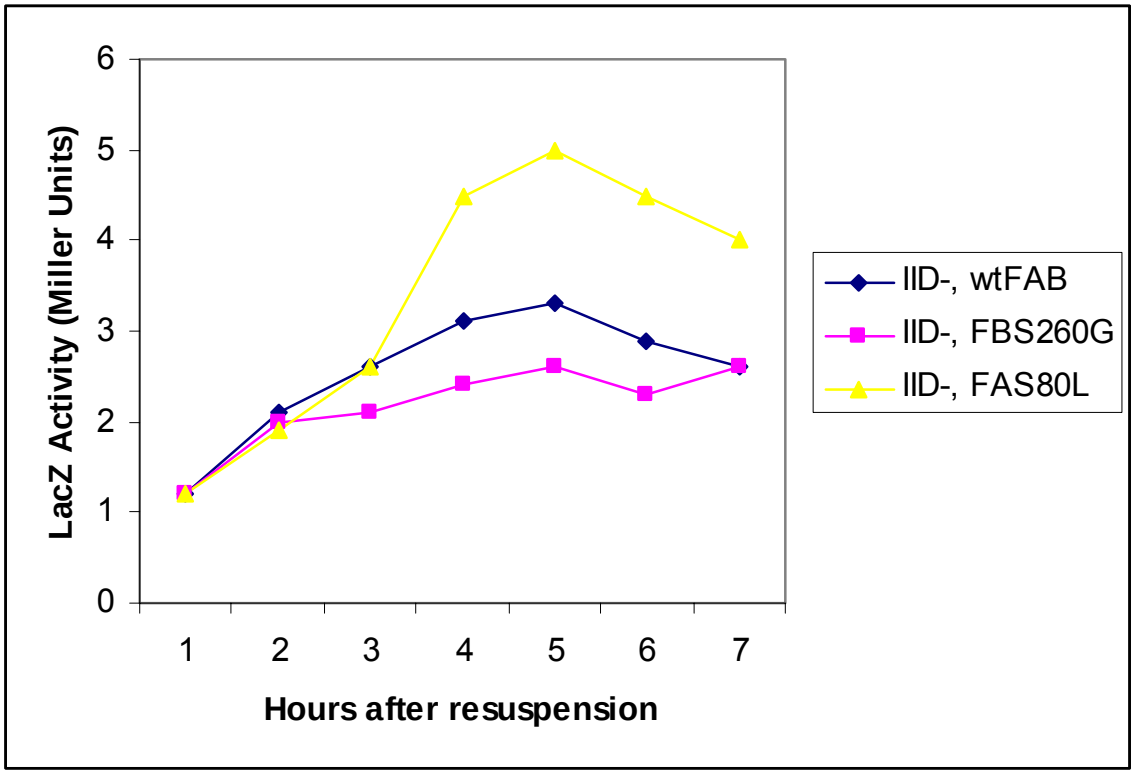

Figure 8. Activity of the *cotD-lacZ* fusion in engulfment-impaired strains (IID298) In a background where engulfment is impaired (IID298), each strain is unable to activate the *cotD-lacZ* fusion. In the SpoIID-minus background, neither FB-S260G (squares), FA-S80L (triangles), nor wild-type SpoIVFAB (diamonds) is able to activate the fusion to significant levels. This shows their inability to bypass the engulfment checkpoint while the forespore checkpoint is still active.

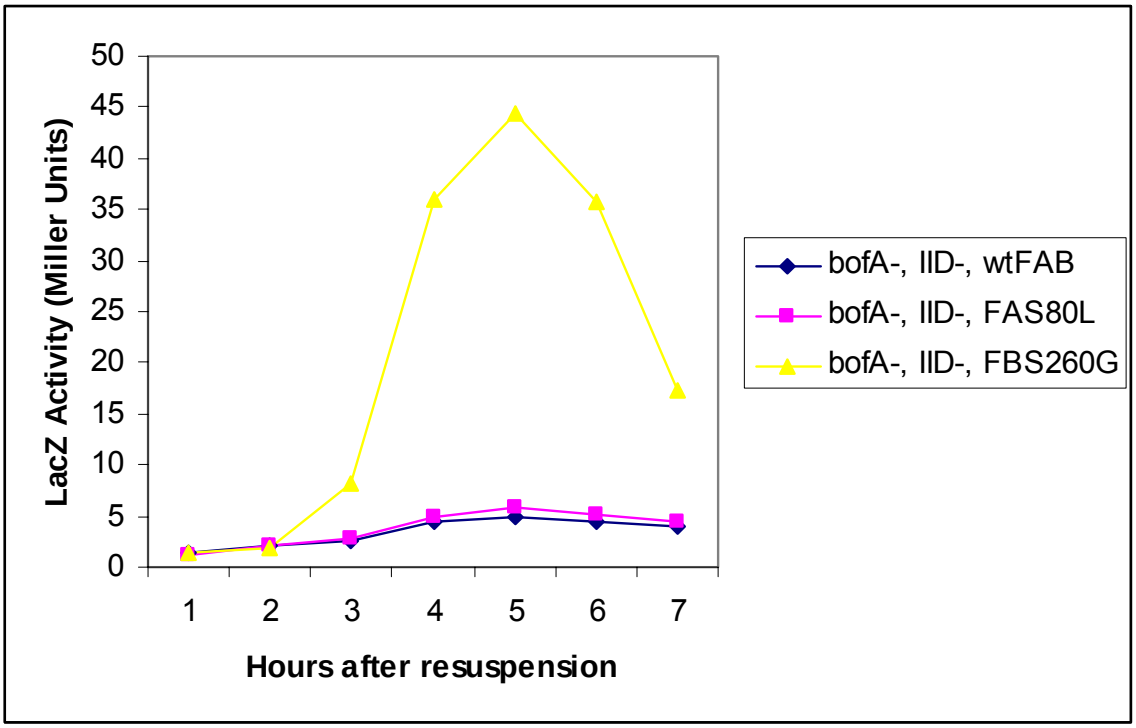

Figure 9. Activity of the *cotD-lacZ* fusion in engulfment-impaired strains (IID298) also lacking *bofA*

The *cotD-lacZ* fusion is not activated to significant levels in wild-type SpoIVFAB (diamonds) or in FA-S80L (squares) in the absence of *bofA* and engulfment. A *bofA* mutation is thus shown not sufficient to activate the fusion (in these strains) in the absence of engulfment, lending further credit to the argument for a separate engulfment checkpoint. A boe mutant, FB-S260G (triangles), is able to activate the fusion. FB-S260G can bypass the engulfment checkpoint in the absence of *bofA*. The forespore and engulfment checkpoints are thus believed to be separable.

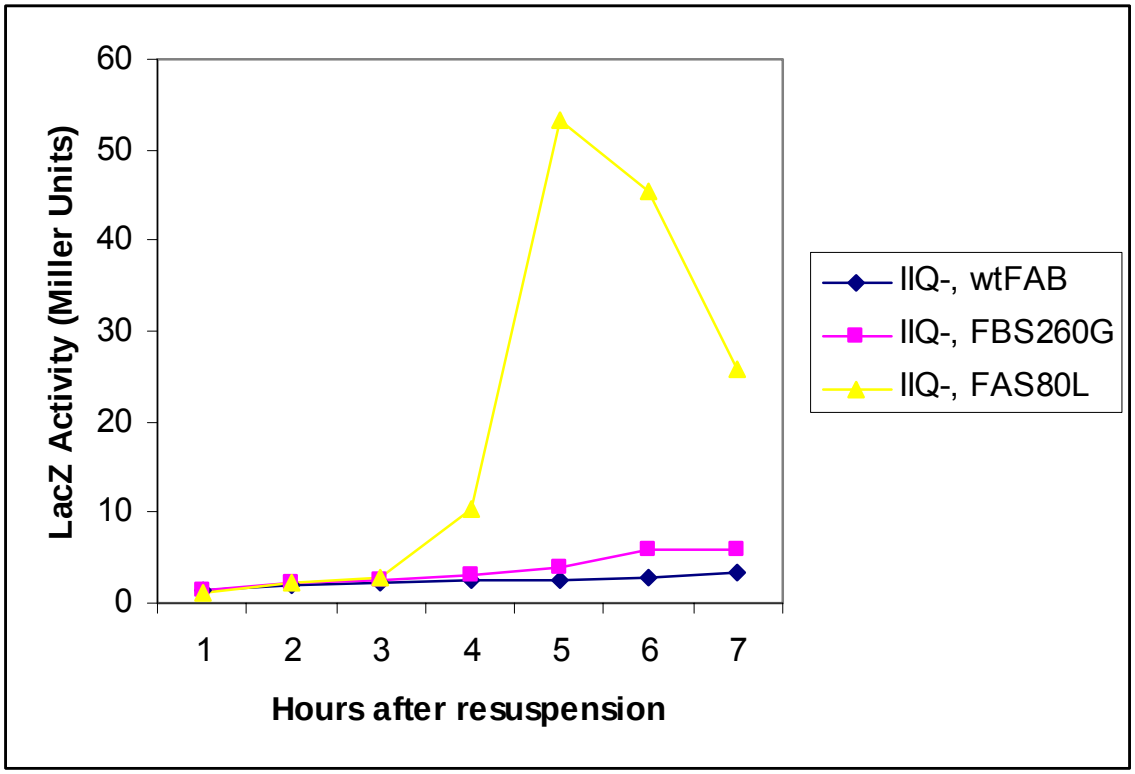

Figure 10. Activity of the *cotD-lacZ* fusion in engulfment-impaired strains lacking *spoIIQ*

Wild-type SpoIVFAB in a strain lacking *spoIIQ* fails to activate the *cotD-lacZ* fusion to adequate levels (diamonds). In the same background, FB-S260G also fails to activate the fusion (squares). These results are expected due to the fact that the forespore checkpoint cannot be bypassed by these strains in the presence of *bofA*. FA-S80L in a strain lacking *spoIIQ* is able to activate the *cotD-lacZ* fusion (triangles). This result is expected due to the bof phenotype of FA-S80L. *spoIIQ* deletion strains still complete engulfment, albeit very slowly. However, synthesis of σ^G is impaired, preventing SpoIVFB activation. FA-S80L is bypassing the forespore checkpoint to activate the fusion in this strain.

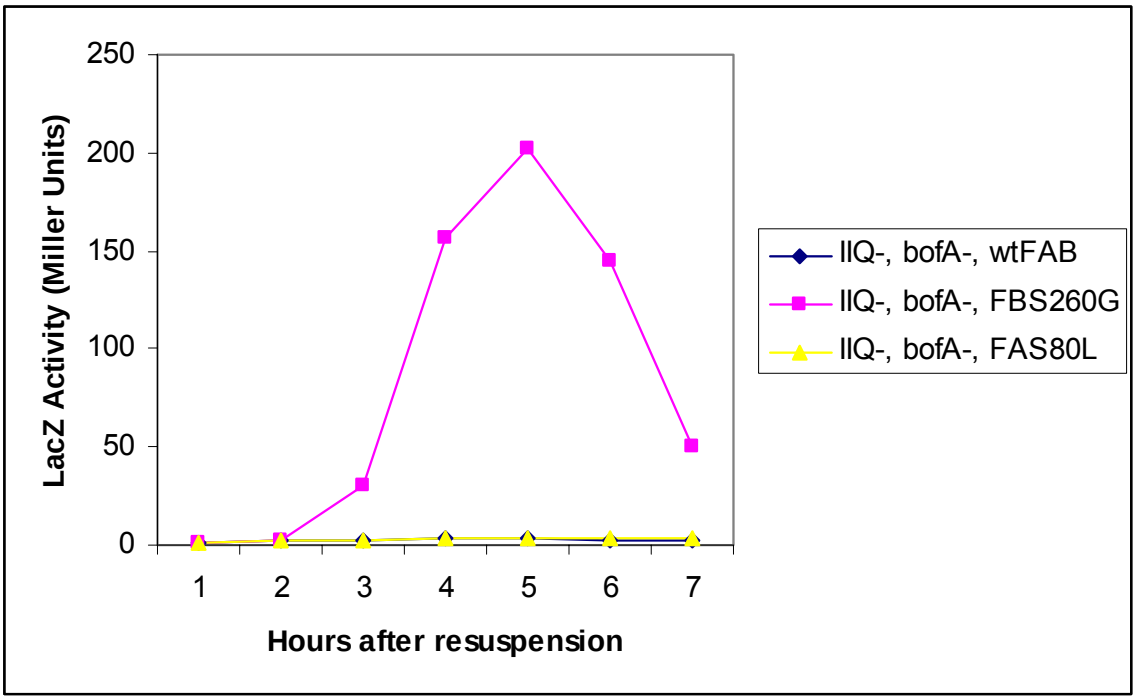

Figure 11. Activity of the *cotD-lacZ* fusion in engulfment-impaired strains lacking *spoIIQ* and *bofA*

In strains lacking *spoIIQ* and *bofA*, neither wild-type SpoIVFAB (diamonds), nor FA-S80L (triangles) activate the *cotD-lacZ* fusion. Engulfment is impaired in this background, thus this result is expected. FB-S260G (squares) is able to activate the fusion early, at t3, and to significant levels in this background. This is expected due to the boe phenotype of this mutant.

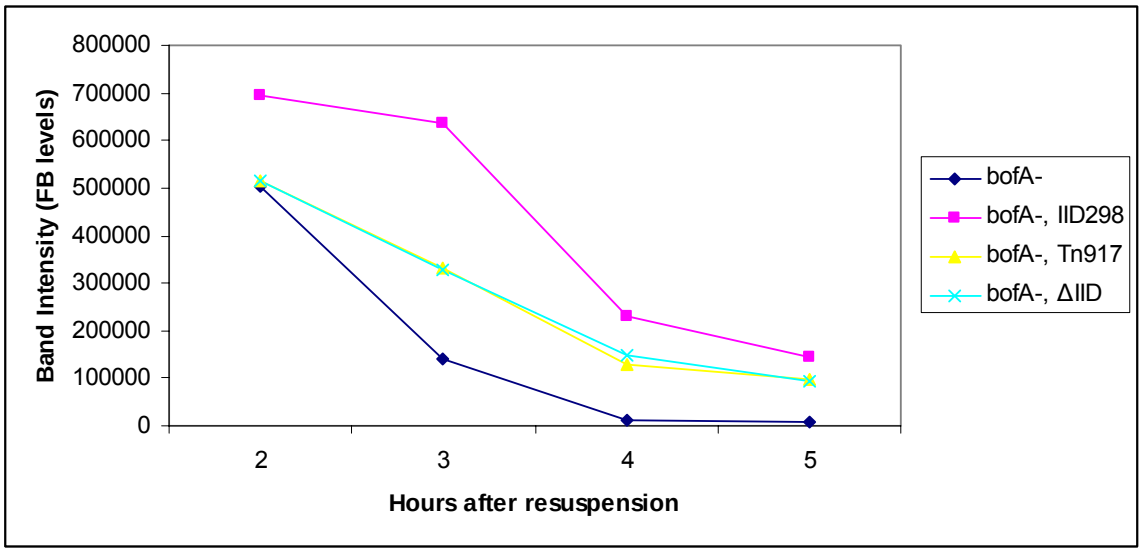

Figure 12. SpoIVFB protein levels in strains lacking *bofA* and engulfment
Wild type SpoIVFB protein levels are significantly reduced in a wild-type strain lacking *bofA* (diamonds). Engulfment impaired strains also lacking *bofA* actually show slightly higher levels of SpoIVFB protein than the strain where only *bofA* is deleted (squares, triangles, x's). Our main engulfment-negative construct, IID298, also lacking *bofA*, shows slightly higher levels of SpoIVFB than the other two constructs, and SpoIVFB levels are again higher than the *bofA* deletion strain.

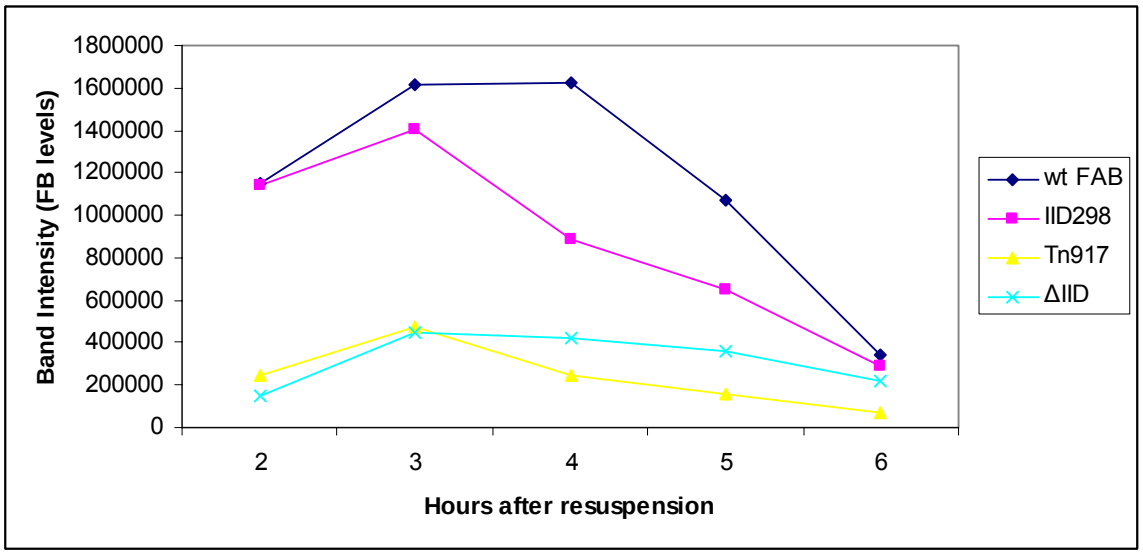

Figure 13. SpoIVFB levels in engulfment-defective strains
The IID298 construct (squares) has slightly less SpoIVFB protein than the wild-type strain (diamonds). The other two constructs, ΔIID (x's) and Tn917 (triangles), have slightly lower SpoIVFB levels than those present in IID298 and wild-type. This difference in levels of SpoIVFB is inconsequential, due to the fact that no strain can activate σ^K in the presence of *bofA*.

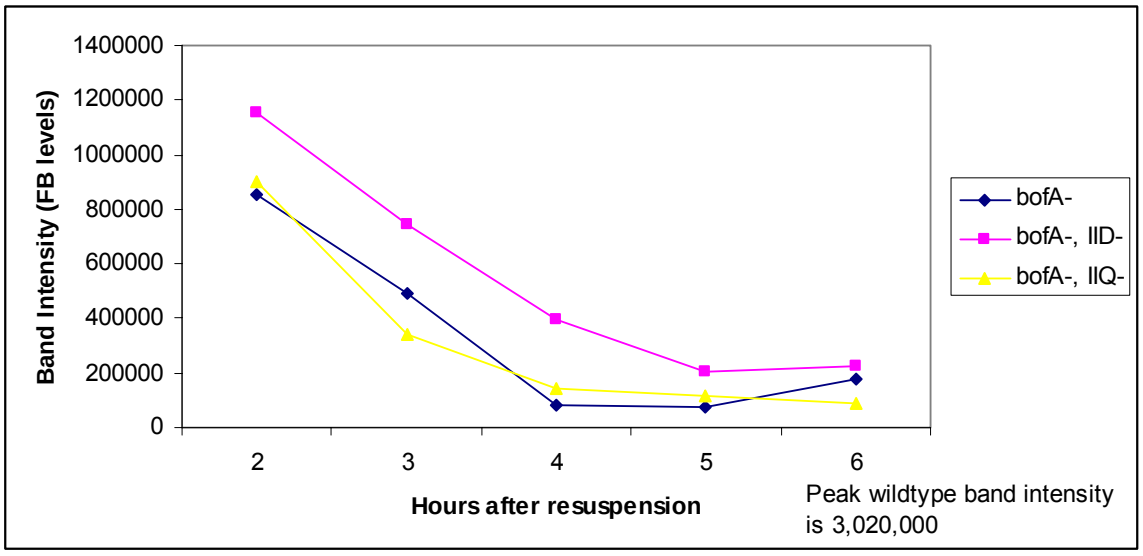

Figure 14. SpoIVFB levels in strains lacking *bofA* and SpoIID or SpoIIQ
SpoIVFB levels in an engulfment-defective strain lacking *bofA* and SpoIID (squares) are slightly higher than levels in a Δ*bofA* only strain (diamonds). Levels in a *bofA* and *spoIIQ* deletion strain (triangles) are equivalent to those in the strain lacking only *bofA*. Since only the *bofA*-minus strain activates σ^K, SpoIVFB levels are inconsequential for activation. The other two strains do not activate σ^K because they are unable to bypass the engulfment checkpoint. (For comparison, peak band intensity for wild-type levels in the same membrane is included).

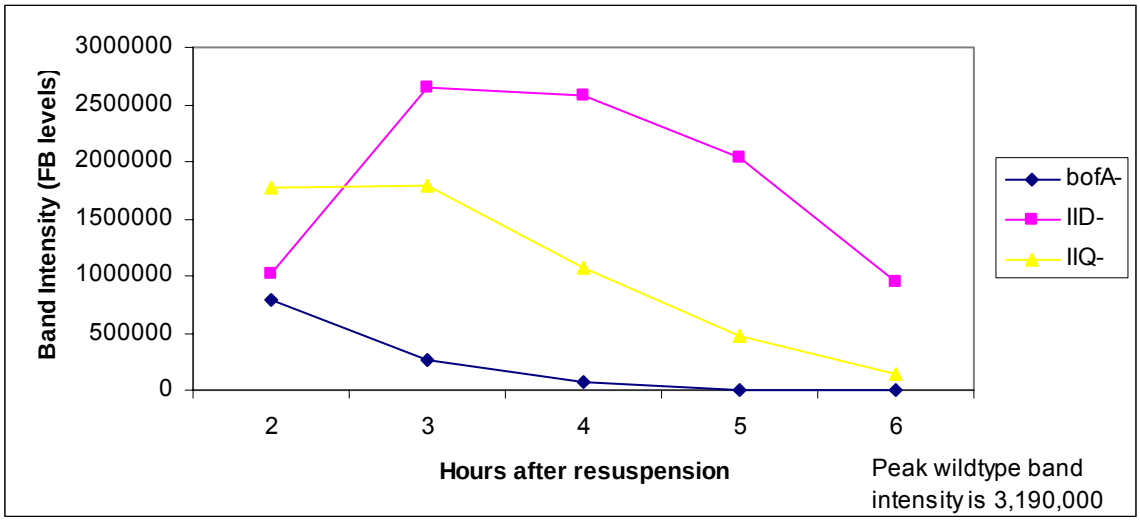

Figure 15. SpoIVFB levels in strains lacking *bofA*, SpoIID, or SpoIIQ
SpoIVFB levels in a strain lacking SpoIID (squares) are higher than those of strains lacking *bofA* (diamonds) or *spoIIQ* (triangles). Also, SpoIVFB levels in this mutant are close to those of wild-type (slightly less). Deleting *spoIIQ* effects a greater decrease in SpoIVFB levels than does mutating *spoIID*. Peak wild-type intensity is included for comparison.

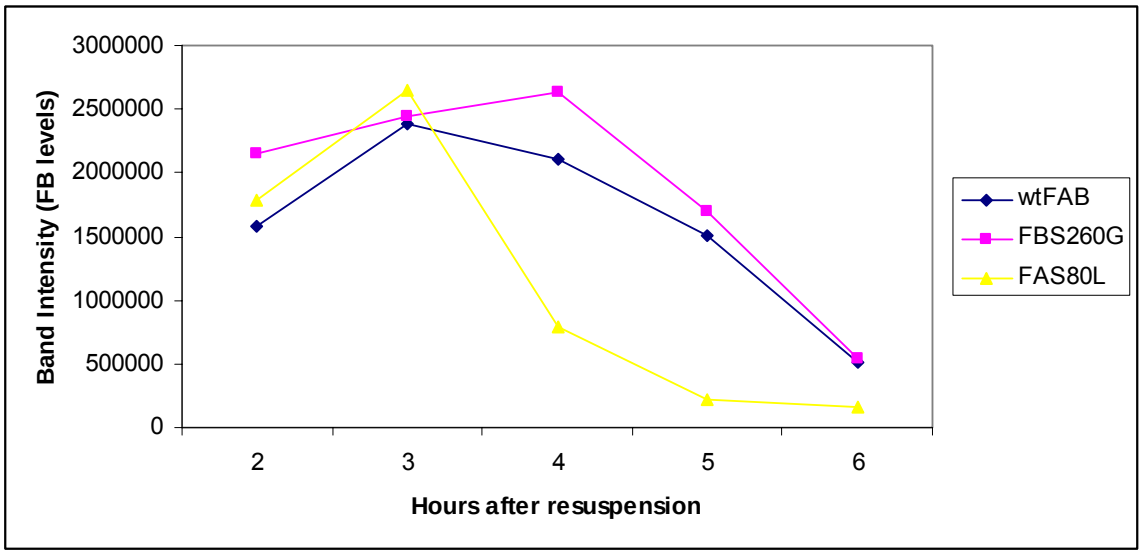

Figure 16. SpoIVFB levels in SpoIVFB and FA mutants
In a wild-type background, FB-S260G (squares) has slightly higher levels of SpoIVFB protein at t4 than wild-type SpoIVFB (diamonds). Other than this difference, levels between these two strains are similar. SpoIVFB levels in a strain containing FA-S80L (triangles) start out close to those of wild-type, but drop drastically over time. This is similar to mutants in *bofA*, accounted for by FA-S80L's bof phenotype.

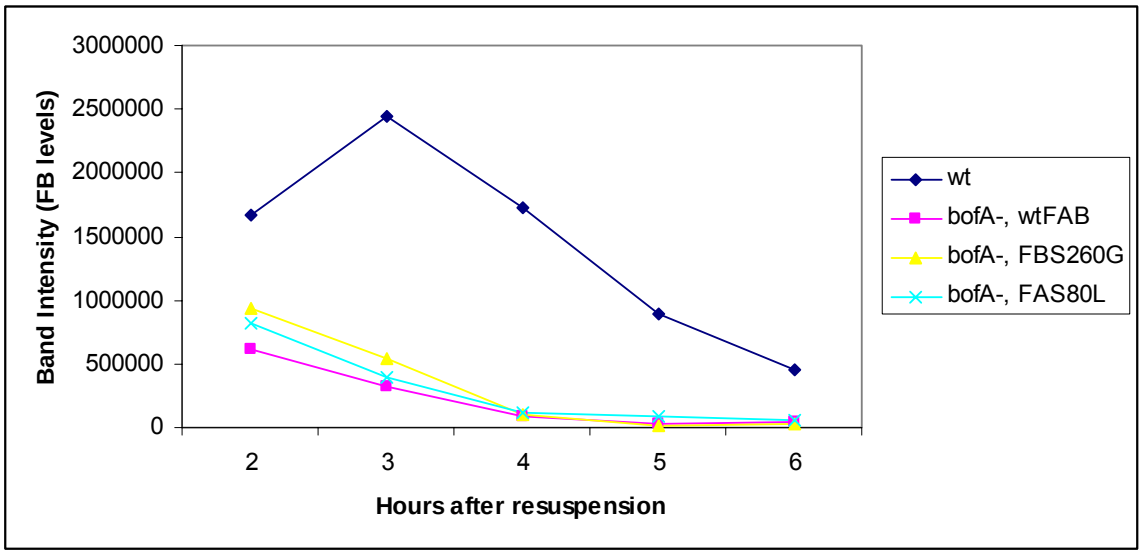

Figure 17. SpoIVFB levels in a *bofA* deletion
In strains lacking *bofA* and containing wild-type SpoIVFAB (squares), FB-S260G (triangles), or FA-S80L (x's), SpoIVFB levels are nearly identical. Each strain lacking *bofA* has SpoIVFB levels that are significantly lower than wild-type.

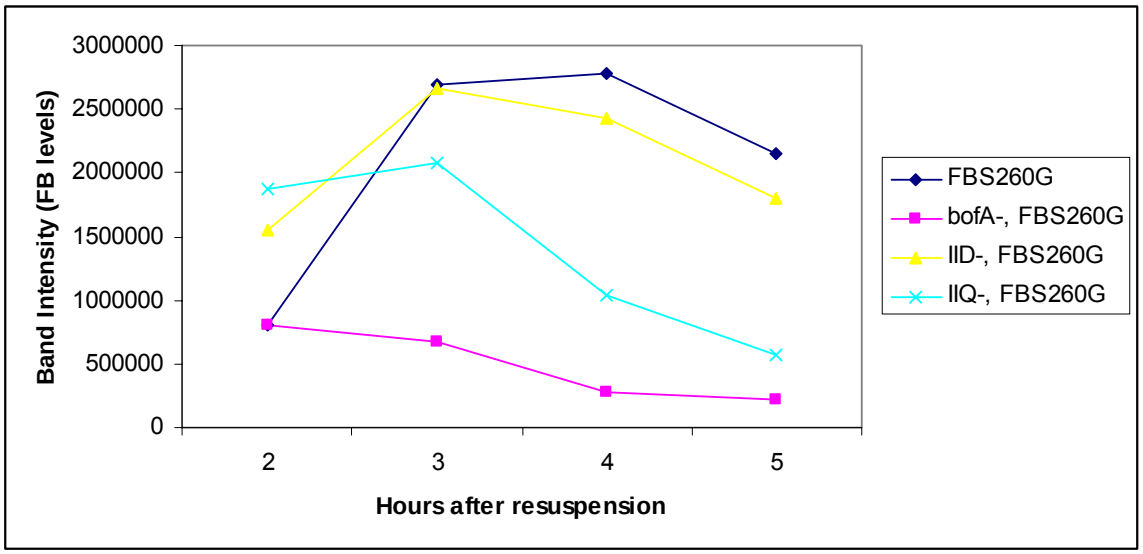

Figure 18. Levels of FB-S260G in strains lacking *bofA*, SpoIID, or SpoIIQ
In strains containing FB-S260G and lacking either *bofA*, SpoIID, or SpoIIQ, SpoIVFB protein levels vary. In the strain lacking SpoIID (triangles), SpoIVFB levels are only slightly lower than those in a wild-type background (diamonds). In the strain lacking SpoIIQ (x's), SpoIVFB levels start out close to those of wild-type FB-S260G, but eventually decrease to less than 50% of wild-type levels. As expected, the strain lacking *bofA* (squares) has significantly reduced levels of SpoIVFB when compared to wild-type FB-S260G.

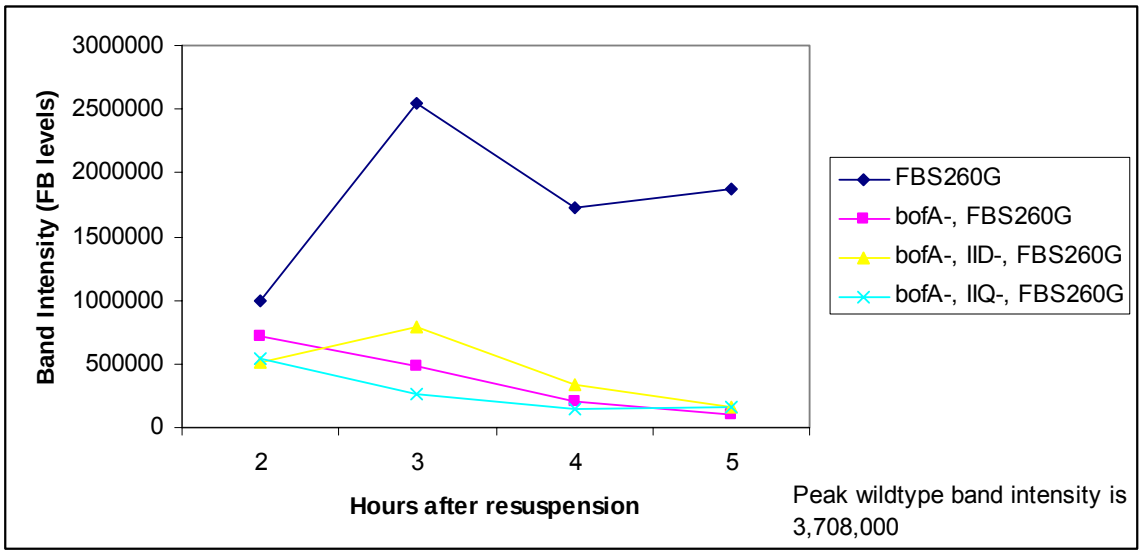

Figure 19. Levels of FB-S260G in strains lacking *bofA* and SpoIID or SpoIIQ
In strains containing FB-S260G and lacking *bofA* and either SpoIID or SpoIIQ, SpoIVFB protein levels are much lower than those of wild-type FB-S260G. SpoIVFB levels in strains lacking *bofA* (squares), *bofA* and SpoIID (triangles), and *bofA* and SpoIIQ (x's) are significantly decreased compared to levels of SpoIVFB in a strain containing FB-S260G (diamonds). SpoIVFB levels in the double-mutants are similar to those in the strain lacking only *bofA*.

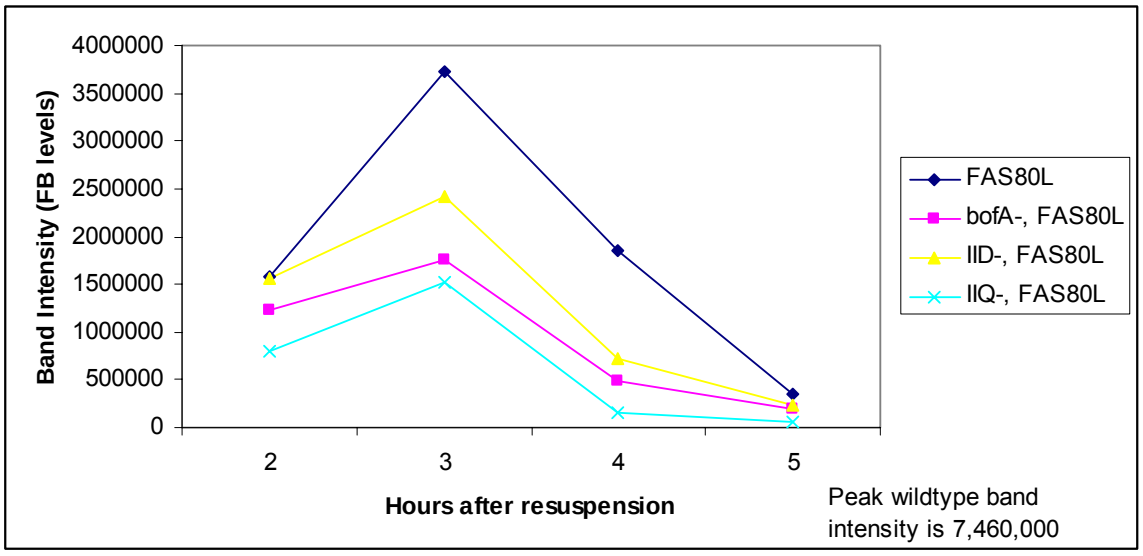

Figure 20. SpoIVFB levels in FA-S80L strains lacking *bofA*, SpoIID, or SpoIIQ
Using peak wild-type SpoIVFAB band intensity as a control, it can be seen once again that SpoIVFB levels in a strain containing FA-S80L (diamonds) are lower than those in a completely wild-type strain. SpoIVFB levels decrease slightly in the FA-S80L strain lacking SpoIID (triangles) when compared to FA-S80L in a wild-type background. Unlike the wild-type SpoIVFAB (Figure 15) and FB-S260G strains (Figure 18) in the same background, deleting *spoIIQ* in the FA-S80L strain (x's) causes SpoIVFB levels to decrease to slightly lower than those in the FA-S80L strain lacking only *bofA* (squares).

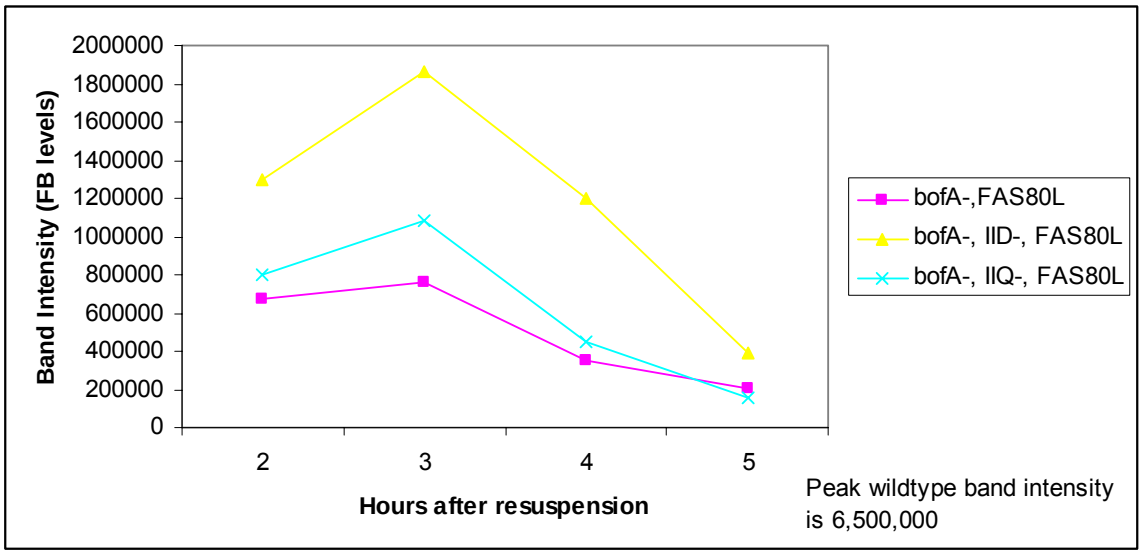

Figure 21. SpoIVFB levels in FA-S80L strains lacking *bofA* and SpoIID or SpoIIQ
Using wild-type SpoIVFAB as a control, it can be seen that deleting *bofA* and either SpoIID or SpoIIQ in a strain containing FA-S80L decreases SpoIVFB levels significantly. The lowest SpoIVFB levels are in the FA-S80L strain lacking *bofA* only (squares). Slightly higher levels are seen in the FA-S80L strain lacking *bofA* and SpoIIQ (x's). SpoIVFB levels in the SpoIID/engulfment-defective FA-S80L strain also lacking *bofA* (triangles) are appreciably higher than levels observed in the other two mutant strains.

Table 1. *cotD-lacZ* activity in *spoIVFAB* mutants in varying backgrounds

σ^K Activity (Miller Units)			
Mutant/Background	**wt FAB**	**FB-S260G**	**FA-S80L**
wt	189.4	137.6	417.2
bofA-	95.2	245.6	155.9
IID-	3.3	2.6	5.0
bofA-, IID-	5.0	44.4	5.9
IIQ-	2.6	4.0	53.4
bofA-, IIQ-	3.3	202.0	3.5

Activation of the *cotD-lacZ* fusion at five hours after resuspension is shown. The *cotD-lacZ* marker was used to quantify σ^K activity. Data are the average of two or more independent experiments. A *spoIVFAB* deletion strain was used as a negative control and, at 2.5 units at five hours after resuspension has, essentially, no activity (Shown in Figure 6).

I. References

1. Carniol, K., Ben-Yehuda, S., King, N., and Losick, R. (2005) Genetic dissection of the sporulation protein SpoIIE and its role in asymmetric division in *Bacillus subtilis*. *J. Bacteriol.* **187,** 3511-3520.

2. Barak, I., and Youngman, P. (1996) SpoIIE mutants of *Bacillus subtilis* comprise two distinct phenotypic classes consistent with a dual functional role for the SpoIIE protein. *J. Bacteriol.* **178,** 4984-4989.

3. Ben-Yehuda, S., and Losick, R. (2002) Asymmetric cell division in *B. subtilis* involves a spiral-like intermediate of the cytokinetic protein FtsZ. *Cell* **109,** 257-266.

4. Feucht, A., Magnin, T., Yudkin, M. D., and Errington, J. (1996) Bifunctional protein required for asymmetric cell division and cell-specific transcription in *Bacillus subtilis*. *Genes Dev.* **10,** 794-803.

5. Aung, S., Shum, J., Abanes-De Mello, A., Broder, D. H., Fredlund-Gutierrez, J., Chiba, S., and Pogliano, K. (2007) Dual localization pathways for the engulfment proteins during *Bacillus subtilis* sporulation. *Mol. Microbiol.* **65,** 1534-1546.

6. Abanes-De Mello, A., Sun, Y. L., Aung, S., and Pogliano, K. (2002) A cytoskeleton-like role for the bacterial cell wall during engulfment of the *Bacillus subtilis* forespore. *Genes Dev.* **16,** 3253-3264.

7. Liu, N. J., Dutton, R. J., and Pogliano, K. (2006) Evidence that the SpoIIIE DNA translocase participates in membrane fusion during cytokinesis and engulfment. *Mol. Microbiol.* **59,** 1097-1113.

8. Broder, D. H., and Pogliano, K. (2006) Forespore engulfment mediated by a ratchet-like mechanism. *Cell* **126,** 917-928.

9. Nicholson, W. L., Munakata, N., Horneck, G, Melosh, H. J., and Setlow, P. (2000) Resistance of bacterial endospores to extreme terrestrial and extraterrestrial environments. *Microbiol. Mol. Biol. Rev.* **64,** 548-572.

10. Nicholson, W. L., Schuerger, A. C., Setlow, P. (2005) The solar UV environment and bacterial spore UV resistance: Considerations for Earth-to-Mars transport by natural processes and human spaceflight. *Mutat Res* **571,** 249-264.

11. Moeller, R., Setlow, P., Horneck, G., Berger, T., Reitz, G., Rettberg, P., Doherty, A. J., Okayasu, R., and Nicholson, W. L. (2008) Roles of the major, small, acid-soluble spore proteins and spore-specific and universal DNA repair mechanisms in resistance of *Bacillus subtilis* spores to ionizing radiation from X rays and high-energy charged-particle bombardment. *J. Bacteriol.* **190,** 1134-1140.

12. Errington, J. (2003) Regulation of endospore formation in *Bacillus subtilis*. *Nat Rev Microbiol.* **1,** 117-126.

13. Errington, J. (1996) Determination of cell fate in *Bacillus subtilis*. *Trends Genet.* **12,** 313-334.

14. Stragier, P., and Losick, R. (2001) Molecular genetics of sporulation in *Bacillus subtilis*. *Annu. Rev. Genet.* **30,** 297-341.

15. Kroos, L. (2007) The *Bacillus* and *Myxococcus* developmental networks and their transcriptional regulators. *Annu Rev Genet* **41,** 13-39.

16. Wang, L., Perpich, J., Driks, A., and Kroos, L. (2007) One perturbation of the mother cell gene regulatory network suppresses the effects of another during sporulation of *Bacillus subtilis*. *J. Bacteriol.* **189,** 8467-8473.

17. Karmazyn-Campelli, C., Rhayat, L., Carballido-Lopez, R., Duperrier, S., Frandsen, N., and Stragier, P. (2008) How the early sporulation sigma factor sigma(F) delays the switch to late development in *Bacillus subtilis*. *Mol. Microbiol.* **67,** 1169-1180.

18. Wang, S. T., Setlow, B., Conlon, E. M., Lyon, J. L., Imamura, D., Sato, T., Setlow, P., Losick, R., and Eichenberger, P. (2006) The forespore line of gene expression in *Bacillus subtilis*. *J. Mol. Biol.* **358,** 16-37.

19. Gomez, M., and Cutting, S. M. (1996) Expression of the *Bacillus subtilis spoIVB* genes is under dual sigma F/sigma G control. *Microbiol.* **142,** 3453-3457.

20. Kellner, E. M., Decatur, A., and Moran, C. P., Jr. (1996) Two-stage regulation of an anti-sigma factor determines developmental fate during bacterial endospore formation. *Mol. Microbiol.* **21,** 913-924.

21. Rudner, D. Z., and Losick, R. (2002) A sporulation membrane protein tethers the pro-sigmaK processing enzyme to its inhibitor and dictates its subcellular localization. *Genes Dev* **16,** 1007-1018.

22. Zhou, R., and Kroos, L. (2004) BofA protein inhibits intramembrane proteolysis of pro-sigmaK in an intercompartmental signaling pathway during *Bacillus subtilis* sporulation. *Proc Natl Acad Sci USA* **101,** 6385-6390.

23. Zhou, R., and Kroos, L. (2005) Serine proteases from two cell types target different components of a complex that governs regulated intramembrane proteolysis of pro-sigmaK during *Bacillus subtilis* development. ***Mol. Microbiol.*** **58,** 835-846.

24. Campo, N, and Rudner, D. Z. (2007) SpoIVB and CtpB are both forespore signals in the activation of the sporulation transcription factor sigmaK in *Bacillus subtilis*. *J Bacteriol.* **189,** 6021-6027.

25. Campo, N., and Rudner, D. Z. (2006) A branched pathway governing the activation of a developmental transcription factor by regulated intramembrane proteolysis. *Mol Cell* **23,** 25-35.

26. Chiba, S., Coleman, K., and Pogliano, K. (2007) Impact of membrane fusion and proteolysis on SpoIIQ dynamics and interaction with SpoIIIAH. *J Biol Chem.* **282,** 2576-2586.

27. Makinoshima, H., and Glickman, M. S. (2006) Site-2 proteases in prokaryotes: regulated intramembrane proteolysis expands to microbial pathogenesis. *Microbes Infect.* **8,** 1882-1888.

28. Brown, M. S., Ye, J., Rawson, R. B., and Goldstein, J. L. (2000) Regulated intramembrane proteolysis: a control mechanism conserved from bacteria to humans. *Cell* **100,** 391-398.

29. Yu, Y. T., and Kroos, L. (2000) Evidence that SpoIVFB is a novel type of membrane metalloprotease governing intercompartmental communication during *Bacillus subtilis* sporulation. *J. Bacteriol.* **182,** 3305-3309.

30. Rudner, D. Z., Fawcett, P., and Losick, R. (1999) A family of membrane-embedded metalloproteases involved in regulated proteolysis of membrane-associated transcription factors. *Proc Natl Acad Sci USA* **96,** 14765-14770.

31. Zelenski, N. G., Rawson, R. B., Brown, M. S., and Goldstein, J. L. (1999) Membrane topology of S2P, a protein required for intramembranous cleavage of sterol regulatory element-binding proteins. *J. Biol. Chem* **274,** 21973-21980.

32. Lee, K., Tirasophon, W., Shen, X., Michalak, M., Prywes, R., Okada, T., Yoshida, H., Mori, K., and Kaufman, R. J. (2002) IRE1-mediated unconventional mRNA splicing and S2P-mediated ATF6 cleavage merge to regulate XPB1 in signaling the unfolded protein response. *Genes Dev.* **16,** 452-466.

33. Chen, J. C., Viollier, P. H., and Shapiro, L. (2005) A membrane metalloprotease participates in the sequential degradation of a *Caulobacter* polarity determinant. *Mol. Microbiol.* **55,** 1085-1103.

34. Bolter, B., Nada, A., Fulgosi, H., and Soll, J. (2006) A chloroplastic inner envelope membrane protease is essential for plant development. *FEBS Lett.* **580,** 789-794.

35. Jiang, X., Rubio, A., Chiba, S., and Pogliano, K. (2005) Engulfment-related proteolysis of SpoIIQ: evidence that dual checkpoints control σ^K activity. *Mol. Microbiol.* **58,** 102-115.

36. Ricca, E., Cutting, S., and Losick, R. (1992) Characterization of *bofA*, a gene involved in intercompartmental regulation of pro-sigma K processing during sporulation in *Bacillus subtilis*. *J. Bacteriol.* **174,** 3177-3184.

37. Cutting, S., Oke, V., Driks, A., Losick, R., Lu, S., and Kroos, L. (1990) A forespore checkpoint for mother cell gene expression during development in *B. subtilis*. *Cell* **62,** 239-250.

38. Karmazyn-Campelli, C., Bonamy, C., Savelli, B., and Stragier, P. (1989) Tandem genes encoding sigma-factors for consecutive steps of development in *Bacillus subtilis*. *Genes Dev.* **3,** 150-157.

39. Partridge, S. R., and Errington, J. (1993) The importance of morphological events and intercellular interactions in the regulation of prespore-specific gene expression during sporulation in *Bacillus subtilis*. *Mol. Microbiol.* **8,** 945-955.

40. Chary, V. K., Xenopoulos, P., and Piggot, P. J. (2006) Blocking chromosome translocation during sporulation of *Bacillus subtilis* can result in prespore-specific activation of sigmaG that is independent of sigmaE and of engulfment. *J. Bacteriol.* **188,** 7267-7273.

41. Doan, T., and Rudner, D. Z. (2007) Perturbations to engulfment trigger a degradative response that prevents cell-cell signaling during sporulation in *Bacillus subtilis*. *Mol. Microbiol.* **64,** 500-511.

42. Londono-Vallejo, J. A., Frehel, C., and Stragier, P. (1997) SpoIIQ, a forespore-expressed gene required for engulfment in *Bacillus subtilis*. *Mol. Microbiol.* **24,** 29-39.

43. Blaylock, B., Jiang, X., Rubio, A., Moran, C. P., Jr., and Pogliano, K. (2004) Zipper-like interaction between proteins in adjacent daughter cells mediates protein localization. *Genes Dev.* **18,** 2916-2928.

44. Doan, T., Marquis, K. A., and Rudner, D. Z. (2005) Subcellular localization of a sporulation membrane protein is achieved through a network of interactions along and across the septum. *Mol Microbiol.* **55,** 1767-1781.

45. Dubnau, D., and Davidoff-Abelson, R. (1971) Fate of transforming DNA following uptake by competent *Bacillus subtilis*. I. Formation and properties of the donor-recipient complex. *J. Mol. Biol.* **56,** 209-221.

46. Sterlini, J. M., and Mandelstam, J. (1969) Commitment to sporulation in *Bacillus subtilis* and its relationship to development of actinomycin resistance. *Biochem. J.* **113,** 29-37.

47. Miller, J. H. (1972) *Experiments in Molecular Genetics*. Cold Spring Harbor, New York, Cold Spring Harbor Laboratory Press.

48. Pogliano, K., Hofmeister, A. E., and Losick, R. (1997) Disappearance of the sigma E transcription factor from the forespore and the SpoIIE phosphatase from the mother cell contributes to establishment of cell-specific gene expression during sporulation in *Bacillus subtilis*. *J. Bacteriol.* **179,** 3331-3341.

49. Perez, A. R., Abanes-De Mello, A., and Pogliano, K. (2000) SpoIIB localizes to active sites of septal biogenesis and spatially regulates septal thinning during engulfment in *Bacillus subtilis*. *J. Bacteriol.* **182,** 1096-1108.

APPENDIX A

Studies of SpoIVB activity at varying pH in assorted buffers

i. Abstract

During sporulation in *Bacillus subtilis*, the cell undergoes an asymmetric division forming a larger mother cell and a smaller compartment, the forespore. After the mother cell engulfs the forespore, a protease secreted into the intermembrane space, SpoIVB, cleaves SpoIIQ and SpoIVFA, leading to the activation of σ^K and its release into the mother cell. It is important that SpoIIQ proteolysis occurs after engulfment and membrane fusion, as SpoIIQ is important for localizing the complex responsible for σ^K activation. Since this proteolysis event occurs within the intermembrane space, an extremely small compartment between the mother cell and forespore, it was suggested that SpoIVB activity could be regulated by a change in pH within this space that occurs just after membrane fusion. This would ensure proper timing of proteolysis, and that SpoIIQ and SpoIVFA would not be cleaved until after membrane fusion. We tested the efficacy of SpoIVB in cleaving SpoIIQ at various pH conditions, and in different pH buffers. It was found that SpoIVB can effectively cleave SpoIIQ in a wide-range of pH conditions and in multiple buffers. A pH change within the intermembrane space is thus judged unlikely to control SpoIVB activity.

ii. Introduction

a. The SpoIVB serine protease

SpoIVB is a serine protease responsible for proteolysis of SpoIIQ and SpoIVFA as part of the forespore checkpoint for σ^K activation. It is a secreted protease from the forespore whose transcription is upregulated by σ^G following engulfment [12,13]. SpoIVB has a PDZ-domain involved in protein-protein interaction and self-cleavage, and a DxxLL motif at position 363 forming a catalytic triad [12]. After membrane fusion, SpoIVB is secreted into the intermembrane space where it undergoes self-cleavage into 3 distinct active species, and then cleaves both SpoIIQ and SpoIVFA (Figure 7) [1,12]. Cleavage of SpoIVFA by SpoIVB leads to the regulated intramembrane proteolysis (RIP) of pro- σ^K, causing the release of active σ^K into the mother cell [1]. The σ^K processing complex is localized to the outer forespore membrane by SpoIIQ [1]. If proteolysis were to occur before membrane fusion, normal signal transduction and σ^K activation may not be possible. It is interesting then to know the mechanism by which SpoIVB activity is regulated.

b. pH regulation in bacteria

pH regulation of proteins in bacteria and eukaryotes is a common theme. Many proteins and genes are regulated by pH in *E. coli*, including those used for flagellar motility, amino acid catabolism, and oxidative stress [3-5]. Other examples of proteins that are regulated by pH include insulin [7], the neonatal Fc receptor [8], ribonuclease A [9], and myoglobin [10]. Protein conformation and activity can be controlled by pH through protonation, changing substrate binding capabilities, catalytic activity, or protein-

protein interactions [11]. A *Lactobacillus* Histidine decarboxylase (HDC) is important for optimal cell growth. This enzyme converts histidine to histamine and CO_2 and the histamine is utilized in an energy-producing reaction. The protein's tertiary structure is regulated by pH: it is active at low pH and inactive at neutral to alkaline pH. At high pH, the protein's substrate-binding pocket is destroyed, while at low pH, it is believed that it is stabilized through protonation [6]. In light of these various examples, it was suggested that SpoIVB's protein conformation, activity in the intermembrane space, and cleavage of substrate proteins SpoIIQ and SpoIVFA, may be regulated by a pH change in the intermembrane space that occurs after membrane fusion. This mechanism would thus temporally regulate proteolysis of SpoIIQ and SpoIVFA, protecting them until after membrane fusion is complete. To test this hypothesis, we performed protease activity assays utilizing purified SpoIVB protein and analyzed its activity under various buffer and pH conditions.

iii. Results and Discussion

a. Finding a reliable assay for SpoIVB protease activity

To have a general test for SpoIVB protease activity, *in vitro* protease assays (Materials and Methods) were performed in various buffers and pH conditions. Samples were run on an SDS-PAGE gel and visualized using various methods. We initially utilized a FITC-labeled casein substrate with purified SpoIVB (Materials and Methods) and visualized the fluorescent bands on a Typhoon scanner. While able to see a breakdown product, this system was not always reliable and results fluctuated. We tried using a beta-casein substrate and visualized the gel bands through Purple staining (Materials and Methods), using the Typhoon scanner once again. Breakdown products resulting from cleavage of the substrate by SpoIVB were observed (Data not shown). This method seemed reliable, but Purple staining is both time-consuming and costly. In addition, protease assays with these substrates required high concentrations of SpoIVB, and our supply of this enzyme was extremely limited. In response to these factors, we searched for other methods for testing SpoIVB's cleavage effectiveness.

While we could see that SpoIVB could cleave various substrates *in vitro* (data not shown), these experiments would not answer the question of SpoIVB's cleavage effectiveness with *in vivo* substrates. We thus decided to use an actual *in vivo* substrate of SpoIVB, SpoIIQ, with a GST-tag. The samples were visualized through Western blotting (Materials and Methods) using anti-SpoIIQ antibodies with a fluorescent secondary antibody. The Typhoon scanner was used to visualize fluorescence. With this method, transfer was an issue, as GST is fairly large and does not transfer well. Also, it

was not possible to see any SpoIIQ breakdown products. We searched again for a reliable test for SpoIVB cleavage.

Success finally came utilizing the GST-SpoIIQ substrate and Purple staining. Although costly, Purple stain allows fluorescent visualization of all proteins in a gel. Since our *in vitro* assays contained only purified proteins, GST-SpoIIQ and SpoIVB, this is actually helpful (this would be troublesome if one were using whole cell lysate). Also, we circumvent problems relating to transfer and other steps of Western blotting.

b. Effects of pH and buffer on SpoIVB activity

In vitro protease assays with SpoIVB and GST-SpoIIQ were performed as described (Materials and Methods). Samples on the gel were visualized by Purple staining and a fluorescence scan on a Typhoon scanner. Four different buffers were used each at four different pH's close to the optimal pH range for each buffer.

SpoIVB protease activity was first tested in Sodium Acetate at pH 4 through pH 7. A GST-SpoIIQ cleavage product accumulated over time at pH 5-7 (Figure 1). Sodium phosphate buffer was then used at pH 5 through pH 8. A cleavage product of GST-SpoIIQ accumulated at all pH levels (Figure 2). In Tris-HCl at pH 6 through pH 9, the GST-SpoIIQ cleavage product again accumulated at all pH levels (Figure 3). Finally, we tested Glycine-NaOH at pH 7 through pH 10. The GST-SpoIIQ cleavage product appeared in all pH levels (Figure 4). In all samples that showed a cleavage product of SpoIIQ, there was also noticeable degradation of the full-length protein. It is thus believed that SpoIVB can cleave GST-SpoIIQ in all of the above listed conditions.

To be certain that this cleavage was due to SpoIVB proteolysis of GST-SpoIIQ, and not to any other factor, protease, or contaminant present in the buffer, *in vitro* protease assays were performed in all conditions and buffers listed above, except only GST-SpoIIQ was added to the reaction, and SpoIVB was left out. The GST-SpoIIQ only results show that there is no accumulation of breakdown product in any buffer at any pH range (Figures 5A-5D). We also used a highly purified SpoIVB protein (Materials and Methods) to confirm this result. To be certain that SpoIVB could actually cleave GST-SpoIIQ, and to make sure no other proteases were present, a protease assay was run using high-purity SpoIVB and GST-SpoIIQ in Tris-HCl, pH 8 (to simulate optimal conditions). It was found that SpoIVB can indeed cleave SpoIIQ and that our results weren't due to any contaminant (Figure 6).

c. Discussion: SpoIVB protease activity is not pH dependent

From the results shown above, it can be seen that SpoIVB is able to cleave GST-SpoIIQ in a wide range of pH and buffer conditions. SpoIVB is active in a pH range of 5-10. Since SpoIVB is responsible for cleavage of both SpoIVFA and SpoIIQ, it is advantageous for it to have activity and proper protein folding in varying conditions. This helps to ensure that reactions that occur as a result of SpoIVB proteolysis, such as σ^K activation, occur even if conditions change slightly in the intermembrane space. SpoIVB appears to have the highest protease activity at pH 6-9 in either Tris-HCl or Glycine-NaOH. It is likely that these conditions best simulate those in the intermembrane space. This result gives insight as to what actual cellular conditions are in this tiny compartment. Although pH obviously does not play a role in regulating SpoIVB

activity, we have helped characterize IVB preferences and expanded our knowledge of this system.

iv. Materials and Methods

a. SpoIVB protein purification

BL21 (DE3)/pZR53 (SpoIVB-His_6) was grown in LB ampicillin (100µg/ml) media, and expression of SpoIVB-His_6 was induced by 1mM isopropyl 1-thio-β-D-galactopyranoside for 1hr at 30°C. Cells were washed by buffer D (20 mM Tris-HCl (pH 8.0), 150 mM NaCl) and disrupted by sonication. After removing debris by centrifugation, cell lysate was added to a nickel affinity column (Sigma) equilibrated in buffer D. The column was washed with buffer D plus 20 mM imidazole and eluted with 300 mM imidazole in the same buffer. Eluted protein was then dialyzed in buffer D. To get SpoIVB protein of extremely high purity, this same process was followed and, after dialysis, protein was loaded on a Hi-Trap Q (Amersham Biosciences) anion-exchange chromatography column previously equilibrated in buffer D. Flow-through fractions that included SpoIVB-His_6 were collected and then loaded onto a Hi-Trap SP (Amersham Biosciences) cation-exchange chromatography column previously equilibrated in buffer D. SpoIVB-His_6 was eluted by a sodium chloride gradient (0-1M) in buffer D. High-purity protocol was performed by Shinobu Chiba [1].

b. *In vitro* protease assay

GST-SpoIIQ and SpoIVB purified proteins (or SpoIIQ alone) were added in 2.6 to 1.0 concentrations to 1.5ml Eppendorf tubes containing 30mM buffer (Sodium Acetate, Sodium Phosphate, Tris-HCl, or Glycine-NaOH) at a specific pH (ranging from 4 to 10). Final concentrations of SpoIIQ and SpoIVB were approximately 0.18µg/µl and 0.07µg/µl, respectively, in a total 60µl reaction. Samples were mixed on ice to prevent

premature activity. 10µl aliquots were added to each of five new Eppendorf tubes labeled t0, t30, t1, t2, and t3. These values correspond to the reaction incubation time, with t30 being 30 minutes and the other values being time in hours. Samples were incubated at 37°C for their respective times. To stop the reaction at each time point, 10µl of 2X SDS (sodium dodecyl sulfate) containing 4 mM DTT (dithiothreitol) was added to each tube. After this, 2µl of 1M Tris-HCl pH 8.0 was added to the respective tube to assure proper pH for SDS-PAGE. Samples were boiled at 80°C for 10 minutes and then applied to a 12.5% gel for SDS-PAGE. Reactions using high-purity SpoIVB and SpoIIQ followed mostly the same procedure. The changes are as follows: 150mM NaCl was added to the buffer. 20ng/µl of GST-SpoIIQ was used either by itself, or with a 1:4 or 1:8 dilution of highly-purified SpoIVB. The only buffer used was Tris-HCl pH 8.0 All other conditions are as above.

c. Purple staining and visualization

The resulting protein gels (four in this case) were first fixed overnight in 7.5% acetic acid with 10% Methanol at room temperature. (New, rinsed, clean gloves and a clean glass dish were used for handling the gel and fixation, as any particles that get on the gel may stain and result in a high-background picture). The gels were then washed in 500ml wash solution (35mM $NaHCO_3$ and 300mM Na_2CO_3) for 30 minutes. Gels were then stained in Nanopure water containing a 1:200 dilution of Deep Purple Total Protein Stain (Amersham) for one hour (kept in the dark for each step starting here). The gels were then washed two separate times for 15 minutes in 7.5% acetic acid and then scanned for fluorescence on a Typhoon scanner.

d. Western blotting

After SDS-PAGE, proteins were transferred to PVDF [2], blocked with 5% nonfat dry milk in PBS-0.5% Tween-20, and probed with a 1:3000 dilution of rabbit polyclonal anti-SpoIIQ antibodies. A 1:2000 diluted anti-rabbit Cy5 or Cy3 fluorescent secondary antibody was then used and membranes were visualized for fluorescence on a Typhoon scanner.

e. Typhoon scanner range calibration

After scanning a Purple stained gel containing multiple serial dilutions of SpoIIQ purified protein, bands were quantified using ImageQuant software and band intensities were graphed in Microsoft Excel to assess the scanner's linear range. Reactions were adjusted to proper concentrations to reflect this range and assure accurate scans. Conditions for scanning Purple stained gels were as follows: A green laser (532nm) was used for excitation with emission of 560LB or 610BP (457 or 488nm) scanning at 450PMT.

v. Figures

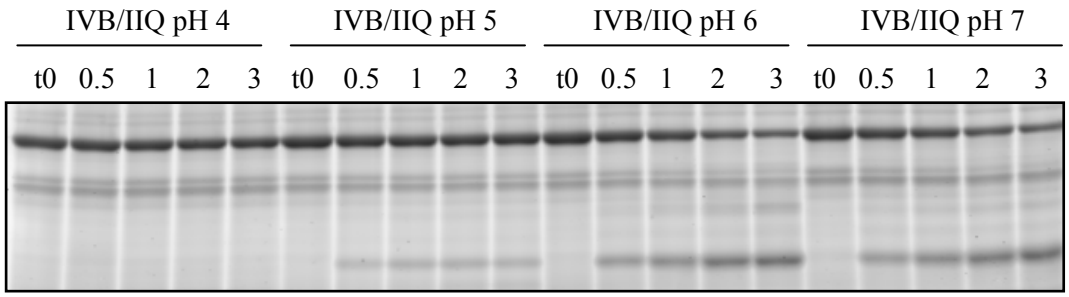

Figure 1. SpoIVB activity in Sodium Acetate
A cleavage product of GST-SpoIIQ accumulates (bottom of gel) at pH 5-7 in Sodium Acetate. There is also a decrease in the full-length SpoIIQ band (top of gel).

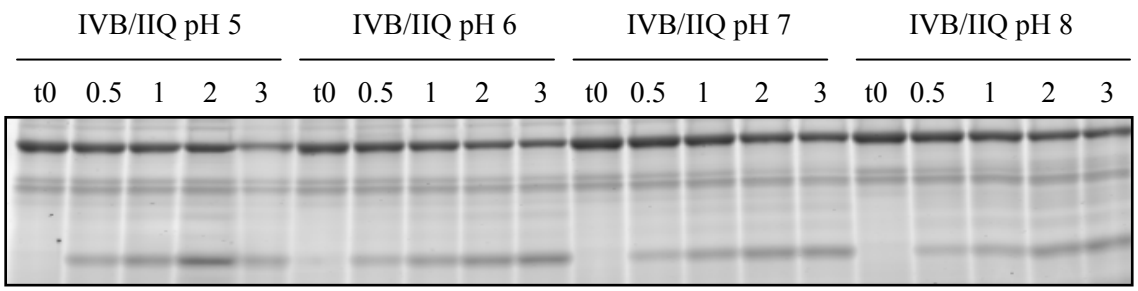

Figure 2. SpoIVB activity in Sodium Phosphate
A cleavage product of GST-SpoIIQ accumulates (bottom of gel) at pH 5-8 in Sodium Phosphate. There is also a decrease in the full-length SpoIIQ band (top of gel).

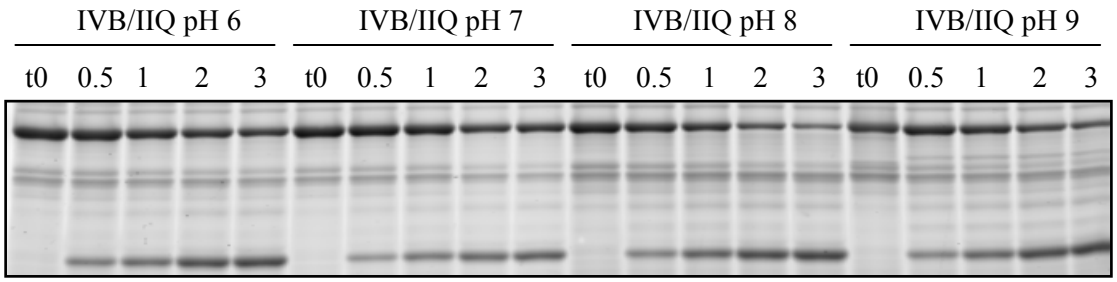

Figure 3. SpoIVB activity in Tris-HCl
A cleavage product of GST-SpoIIQ accumulates (bottom of gel) at pH 6-9 in Tris-HCl. There is also a decrease in the full-length SpoIIQ band (top of gel).

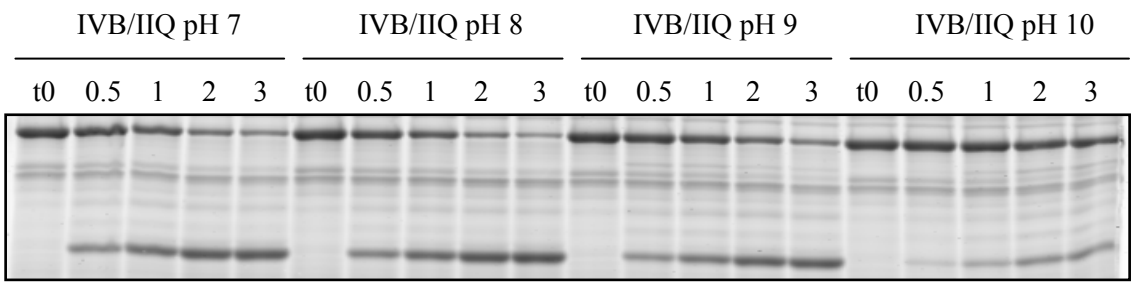

Figure 4. SpoIVB activity in Glycine-NaOH
A cleavage product of GST-SpoIIQ accumulates (bottom of gel) at pH 7-10 in Glycine-NaOH. There is also a decrease in the full-length SpoIIQ band (top of gel).

A. Sodium Acetate

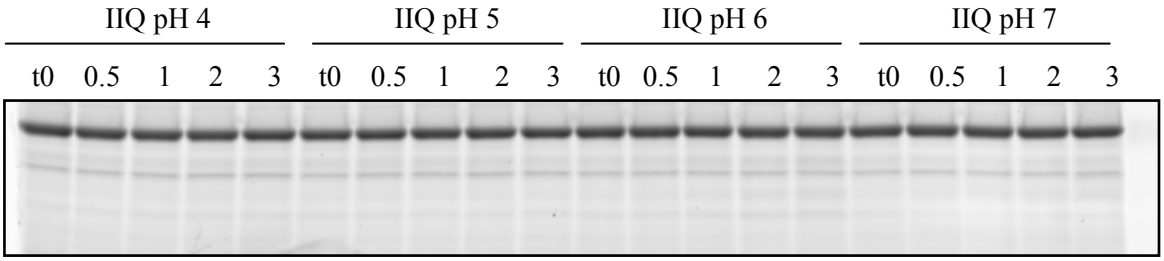

B. Sodium phosphate

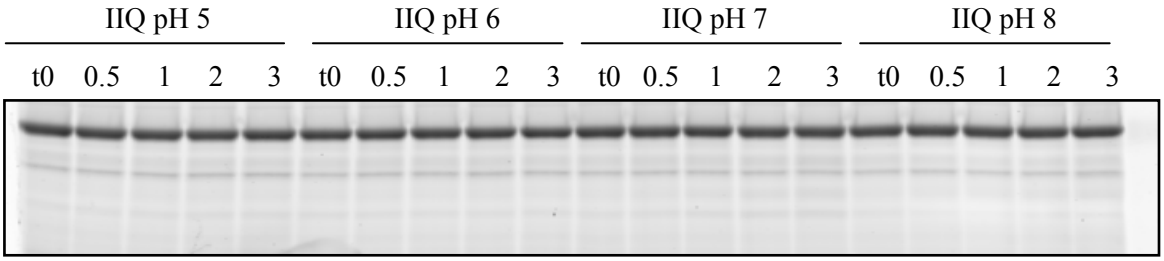

C. Tris-HCl

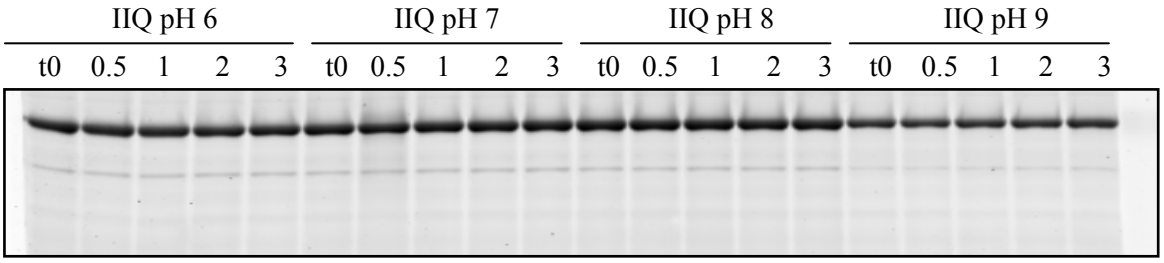

D. Glycine-NaOH

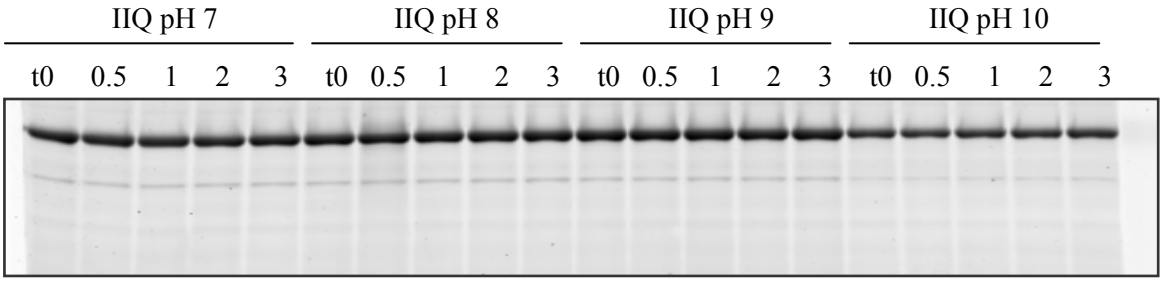

Figure 5. GST-SpoIIQ in pH buffers
Adding only GST-SpoIIQ to the reactions in all above conditions, no cleavage product accumulates. There is also no decrease of the full-length SpoIIQ band. Thus, there are no protease contaminants in any of our buffers.

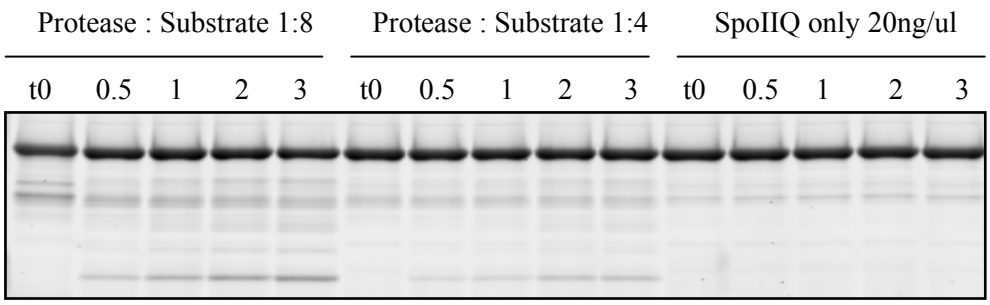

Figure 6. Cleavage of GST-SpoIIQ by SpoIVB
Utilizing highly-purified SpoIVB and GST-SpoIIQ in two different ratios, it can be seen that a cleavage product of SpoIIQ accumulates (bottom of gel). In the absence of the SpoIVB protease (SpoIIQ only, far right of gel), SpoIIQ is not cleaved and no cleavage product accumulates.

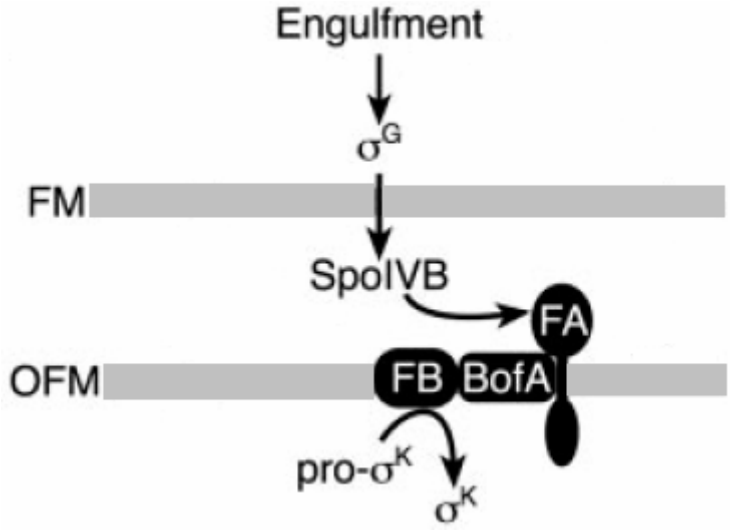

Figure 7. The forespore checkpoint
After engulfment, σ^G leads to upregulation of *spoIVB* causing high levels of SpoIVB protein to accumulate. SpoIVB is secreted into the intramembrane space (between the mother cell and forespore) and cleaves SpoIVFA. This cleavage relieves the BofA-mediated inhibition of SpoIVFB. SpoIVFB then executes regulated intramembrane proteolysis (RIP) of pro- σ^K into active σ^K, which is released into the mother cell. (It is believed that after cleavage of FA by SpoIVB, another protease, CtpB, cleaves FA and BofA.) Modified with permission from [1].

vi. References

1. Chiba, S., Coleman, K., and Pogliano, K. (2007) Impact of membrane fusion and proteolysis on SpoIIQ dynamics and interaction with SpoIIIAH. *J Biol Chem.* **282,** 2576-2586.

2. Perez, A. R., Abanes-De Mello, A., and Pogliano, K. (2000) SpoIIB localizes to active sites of septal biogenesis and spatially regulates septal thinning during engulfment in *Bacillus subtilis*. *J. Bacteriol.* **182,** 1096-1108.

3. Hayes, E. T., Wilks, J. C., Sanfilippo, P., Yohannes, E., Tate, D. P., Jones, B. D., Radmacher, M. D., BonDurant, S. S., and Slonczewski, J. L. (2006) Oxygen limitation modulates pH regulation of catabolism and hydrogenases, multidrug transporters, and envelope composition in *Escherichia coli* K-12. *BMC Microbiol.* **6,** 89.

4. Maurer, L. M., Yohannes, E., BonDurant, S. S., Radmacher, M., and Slonczewski, J. L. (2005) pH regulates genes for flagellar motility, catabolism, and oxidative stress in *Escherichia coli* K-12. *J. Bacteriol.* **187,** 304-319.

5. Slonczewski, J. L., and Foster, J. W. (1996) pH-regulated genes and survival at extreme pH. *E. coli and Salmonella: cellular and molecular biology Volume 1.* 1539-1549

6. Schelp, E., Worley, S., Monzingo, A. F., Ernst, S., and Robertus, J. D. (2001) pH-induced structural changes regulate histidine decarboxylase activity in *Lactobacillus 30a*. **306,** 727-732.

7. Diao, J. (2003) Crystallographic titration of cubic insulin crystals: pH affects GluB13 switching and sulfate binding. *Acta Crystallogr D Biol Crystallogr* **59,** 670-676.

8. Vaughn, D. E., and Bjorkman, P. J. (1998) Structural basis of pH-dependent antibody binding by the neonatal Fc receptor. *Structure* **6,** 63-73.

9. Berisio, R., Sica, F., Lamzin, V. S., Wilson, K. S., Zagari, A., and Mazzarella, L. (2002) Atomic resolution structures of ribonuclease A at six pH values. *Acta Crystallogr D Biol Crystallogr* **58,** 441-450.

10. Yang, F., and Phillips, G. N., Jr. (1996) Crystal structures of CO-, deoxy-, and met-myoglobins at various pH values. *J. Mol. Biol.* **256,** 762-774.

11. Srivastava, J., Barber, D. L., and Jacobson, M. P. (2007) Intracellular pH sensors: design principles and functional significance. *Physiology* **22,** 30-39.

12. Hoa, N. T., Brannigan, J. A., and Cutting, S. M. (2002) The *Bacillus subtilis* signaling protein SpoIVB defines a new family of serine peptidases. *J. Bacteriol.* **184,** 191-199.

13. Wakeley, P. R., Dorazi, R., Hoa, N. T., Bowyer, J. R., and Cutting, S. M. (2000) Proteolysis of SpoIVB is a critical determinant in signaling of Pro-sigmaK processing in *Bacillus subtilis*. *Mol. Microbiol.* **36,** 1336-1348.

APPENDIX B

Strain list

Strain	Genotype	Source
PY79	Wild Type	(3)
KP 8	*spoIID::Tn917(mls)*	Lab Stock
KP 47	*ΔspoIID::cat*	Lab Stock
KP 468	*ΔspoIVB::spc*	(2)
KP 575	*ΔspoIIQ::spc*	(1)
ECE 74	*cat::spc*	Lab Stock
ECE 80	*mls::spc*	Lab Stock
ALD 34	*spoIID298, ΔbofA::cat::tet, thrC::cotD-lacZΩmls, ΔspoIVFABΩcat, amyE::spoIVFABΩkan*	Lab Stock
ALD 40	*spoIID298, thrC::cotD-lacZΩmls, ΔspoIVFABΩcat*	Lab Stock
ALD 63	*thrC::cotD-lacZΩmls, ΔspoIVFABΩcat*	Lab Stock
ALD 167	*spoIID298, ΔbofA::cat::tet, thrC::cotD-lacZΩmls, ΔspoIVFABΩcat, amyE::spoIVFA-S80L(bof8)-FBΩkan*	Lab Stock
ALD 246	*spoIID298, ΔbofA::cat::tet, thrC::cotD-lacZΩmls, ΔspoIVFABΩcat, amyE::spoIVFA-FB-S260GΩkan*	Lab Stock
ALD 270	*ΔbofA::cat::tet, thrC::cotD-lacZΩmls, ΔspoIVFABΩcat, amyE::spoIVFABΩkan*	Lab Stock
ALD 271	*ΔbofA::cat::tet, thrC::cotD-lacZΩmls, ΔspoIVFABΩcat, amyE::spoIVFA-FB-S260GΩkan*	Lab Stock
ALD 275	*thrC::cotD-lacZΩmls, ΔspoIVFABΩcat, amyE::spoIVFABΩkan*	Lab Stock
ALD 288	*spoIID298, thrC::cotD-lacZΩmls, ΔspoIVFABΩcat, amyE::spoIVFABΩkan*	Lab Stock
ALD 312	*thrC::cotD-lacZΩmls, ΔspoIVFABΩcat, amyE::spoIVFA-FB-S260GΩkan*	Lab Stock
ALD 332	*ΔspoIVFABΩcat::tet, amyE::spoIVFA-FB-S260GΩkan*	Lab Stock
ALD 334	*ΔspoIVFABΩcat::tet, amyE::spoIVFA-FB-S260EΩkan*	Lab Stock
ALD 358	*thrC::cotD-lacZΩmls, ΔspoIVFABΩcat, amyE::spoIVFA-S80L(bof8)-FBΩkan*	Lab Stock
KCB 16	*spoIID298, thrC::cotD-lacZΩmls, ΔspoIVFABΩcat, amyE::spoIVFA-FB-S260GΩkan*	This study
KCB 17	*spoIID298, thrC::cotD-lacZΩmls, ΔspoIVFABΩcat, amyE::spoIVFA-FB-S260EΩkan*	This study
KCB 18	*spoIID298, thrC::cotD-lacZΩmls, ΔspoIVFABΩcat, amyE::spoIVFA-S80L(bof8)-FBΩkan*	This study
KCB 19	*ΔbofA::cat::tet, thrC::cotD-lacZΩmls, ΔspoIVFABΩcat, amyE::spoIVFA-S80L(bof8)-FBΩkan*	This study
KCB 20	*ΔspoIID::cat::spc*	This study
KCB 21	*spoIID::Tn917(mls)::spc*	This study
KCB 22	*ΔspoIIQ::spc, thrC::cotD-lacZΩmls, ΔspoIVFABΩcat, amyE::spoIVFA-S80L(bof8)-FBΩkan*	This study
KCB 23	*ΔspoIIQ::spc, thrC::cotD-lacZΩmls, ΔspoIVFABΩcat, amyE::spoIVFABΩkan*	This study
KCB 24	*ΔspoIIQ::spc, thrC::cotD-lacZΩmls, ΔspoIVFABΩcat, amyE::spoIVFA-FB-S260GΩkan*	This study
KCB 25	*ΔspoIIQ::spc, ΔbofA::cat::tet, thrC::cotD-lacZΩmls, ΔspoIVFABΩcat, amyE::spoIVFA-S80L(bof8)-FBΩkan*	This study
KCB 26	*ΔspoIIQ::spc, ΔbofA::cat::tet, thrC::cotD-lacZΩmls, ΔspoIVFABΩcat, amyE::spoIVFABΩkan*	This study

Strain	Genotype	Source
KCB 27	*ΔspoIIQ::spc, ΔbofA::cat::tet, thrC::cotD-lacZΩmls, ΔspoIVFABΩcat, amyE::spoIVFA-FB-S260GΩkan*	This study
KCB 28	*ΔspoIID::cat::spc, thrC::cotD-lacZΩmls, ΔspoIVFABΩcat, amyE::spoIVFA-S80L(bof8)-FBΩkan*	This study
KCB 29	*ΔspoIID::cat::spc, thrC::cotD-lacZΩmls, ΔspoIVFABΩcat, amyE::spoIVFABΩkan*	This study
KCB 30	*ΔspoIID::cat::spc, thrC::cotD-lacZΩmls, ΔspoIVFABΩcat, amyE::spoIVFA-FB-S260GΩkan*	This study
KCB 31	*spoIID::Tn917(mls)::spc, thrC::cotD-lacZΩmls, ΔspoIVFABΩcat, amyE::spoIVFA-S80L(bof8)-FBΩkan*	This study
KCB 32	*spoIID::Tn917(mls)::spc, thrC::cotD-lacZΩmls, ΔspoIVFABΩcat, amyE::spoIVFABΩkan*	This study
KCB 33	*spoIID::Tn917(mls)::spc, thrC::cotD-lacZΩmls, ΔspoIVFABΩcat, amyE::spoIVFA-FB-S260GΩkan*	This study
KCB 34	*spoIID::Tn917(mls)::spc, ΔbofA::cat::tet, thrC::cotD-lacZΩmls, ΔspoIVFABΩcat, amyE::spoIVFA-S80L(bof8)-FBΩkan*	This study
KCB 35	*spoIID::Tn917(mls)::spc, ΔbofA::cat::tet, thrC::cotD-lacZΩmls, ΔspoIVFABΩcat, amyE::spoIVFABΩkan*	This study
KCB 36	*spoIID::Tn917(mls)::spc, ΔbofA::cat::tet, thrC::cotD-lacZΩmls, ΔspoIVFABΩcat, amyE::spoIVFA-FB-S260GΩkan*	This study
KCB 37	*ΔspoIID::cat::spc, ΔbofA::cat::tet, thrC::cotD-lacZΩmls, ΔspoIVFABΩcat, amyE::spoIVFA-S80L(bof8)-FBΩkan*	This study
KCB 38	*ΔspoIID::cat::spc, ΔbofA::cat::tet, thrC::cotD-lacZΩmls, ΔspoIVFABΩcat, amyE::spoIVFABΩkan*	This study
KCB 39	*ΔspoIID::cat::spc, ΔbofA::cat::tet, thrC::cotD-lacZΩmls, ΔspoIVFABΩcat, amyE::spoIVFA-FB-S260GΩkan*	This study